

POLITECNICO DI TORINO



IMPACT OF THE COMBINED USE OF THE BSG AND OF THE E-CLUTCH ON A MICRO-HYBRID VEHICLE

Master's Degree in Mechanical Engineering

Student:
FABRIZIO CUSTORELLA

Academic Tutor:
PROF. EZIO SPESSA
PROF. DANIELA MISUL

Company Tutor:
ING. ANDREA STROPPIANA

ANNO ACCADEMICO 2017-2018

A Federica.

IMPORTANT NOTICE:

This report contains some information which is not intended for publication. Centro Ricerche Fiat S.C.p.A holds all rights on the thesis, including the distribution through electronic media. The content of this work cannot be published or transmitted to third parties without an explicit written authorization.

AVVISO:

Questo lavoro contiene informazioni riservate. È proibito divulgare l'opera o parti di essa senza il consenso scritto da parte di Centro Ricerche Fiat S.C.p.A. Il contenuto di questo lavoro non può essere reso pubblico o trasmesso a terze parti senza esplicita autorizzazione scritta.

Acknowledgments

Innanzitutto vorrei ringraziare il Prof. Ezio Spessa e la Prof.ssa Daniela Misul, in qualità rispettivamente di relatore e correlatrice della mia tesi. La loro incredibile conoscenza tecnica, il loro aiuto e soprattutto la disponibilità che hanno avuto nei miei riguardi sono stati fondamentali per portare a termine il progetto e raggiungere gli obiettivi che avevamo prefissato.

Vorrei inoltre ringraziare il Centro Ricerche Fiat per la splendida opportunità di internship che mi è stata concessa, tutto il dipartimento di “Gasoline & Alternative Fuel Advanced Engineering” e in particolar modo l’Ing. Andrea Stroppiana e l’Ing. Fulvio Reviglio per il loro supporto tecnico, per gli incoraggiamenti e per avermi fatto sentire sin da subito parte integrante del team.

Un ringraziamento speciale va alle persone che mi sono state sempre vicino durante il mio percorso universitario.

Ai miei genitori Alfio e Loredana, che mi hanno sempre sostenuto ed aiutato di fronte a qualsiasi difficoltà non lasciandomi mai solo. La mia dedizione al lavoro e la voglia di superare sempre i miei limiti sono frutto dei vostri insegnamenti: chi sono io oggi è solo merito vostro. Io sarò il bastone della vostra vecchiaia, voi siete stati e sarete le gambe forti della mia gioventù.

A mia sorella Federica, la mia forza. Con i tuoi consigli, mi hai preso per mano e mi hai indicato sempre la strada giusta. Tutte le mie soddisfazioni più grandi sono dedicate a te.

A mia nonna, esempio di straordinaria risolutezza. La tua incredibile forza di volontà mi ha insegnato che nella vita si può sempre ottenere tutto quello si desidera, “*sempre avanti*” e non sarà mai troppo tardi.

A Marco e Paolo, per la meravigliosa amicizia che ci lega. Per tutte le emozioni che abbiamo vissuto e per tutte quelle che ancora dovremmo vivere, insieme.

A Sara, per esserci, da sempre.

A Tano, che mi è stato vicino in uno dei momenti più difficili della mia vita.

A Riccardo, Antonio, al team Engioi e a tutto il resto del magnifico e numeroso gruppo di amici conosciuti qui a Torino. Grazie per le risate e la spensieratezza: ognuno di voi, mi ha insegnato qualcosa che porterò sempre con me.

Alle persone che ci sono state e a quelle che in parte hanno camminato al mio fianco durante questo percorso, ma che poi hanno preso strade diverse.

Grazie.

Abstract

The increasing awareness of the environmental damage caused to the environment and to mankind by pollutants emitted by internal combustion engines has led to the introduction by the competent authorities of increasingly stringent limits for the approval of vehicles. The objective of this work is to show the results in terms of CO₂ reduction on the main type-approval cycles, obtained through the simulation of a kinematic model built taking as reference a micro-hybrid vehicle with P1f architecture in which a Belt Starter Generator and an E-Clutch are installed. The validation of the model was made by comparing the benefits in terms of CO₂ reduction obtained from the simulation with the experimental data of the Fiat Research Center. After validation, the impact of the combined use of the Belt Starter Generator and the E-Clutch on the vehicle and the energy losses that characterize this type of architecture was assessed.

Sommario

La sempre maggiore consapevolezza dei danni ambientali inferti all'ambiente e all'uomo dalle sostanze inquinanti emesse dai motori a combustione interna, ha comportato l'introduzione da parte delle autorità competenti di sempre più stringenti limiti per l'omologazione dei veicoli. L'obiettivo di questo lavoro è quello di mostrare i risultati in termini di riduzione di CO₂ sui principali cicli guida omologativi, ottenuti mediante la simulazione di un modello cinematico costruito prendendo come riferimento un veicolo micro-hybrid con architettura P1f in cui sono installati un Belt Starter Generator e un E-Clutch. La validazione del modello è stata realizzata confrontando i benefits in termini di riduzione di CO₂ ottenuti dalla simulazione con i dati sperimentali del Centro Ricerche Fiat. Dopo la validazione si è valutato l'impatto dell'uso combinato del Belt Starter Generator e dell'E-Clutch sul veicolo e le perdite energetiche che caratterizzano questo tipo di architetture.

Contents

- 1. INTRODUCTION..... 1**
 - 1.1. AIM AND SCOPE..... 2
 - 1.2. OUTLINE OF THE THESIS..... 2

- 2. HYBRID VEHICLES 3**
 - 2.1. MOTIVATION AND HISTORY 3
 - 2.2. MAIN ADVANTAGES AND FUNCTIONS 5
 - 2.3. CLASSIFICATION 7
 - 2.3.1. *HEVs Types*..... 7
 - 2.3.2. *HEVs Levels*..... 10
 - 2.3.3. *Electric machine position* 12

- 3. HYBRID ELECTRIC VEHICLE HOMOLOGATION.....14**
 - 3.1. NEDC 14
 - 3.2. WLTC..... 22

- 4. FIAT PANDA-DEMO CAR.....29**
 - 4.1. VEHICLE GENERAL ARCHITECTURE 29
 - 4.2. BELT STARTER GENERATOR..... 30
 - 4.2.1. *BSG functionalities*..... 33
 - 4.3. ELECTROMECHANICAL CLUTCH..... 36
 - 4.3.1. *Idle Coasting*..... 40
 - 4.4. LI-ION BATTERY 42

- 5. VEHICLE MODEL44**

5.1.	DRIVELINE MODEL	45
5.1.1.	<i>Resistance to motion</i>	45
5.1.2.	<i>Driveline components inertial power</i>	46
5.2.	E-CLUTCH MODEL.....	49
5.3.	ENGINE MODEL	50
5.4.	BSG MODEL.....	51
5.5.	BATTERY MODEL.....	54
5.6.	VEHICLE PERFORMANCES AND EMISSIONS.....	56
6.	STRATEGY.....	58
6.1.	DATA PRE-PROCESSING	58
6.1.1.	<i>Chassis dynamometer emission testing</i>	58
6.1.2.	<i>Vehicle testing Analyzer Tool</i>	60
6.2.	BSG FUNCTION	63
6.2.1.	<i>Enhanced Start & Stop</i>	63
6.2.2.	<i>Regenerative Braking</i>	64
6.2.3.	<i>E-Assist</i>	69
6.3.	E-CLUTCH FUNCTION	73
6.3.1.	<i>Driver Behaviour</i>	73
6.3.2.	<i>Idle Coasting</i>	76
7.	RESULTS	80
7.1.	BSG BENEFITS	81
7.1.1.	<i>NEDC and model validation</i>	81
7.1.2.	<i>WLTC</i>	87
7.2.	E-CLUTCH BENEFITS	91
7.2.1.	<i>WLTC and model validation</i>	91

7.3. COMBINED USE OF THE BSG AND OF THE E-CLUTCH	95
7.3.1. <i>Energy analysis</i>	99
8. CONCLUSION.....	103
BIBLIOGRAPHY	105

List of Figures

Figure 1-Series hybrid.....	8
Figure 2-Parallel hybrid.....	9
Figure 3-Series/Parallel hybrid.....	10
Figure 4-Start&Stop and regenerative braking for a Micro-Hybrid.....	11
Figure 5-Passing phase for a Mild-Hybrid.....	12
Figure 6-Electric driving and normal cruising for a Full-Hybrid.....	12
Figure 7-Electric Machine position in hybrid powertrain.....	13
Figure 8-New European Driving Cycle.....	15
Figure 9-SOC in function of time for condition A (CD).....	18
Figure 10-SOC in function of time for the condition B (CS).....	19
Figure 11-WLTC speed profile.....	24
Figure 12-FIAT Panda Demo-Car.....	29
Figure 13-FIAT Panda Demo-Car Architecture.....	30
Figure 14-BSG installed in FIAT Demo-Car.....	32
Figure 15-Coupling between BSG and engine.....	32
Figure 16-Decoupling tensioner.....	33
Figure 17-BSG main functions.....	34
Figure 18-BSG motoring torque [15].....	35
Figure 19-BSG generating torque.....	36
Figure 20-Hydraulic and mechanical link in manual transmission.....	37
Figure 21-Design and component of the electromechanical clutch system.....	38
Figure 22-System overview of a clutch by wire system.....	39

Figure 24-Rolling distance with and without Idle Coasting [21]	41
Figure 25-Idle Coasting such as a transition mode between driving at constant speed and braking/recuperation.....	42
Figure 26-Li-ion Battery installed in the Demo-Car	43
Figure 27-DemoBE driveline	45
Figure 28-Main rotating components in the driveline	47
Figure 29-Wheels inertial power	48
Figure 30-Final Drive inertial power	48
Figure 31-Gearbox inertial power	49
Figure 32-BSG Efficiency map	52
Figure 33-Power flow in RG-mode	53
Figure 34-Power flow in EA-mode	53
Figure 35-Battery equivalent resistance circuit.....	54
Figure 36-OCV versus SOC.....	55
Figure 37-Internal resistance versus SOC.....	55
Figure 38-Battery current limitations.....	56
Figure 39-BSFC map	57
Figure 40-Matlab dialog box for the choice of tests.....	61
Figure 41-Matlab dialog box for the choice of polluting substances	61
Figure 42-Matlab dialog box for the choice of VCU signals.....	62
Figure 43-Enhanced Start & Stop strategy flow chart.....	64
Figure 44-BSG MM_STATE signal.....	65
Figure 45-BSG MM_STATE signal-RG Mode	65
Figure 46-Engine speed and MM_STATE-RG Mode.....	66
Figure 47-Regenerative braking partial strategy flow chart	67

Figure 48-Regenerative braking strategy flow chart	68
Figure 49-Regenerative braking SOC check.....	69
Figure 50-BSG MM_STATE signal-EA Mode	70
Figure 51-Engine speed and MM_STATE-EA Mode.....	71
Figure 52-E-Assist SOC check.....	72
Figure 53-E-Assist strategy flow chart	73
Figure 54-Gas pedal model	74
Figure 55-Accelerator pedal travel over the cycle.....	75
Figure 56- Accelerator pedal ECU signal	75
Figure 57-Brake pedal travel over the WLTC cycle.....	76
Figure 58-E-Clutch COASTING_PHASE_STATE signal.....	77
Figure 59-E-Clutch COASTING_PHASE_STATE Active.....	78
Figure 60-Idle Coasting strategy flow chart.....	79
Figure 61-BSG functions over the NEDC	81
Figure 62-BSG electric functions duration over the NEDC	82
Figure 63-BSG operative points- NEDC	83
Figure 64-SOC level-NEDC	83
Figure 65-BSG CO2 benefits - NEDC.....	85
Figure 66-Cumulative CO2 emission with BSG-NEDC	86
Figure 67- Zoom of the cumulative CO2 emission with BSG-NEDC	86
Figure 68-BSG functions over the WLTC.....	87
Figure 69-BSG functions duration over the WLTC	88
Figure 70-BSG operative points-WLTC.....	88
Figure 71-SOC level-WLTC	89
Figure 72-BSG CO2 benefits-WLTC	90

Figure 73-Cumulative CO2 emission with BSG-WLTC.....	91
Figure 74-Zoom of the cumulative CO2 emission with BSG-WLTC.....	91
Figure 75-Idle-Coasting operative points over the WLTC	92
Figure 76-Gear variation during the Idle-Coasting	92
Figure 77-E-Clutch function duration over the WLTC	93
Figure 78-E-Clutch CO2 benefit-WLTC	94
Figure 79-Cumulative CO2 emission with E-Clutch-WLTC.....	95
Figure 80-Zoom of the cumulative CO2 emission with E-Clutch-WLTC	95
Figure 81-BSG and E-Clutch functions over the WLTC.....	96
Figure 82-BSG and E-Clutch CO2 benefits-WLTC.....	97
Figure 83-Cumulative CO2 emission with BSG and E-Clutch-WLTC.....	98
Figure 84-Zoom of the cumulative CO2 emission with BSG and E-Clutch-WLTC	98
Figure 85-Energy recover analysis	99
Figure 86-Energy recover percentage reduction	99
Figure 87-Energy supply analysis	100
Figure 88-Energy supply percentage reduction.....	101
Figure 89-Kinetic energy retained.....	102

List of Tables

Table 1-Hybrid Electric Vehicle classification for NEDC regulation.....	16
Table 2-Speed phase sequence for HEV and PHEV in WLTC	23
Table 3-Speed phase sequences characteristics for HEV and PHEV in WLTC	24
Table 4-Test modes for HEV,PHEV and EV in WLTC	25
Table 5-RCB correction criteria values	26
Table 6-RG Mode strategy rules A.....	66
Table 7-RG Mode strategy rules B.....	67
Table 8-EA Mode strategy rules A.....	70
Table 9-EA Mode strategy rules B	71
Table 10-IDLC Mode strategy rule A.....	78
Table 11-IDLC Mode strategy rules B	78
Table 12-IDLC Mode strategy rules C	79
Table 13-Contribution of each BSG functionalities for CO2 reduction-NEDC	85
Table 14-Contribution of each BSG functionalities for CO2 reduction-WLTC.....	90
Table 15- Contribution of E-Clutch function for CO2 reduction-WLTC.....	94
Table 16- Contribution of BSG and E-Clutch functions for CO2 reduction-WLTC	97

Acronyms

ICE	Internal Combustion Engine
FC	Fuel Consumption
HEV	Hybrid Electric Vehicle
CRF	FIAT Research Center
EM	Electric Motor
AC	Alternate Current
DC	Direct Current
PHEV	Plug-in Hybrid Electric Vehicle
BSG	Belt Starter Generator
NEDC	New European Driving Cycle
OPS	Operating Mode Switch
CD	Charge Depleting
SOC	State of Charge
CS	Charge Sustaining
WLTC	Worldwide Harmonized Light Vehicles Test Cycles
REESS	Rechargeable Electric Energy Storage System
RCB	Rechargeable Electric Energy Storage System Charging Balance
SG	Starter Generator
S&S	Start&Stop
EA	Electric Assist
RG	Regenerative braking
CCU	Clutch Control Unit

IDLC	Idle Coasting
DemoBE	Model of the FIAT Panda Demo-Car
OVC	Open Circuit Voltage
BMEP	Break Mean Effective Pressure
VCU	Vehicle Control Unit
BCU	BSG Control Unit
ECU	Engine Control Unit
ENHSS	Enhanced Start&Stop
TWC	Three Way Catalyst

Chapter 1

1. Introduction

Since the beginning of the 21st century the environmental issues such as the climate change, the global warming and the air pollution have become a hot topic in the political agenda of many countries. Indeed the discussion related on how to support one of the major consequences of the economic growth of many nations, and in particular of developing countries such China and India, has become one of the main goals to achieve some of the “Sustainable Development Goals” according to United Nations.

But why the word sustainability has become so much fundamental nowadays? The new concept of sustainability deals with the fundamental idea of preventing pollution rather than fixing problems in order to both avoid and address many environmental problems.

As a response the more restrictive limits for the vehicles homologation in terms of CO₂ emissions, imposed by the regulations, have forced the manufacturers to invest in new different solutions to propel the vehicles with respect to the conventional propulsion by Internal Combustion Engines (ICE). Although the ICE, taking into account its energy storage system, presents the highest weight/power ratio with respect to the others propulsion systems, it is very disadvantageous in terms of polluting substances emissions. Nowadays the best solution it is said to be the vehicle electrification in order to not renounce to the performances and to reduce the fuel consumption (FC) and the emissions by meeting the regulation targets.

1.1. Aim and scope

The Hybrid Electric Vehicles (HEVs) combine two or more sources of power that can directly or indirectly provide propulsion. The aim of this Master's thesis project is the simulation of a P1f micro-hybrid vehicle, with BSG and E-Clutch, on the main type-approval cycles.

1.2. Outline of the thesis

The remainder of this paper is organized as follows. Section two presents a HEVs literature review about their history and development since the last century until nowadays. The different possible classifications (in terms of drivetrain architecture, electrification degree and coupling electric motor-engine) and their main functionalities have been described. The new regulations for the hybrid vehicles and the procedures for their homologation on the type-approval cycles have been analysed. Secondly starting from the components analysis of real reference vehicle actually tested on the chassis dynamometer in FIAT Research Center (CRF) in Orbassano (Turin), a kinematic model has built. The strategies, completely independent by the type-approval cycle, for the activation of the functionalities of the innovative devices that guarantee a CO₂ emissions reduction have been defined by means of the use of a Tool Analyzer (as a part of this Master's thesis project). The results in terms of CO₂ benefits after the model simulation have been evaluated and through a comparison with the CRF experimental data the model was validated. Finally the impact of the combined use of the BSG and of the E-Clutch over the WLTC, not valuated in CRF yet, was calculated and an energetic analysis was carried out about the energy supplied and recovered when the functions are on.

Chapter 2

2. Hybrid vehicles

2.1. Motivation and history

The human life and habits have totally changed since the invention of the Internal Combustion Engine by Nicolas Otto in 1876. During the last century the automobile evolution has been focused mainly on the performance of the cars in terms of power and driveability but the possibility of pollution due to the vehicles emissions has never been taken into account.

In this regard one of the most important cause has been the combustion of hydrocarbon fuels in combustion engine to derive the energy necessary for the propulsion. The products of an ideal combustion are only carbon dioxide (CO_2) and water which do not harm the environment. The carbon dioxide is absorbed by the green plants for the photosynthesis and then it is fundamental for the vegetal life. Actually the combustion that occurs in the ICE is not ideal and the combustion products contain an huge amount of nitrogen oxides (NO_x), carbon monoxides (CO), and unburned hydrocarbons (HC), all of which are toxic to human health. Moreover the large amount of carbon dioxide released in the atmosphere by human activity (the transportation sector is the major contributor) can not be assimilated by the plants, resulting in an accumulation of carbon dioxide.

Thus global warming is a result of the greenhouse effect induced by the presence of carbon dioxide and other gases, greenhouse gases, such as methane, in the atmosphere.

Furthermore the majority of fuels used for the transportation are liquid fuels originating from petroleum. Petroleum is a fossil fuel that has been created by a slow process of millions of years under particular conditions. Many researches showed how the Earth resources of fossil fuel are coming to a end.

All these circumstances, as mentioned before, have recently raised the awareness of the institution by researching different propulsion systems. The necessity for the energetic consumption and pollutant emissions reduction have encouraged the development of Hybrid Electric Vehicles, in which the useful power comes from more actuators. The hybrid vehicle combines the benefits of ICE and Electric Motor (EM), which can work simultaneously or alternatively, to provide improved fuel economy.

The history of electric and hybrid electric vehicles, however, began shortly after the dawn of the 20th century [1]:

- 1900: The Lohner-Porsche Elektromobil makes its debut at the Paris Exposition. Although initially a purely electric vehicle, the designer Ferdinand Porsche added an internal combustion engine to recharge the batteries. It was the first hybrid electric vehicle.
- 1965: US General Motors initiates an electric car development programme. The prototypes Electrovair and Electrovan had a three-phase AC drive system with power either from a silverzinc battery or a fuel cell.
- 1967: The research Staff at the British Ford Motor Company builds a prototype of a small urban electric car: Comuta. With lead batteries it had a maximum range of about 60 km at a speed of 40 km/h, and a maximum speed of somewhat above 60 km/h.

- 1970: A group of engineers at the French electric utility company makes an electric car called VEL.
- 1989: Audi demonstrates the experimental Audi Duo. It combines a 12-horsepower electric motor with a 139-horsepower internal combustion engine. Audi has developed further generations of the Duo during the following decade.
- 1997: In response to a challenge from Executive Vice President Akihiro Wadi to develop more fuel-efficient vehicles, Toyota introduces the Prius and begins marketing it in Japan and in 2000 in the United States.
- 1999: Honda introduces the Insight.
- 2004: Ford introduces the first hybrid SUV, the 2005 Ford Escape.

2.2. Main advantages and functions

A Hybrid Electric Vehicle has at least two sources of power for propulsion: the internal combustion engine and an electric motor.

The combination of a combustion engine and electric machine provides different advantages [2]:

- The presence of EM reduces the demands on a hybrid gasoline engine, which in turn can be downsized and more efficiently operated (working near the optimum operating line in the most fuel-efficient points). The gasoline engine produces less power, but when combined with electric motors, the system total power can be equal or higher than that of a conventional vehicle.
- The gear ratios of the transmission can be lowered, to keep the engine at lower speed operating points, because the electric motor can deliver instant torque

request from the driver improving at the same time the torque response of the powertrain.

- Conventional cars rely entirely on friction brakes to slow down, dissipating the vehicle kinetic energy as heat. The presence of a reversible electric machine allows some of that energy to be captured, turned into electricity, and stored in the batteries. This stored electricity can later be used to run the motor and accelerate the vehicle.

In function of the degree of hybridization and the kind of hybrid an HEV can perform at least one or more of the following functions:

- **Engine Start&Stop:** this function turns off the engine when the vehicle is stopped without the intervention of the driver (through the ignition key), saving fuel. When the driver presses the clutch pedal or releases the brake pedal the engine is restarted automatically. The battery provides energy for the air conditioner and accessories (they can be electrified) while the vehicle idles at stop lights or in traffic, and the electric motor can start the vehicle moving again.
- **Electric Torque Assistance:** the electric motor can provide additional torque to the powertrain, improving the overall torque response. The torque can be provided by the EM during the transient phase to compensate for the engine torque response delay: torque fill. Otherwise the torque delivered can be used to increase the maximum overall torque of the powertrain, this function is called torque boost.

- **Electric Driving:** If the electric machine is powerful enough and it can provide all the necessary power for the propulsion, the internal combustion engine is switched off and the vehicle can be driven in electric mode.
- **Battery Charging and Regenerative Braking:** The Plug-in Hybrid Vehicles (PHEV) can be charged from the grid to store the electric energy on the battery. This kind of hybrid vehicle has a rectifier which converts the alternate current of the power socket into direct current and stored into the high voltage battery. Instead the conventional hybrid vehicle has usually a belt or integrated starter generator, which is connected to the engine and during the vehicle braking works as generator charging the battery (regenerative braking).

2.3. Classification

2.3.1. HEVs Types

The HEVs type, first classification for hybrid vehicles, is determined by the drivetrain design. The drivetrain effects the vehicle mechanical efficiency, the fuel consumption and the purchasing price. In hybrid-electric cars the drivetrain architecture identifies the coupling between electric motor and conventional engine and how they work together. Three different types are determined [3]:

- **Series Hybrid:** Electric hybridization. The drivetrain receives mechanical power from the electric motor, which is run by either a battery or a gasoline-powered generator.
- **Parallel Hybrid:** Powertrain hybridization with a mechanical coupling. The electric motor and internal combustion engine can provide mechanical power simultaneously.

- **Series/Parallel Hybrid:** The drivetrain enables the engine and electric motor to provide power independently or in conjunction with one another.

In the figure below is presented a series drivetrain. The mechanical coupling between ICE and vehicle is absent, the combustion engine drives an electric generator instead of directly driving the wheels. The ICE mechanical energy is converted in electrical energy totally by the generator and it can be used to charge the battery or to provide power to electric motor that moves the vehicle. The electric motor is the only one which provides power to the wheels. The motor receives electric power from either the battery pack or from a generator run by a gasoline engine. The connection of the powers developed by engine and provided from the battery is electrical. Series hybrids perform at their best during stop-and-go traffic, where gasoline and diesel engines are inefficient. The engine is typically smaller in a series drivetrain because it has only to meet certain power demands; the battery pack is generally more powerful than the one in parallel hybrids in order to provide the remaining power needs. For these reasons, series hybrids may also be referred to as Range-Extended Electric Vehicles.

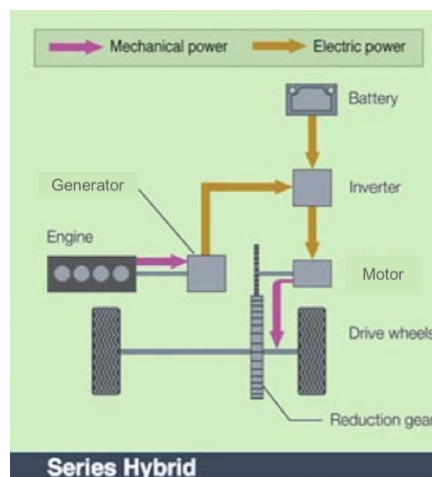


FIGURE 1-SERIES HYBRID

A parallel hybrid (Figure 2) is propelled by both an internal combustion engine and an electric motor connected to a mechanical transmission. Power distribution between the engine and the motor is varied so both run in their optimum operating region as much as possible. Whenever the generator's operation is needed, for example to charge the battery, the electric machine works as a generator. Instead, the motor working is active only when a boost is needed. Parallel hybrids tend to use a smaller battery pack than series drivetrains, relying on regenerative braking to keep it recharged. When power demands are low, parallel hybrids utilize also the motor as a generator for supplemental recharging such as an alternator in conventional cars.

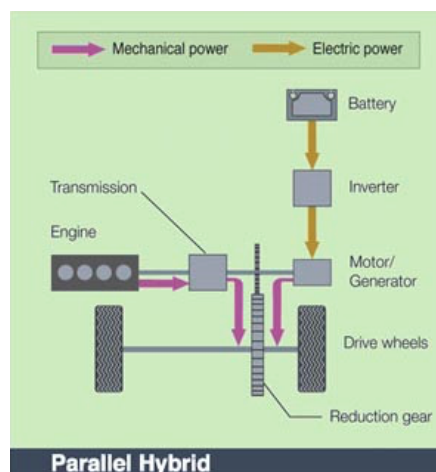


FIGURE 2-PARALLEL HYBRID

The last configuration is a mixture of the previous two architectures. The vehicles that use this architecture are referred Series/Parallel hybrids. This kind of drivetrains merges the advantages and complications of the parallel and series configuration. The engine and the electric motor can both drive the wheels directly (as in the parallel hybrids) or they can be effectively disconnected with only the electric motor providing power (as in the series hybrids). Moreover the power delivered by the ICE can be used to move the

vehicle and at the same time it can be converted in electrical energy by a generator to supply energy to electric motor or to charge the battery. Power distribution between the ICE and EM is designed so that the engine can run in its optimum operating range as much as possible. At lower speeds, it operates more as a series vehicle, while at high speeds, where the series drivetrain is less efficient, the engine takes over and energy loss is minimized. [4]

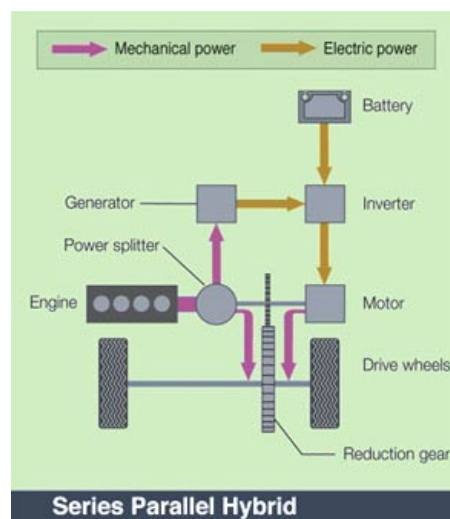


FIGURE 3-SERIES/PARALLEL HYBRID

2.3.2. HEVs Levels

A second classification can be done in function of the degree of hybridization. The term hybrid refers to a type of vehicle but there are different levels of hybridization:

- **Micro-Hybrid**
- **Mild-Hybrid**
- **Full-Hybrid**

The category of micro-hybrid is the simplest in terms of working and architecture. The micro HEV is a vehicle with an integrated alternator/starter or a belt driven starter generator (BSG) that uses start/stop technology and allows the regenerative braking. During the cruise, the vehicle is propelled only by the internal combustion engine (very similar to the conventional vehicle engine) and the vehicle never moves in electric driving. Typical fuel efficiency increase is around 10% compared to a non-hybrid.

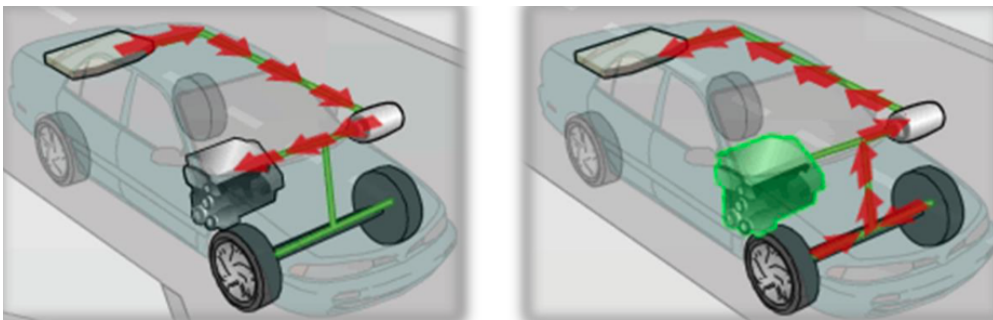


FIGURE 4-START&STOP AND REGENERATIVE BRAKING FOR A MICRO-HYBRID

The mild-hybrids is very similar to a micro HEV with the exception that the BSG is upgraded with stronger electric components that could assist the ICE in vehicle propulsion when the power required by the vehicle is high. Indeed during the “passing phase” the power is provided by the ICE and the EM both. The electric motor works also in generator mode to realize the regenerative braking or to convert the energy provided by the engine to charge the battery. During a stop the engine and the electric motor switch off and the accessories are alimented only by the battery. The engine is downsized with respect to the micro-hybrid engine and the typical fuel efficiency increase is around 20-25% compared to a non-hybrid.

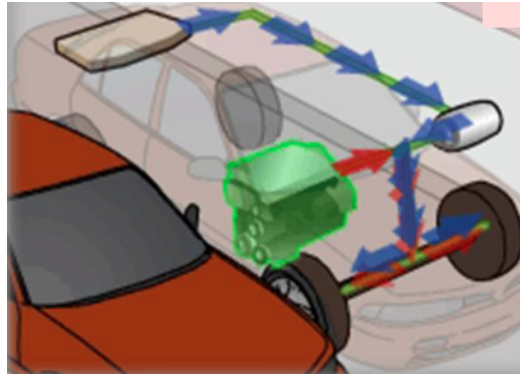


FIGURE 5-PASSING PHASE FOR A MILD-HYBRID

A Full HEV is the most complex and functional hybrid level. The components are similar with respect to that used by a mild HEV but they are much larger in size and moreover a full HEV needs a power split device. The additional functions of a Full Hybrid are the electrical driving for low speed and the possibility to improve the engine working conditions during the normal cruising. The typical fuel efficiency increasing is around 40-45%. [5]

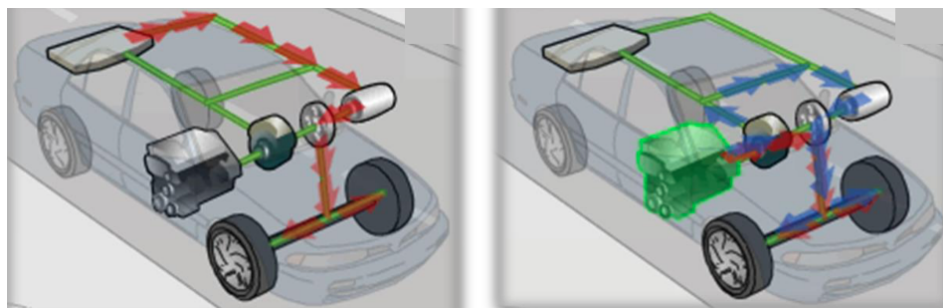


FIGURE 6-ELECTRIC DRIVING AND NORMAL CRUISING FOR A FULL-HYBRID

2.3.3. Electric machine position

The last classification is based on the electric machine position relative to the other powertrain components [2]:

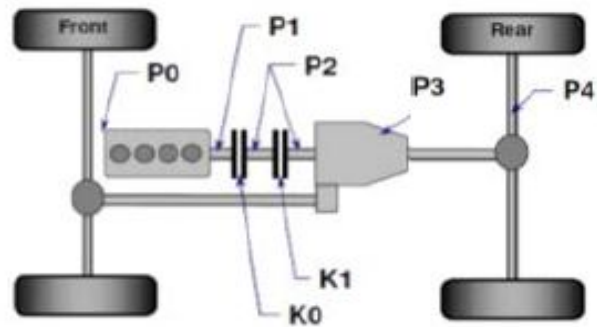


FIGURE 7-ELECTRIC MACHINE POSITION IN HYBRID POWERTRAIN

- **P1f/P0:** The electric machine is connected with the ICE through a belt on the Front End Accessory Drive (FEAD).
- **P1r:** The electric machine is connected directly with the crankshaft of the internal combustion engine: rear position.
- **P2:** The electric machine is between the internal combustion engine and the transmission.
- **P3:** The electric machine is connected through a gear with the transmission.
- **P4:** The electric machine is connected through a gear on the rear axle of the vehicle. It can be located also in the wheels hub.

Chapter 3

3. Hybrid Electric Vehicle homologation

The higher circulation of hybrid vehicles and their success in the world market caused the necessity to define type-approvals for the vehicles homologation. In this chapter the main type-approvals cycles and their relative homologation procedures will be analysed and described.

3.1. NEDC

The current European regulations assert that the fuel consumption and the emission of polluting substance emissions should be evaluated over the New European Driving Cycle (NEDC). It is a speed profile in function of time that must be done on the chassis dynamometer by the vehicle respecting the regulation constraints. The cycle (figure below) consists in two different parts: the urban cycle, formed by four elementary cycles, and an extra urban cycle for a total of 1180 s.

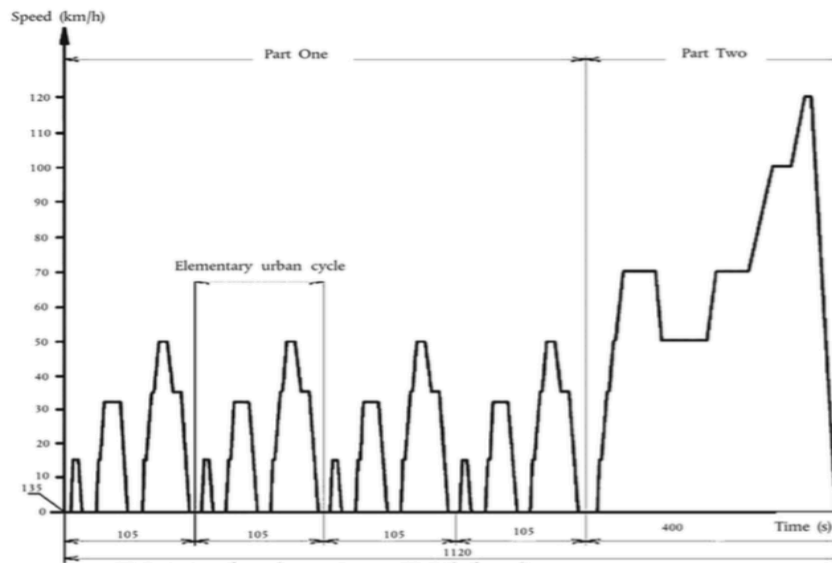


FIGURE 8-NEW EUROPEAN DRIVING CYCLE

The regulation [6] defines in detail the acceleration and deceleration time, the gear shift profile with the relative shifting points and the speed tolerance. The gear shift profile depends on the vehicle gearbox. Different test mode are described in function of the gearboxes: manual gearboxes, semi-automatic-shift gearboxes or automatic-shift gearboxes.

A tolerance of ± 2 km/h shall be allowed between the indicated speed and the theoretical speed during acceleration, during steady speed, and during deceleration when the vehicle brakes are used.

About the hybrid electric vehicles, defined as “Hybrid electric vehicle means a vehicle that, for the purpose of mechanical propulsion, draws energy from both of the following on-vehicle sources of stored energy/power: (a) a consumable fuel; (b) an electrical energy/power storage device (e.g. battery, capacitor, flywheel/generator, etc.)” the reference is the Regulation No 101 [7]. This one is structured in different sections in function of the HEV classification.

The table below shows the principal classification criteria used for hybrid vehicle:

Vehicle charging	Off-vehicle charging ^(a) OVC/PHEV		Not Off-vehicle charging ^(b) NOVC/HEV	
Operating mode switch	Without	With	Without	With
(a) Also known as “externally chargeable”: Plug-in hybrid vehicle				
(b) Also known as “not externally chargeable”: Conventional hybrid vehicle				

TABLE 1-HYBRID ELECTRIC VEHICLE CLASSIFICATION FOR NEDC REGULATION

Beyond the general classification about the charging mode that discerns two categories (PHEV and HEV), the regulation takes into account the installation of an Operating Mode Switch (OPS) which allows to choose the vehicle working mode:

- **Hybrid**
- **Fuel Consuming**
- **Most Electric Hybrid Mode:** The hybrid mode which can be proven to have the highest electricity consumption of all selectable hybrid modes.
- **Most Fuel Consuming Mode:** The hybrid mode which can be proven to have the highest fuel consumption of all selectable hybrid modes.

Since the reference vehicle is a conventional hybrid vehicle not externally chargeable, only the type-approval procedures for the conventional HEVs are described.

For a Conventional Hybrid Electric Vehicles and therefore for all those vehicles not externally chargeable, the OPS presence or absence does not change the type-approval procedure. In the event different vehicle working mode are possible, the homologation test shall be carried out in the mode that is automatically set after turn on of the ignition key (normal mode).

Emission of carbon dioxide and fuel consumption shall be determined separately for the Part One (urban driving) and the Part Two (extra-urban driving) of the specified driving cycle.

Two test shall be performed under the following conditions:

- **Condition A:** Test shall be carried out with a fully charged electrical energy/power storage device: Charge Depleting (CD) test. The procedure starts with the discharge of the electrical energy/power storage device according to the possible ways. Secondly the application of a normal overnight charge shall be applied to the electrical energy/power storage device and the test can be carried out. The vehicle shall be driven using the applicable driving cycle and gear shifting prescription as defined by the regulation. The exhaust gases are analyzed and the test results of CO₂ and fuel consumption on the combined cycle for the condition A shall be recorded respectively in m_1 [g] and c_1 [l]. Within the thirty minutes after the conclusion of the cycle, the electrical energy/power storage device is charged again and the energy measurement equipment measures the electric energy consumption for the condition A in e_1 [Wh]. In the figure below is illustrated battery State of Charge (SOC) trend in function of time for the condition A:

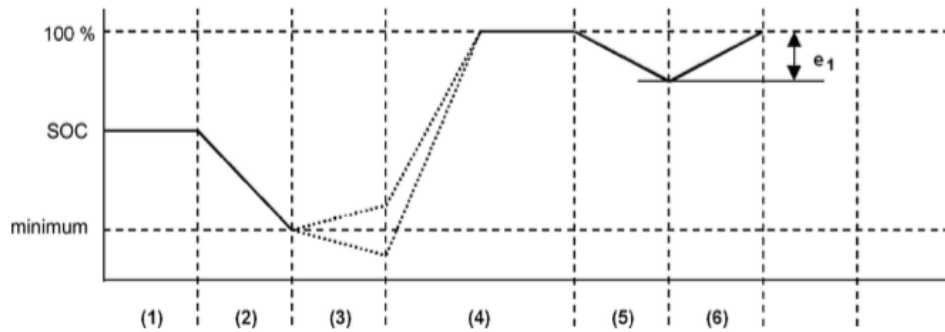


FIGURE 9-SOC IN FUNCTION OF TIME FOR CONDITION A (CD)

- **Condition B:** Test shall be carried out with an electrical energy/power storage device in minimum state of charge (maximum discharge of capacity): Charge Sustaining (CS) test. The test procedure and the exhaust gases analyses are the same of the procedure A. The results on the combined cycle for the condition B are recorded in m_2 [g] (CO_2) and c_2 [l] (FC). Within the thirty minutes after the conclusion of the cycle the battery is charged again and the charge energy e_2 [Wh] is measured. The electrical energy/power storage device of the vehicle shall be discharge and secondly charged to measure the charge energy e_3 [Wh]. From this value the electric energy consumption e_4 [Wh] is obtained:

$$e_4 = e_3 - e_2 \quad (3.1)$$

The figure below shows the SOC for the condition B:

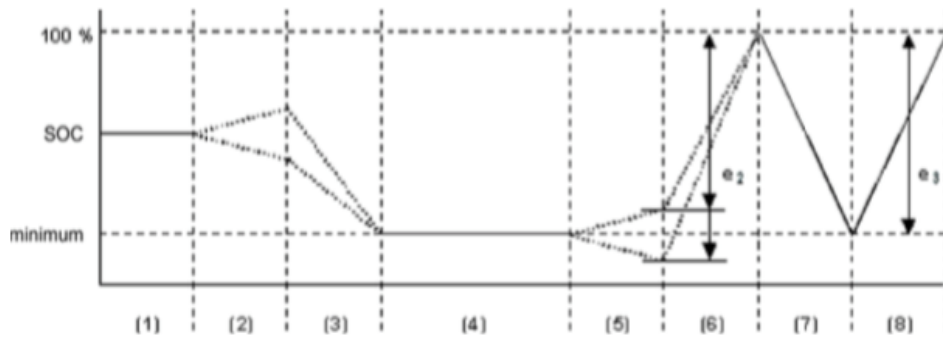


FIGURE 10-SOC IN FUNCTION OF TIME FOR THE CONDITION B (CS)

Later the testing of the two conditions test results shall be analysed to obtain the weighted values of CO₂, fuel consumption and energy consumption.

The weighted values of CO₂ shall be calculated as below:

$$M = (D_e \cdot M_1 + D_{av} \cdot M_2) / (D_e + D_{av}) \quad (3.2)$$

where

- D_e =vehicle's electric range [km].

- D_{av} =25 km (assumed average distance between two battery recharges).

- M_1 =mass emission of CO₂ with a fully charge electrical energy/power storage device [g/km] calculated by m_1/D_{test1} where D_{test1} is the actual driven distance in the test performed under condition A.

- M_2 = mass emission of CO₂ with an electrical energy/power storage device in minimum state of charge [g/km] calculated by m_2/ D_{test2} where D_{test2} is the actual driven distance in the test performed under condition B.

- M = mass emission of CO₂ in grams per kilometer [g/km]

The values of fuel consumption:

$$C = (D_e \cdot C_1 + D_{av} \cdot C_2) / (D_e + D_{av}) \quad (3.3)$$

with

$-C_1$ = fuel consumption with a fully charge electrical energy/power storage device [l/100km] calculated by $100 \cdot c_1 / D_{test1}$ where D_{test1} is the actual driven distance in the test performed under condition A.

$-C_2$ = fuel consumption with an electrical energy/power storage device in minimum state of charge [l/100km] calculated by $100 \cdot c_2 / D_{test2}$ where D_{test2} is the actual driven distance in the test performed under condition B.

$-C$ = fuel consumption in l/100 km.

The value of electric energy consumption instead:

$$E = (D_e \cdot E_1 + D_{av} \cdot E_4) / (D_e + D_{av}) \quad (3.4)$$

$-E_1$ = electric consumption Wh/km with a fully charge electrical energy/power storage device [g/km] calculated by e_1 / D_{test1} where D_{test1} is the actual driven distance in the test performed under condition A.

$-E_4$ = electric consumption Wh/km with an electrical energy/power storage device in minimum state of charge [g/km] calculated by e_4 / D_{test2} where D_{test2} is the actual driven distance in the test performed under condition B.

$-E$ = electric consumption [Wh/km].

Moreover the **test results should be corrected** in function of the vehicle's battery energy balance ΔE_{batt} and of the electricity balance Q [Ah]. This one, measured using the procedure specified in appendix 2 to the Annex 8 in the Regulation 101 [7], is used as a measure of the difference in the vehicle battery energy content at the end of the cycle compared to the beginning of the cycle.

The correction is necessary to take into account the effect of battery recharge made by the ICE, since HEVs do not allow the external recharge of the high voltage battery. The corrected values should correspond to a zero energy balance and are calculated using a correction coefficient described in this section.

It is allowed to the uncorrected measured values C and M as the results:

- in case the manufacturer can prove that there is no relation between the energy balance and fuel consumption.
- in case that ΔE_{batt} always corresponds to a battery charging.
- in case that ΔE_{batt} always corresponds to a battery discharging and ΔE_{batt} is within 1% of the energy content of the total fuel consumption over one cycle.

The change in battery content can be calculated from the measured electricity balance:

$$\Delta E_{batt} = \Delta SOC(\%) \cdot \Delta E_{TEbatt} = 0,0036 * Q * V_{batt} \quad (3.5)$$

With E_{TEbatt} [MJ] the total energy storage capacity of the battery and V_{batt} [V] the nominal battery voltage.

The CO₂ emission correction coefficient [g/km/Ah] and fuel consumption correction coefficient [l/100km/Ah] are defined as below:

$$K_{CO_2} = \frac{(n \cdot \sum Q_i M_i - \sum Q_i \cdot M_i)}{n \cdot \sum Q_i^2 - \sum Q_i^2} \quad (3.6)$$

$$K_{FC} = \frac{(n \cdot \sum Q_i C_i - \sum Q_i \cdot C_i)}{n \cdot \sum Q_i^2 - \sum Q_i^2} \quad (3.7)$$

where

- C_i =fuel consumption measured during i-th manufacturer's test [g/km].

- M_i =CO₂ -emission measured during i-th manufacturer's test [g/km].

- Q_i =electricity balance during i-th manufacturer's test [Ah].

- n =number of measurements performed by the manufacturer.

Separate fuel consumption and CO₂ emission correction coefficients shall be determined for the fuel consumption values measured over the Part One cycle and the Part Two cycle respectively.

The corrected values C_0 and M_0 (type approvals fuel emission and CO₂-emission) are computing using the formulation below:

$$M_0 = M - K_{CO_2} \cdot Q \quad (3.8)$$

$$C_0 = C - K_{FC} \cdot Q \quad (3.9)$$

- C_0 =TA fuel consumption (l/100km).

- M_0 =TA CO₂-emission (g/km).

- C =fuel consumption measured during test [l/100 km].

- M =CO₂-emission at the end of the test [g/km].

- Q = electricity balance measured during test [Ah].

3.2. WLTC

The Worldwide harmonized Light vehicles Test Cycles (WLTC) are chassis dynamometer tests for the determination of emissions and fuel consumption for light-duty vehicle. The WLTC cycles are part of the Worldwide harmonized Light vehicles Test Procedures (WLTP). The WLTP procedures includes several WLTC test cycles created by a succession of speed phase sequences, that recreate almost faithfully to real cycle with respect to the NEDC test. The cycles shall be carried out by the vehicles in

function of the class described by their power-to-mass (PMR) ratio: Class 3 (Divided into 2 subclasses according to their maximum speed, Class3b and Class 3a), Class 2 and Class 1 .

- **Class 1:** vehicles with $PMR \leq 22$ W/kg.
- **Class 2:** vehicles with $22 \text{ W/kg} < PMR \leq 34$ W/kg c
- **Class 3:** vehicles with $PMR > 34$ W/kg. Divided into 2 subclasses according to their maximum speed, Class3b and Class 3a.

The Global technical regulation about the Worldwide harmonized Light vehicles Test Procedure [8] defines in detail the procedure phases and analyses also the type-approval procedures for the hybrid electric vehicles (HEV or PHEV) or electric vehicles (EV).

All these vehicle are in the Class 3 and the speed phase sequences are described below:

Category	PMR	V_max [km/h]	Speed Phase Sequence
Class 3b	PMR>34	$V_{max} \geq 120$	Low 3+Medium 3-2 +Extra High 3
Class 3a		$V_{max} \leq 120$	Low 3+Medium 3-1 +High 3-1+Extra High 3

TABLE 2-SPEED PHASE SEQUENCE FOR HEV AND PHEV IN WLTC

In the table are reported the speed phase sequences characteristic in detail:

Phase	Duration	Stop Duration	Distance	p_stop	v_max	v_ave w/o stops	v_ave w/ stops	a_min	a_max
	s	s	m		km/h	km/h	km/h	m/s ²	m/s ²
Class 3b (v_max ≥ 120 km/h)									
Low 3	589	156	3095	26.5%	56.5	25.7	18.9	-1.47	1.47
Medium 3-2	433	48	4756	11.1%	76.6	44.5	39.5	-1.49	1.57
High 3-2	455	31	7162	6.8%	97.4	60.8	56.7	-1.49	1.58
Extra-High 3	323	7	8254	2.2%	131.3	94.0	92.0	-1.21	1.03
Total	1800	242	23266						
Class 3a (v_max < 120 km/h)									
Low 3	589	156	3095	26.5%	56.5	25.7	18.9	-1.47	1.47
Medium 3-1	433	48	4721	11.1%	76.6	44.1	39.3	-1.47	1.28
High 3-1	455	31	7124	6.8%	97.4	60.5	56.4	-1.49	1.58
Extra-High 3	323	7	8254	2.2%	131.3	94.0	92.0	-1.21	1.03
Total	1800	242	23194						

TABLE 3-SPEED PHASE SEQUENCES CHARACTERISTICS FOR HEV AND PHEV IN WLTC

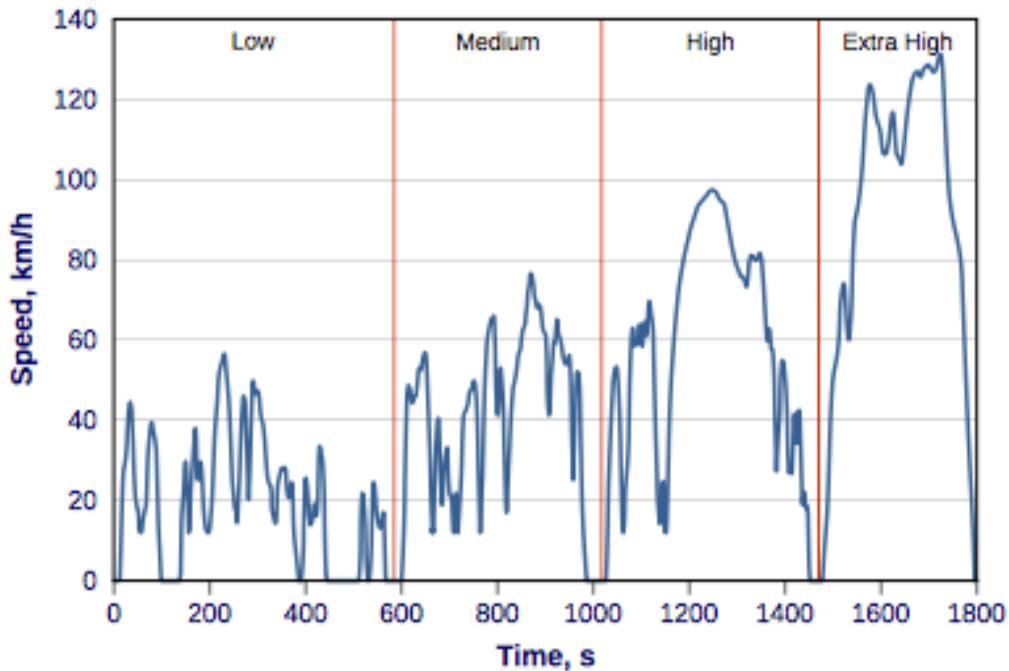


FIGURE 11-WLTC SPEED PROFILE

The matrix shows that the type approvals for hybrid electric vehicle in terms of procedure and conditions (as charge depleting or sustaining for the different categories) are the same of the NEDC. The differences are the parameters of the cycle and consequently the velocity profile in function of the time.

		WLTP		WLTP city
		Charge-depleting	Charge-sustaining	Charge-depleting
PHEV	Class 3a	Low3+ Medium 3-1+ Extra High 3	Low3+ Medium 3-1+ High 3-1+Extra High 3	Low3+ Medium 3-1
	Class 3b	Low 3+ Medium 3-2+ Extra High 3	Low 3+ Medium 3-2+ Extra High 3	Low 3+ Medium 3-2
HEV	Class 3a	--	Low3+ Medium 3-1+ High 3-1+Extra High 3	--
	Class 3b	--	Low 3+ Medium 3-2+ Extra High 3	--
PEV	Class 3a	Low3+ Medium 3-1+ High 3-1+Extra High 3	--	Low3+ Medium 3-1
	Class 3b	Low 3+ Medium 3-2+ High 3-2+ Extra High 3 High 3	--	Low 3+ Medium 3-2

TABLE 4-TEST MODES FOR HEV,PHEV AND EV IN WLTC

The conventional hybrid electric vehicle shall be tested under charge-sustaining (CS) conditions: test results shall be corrected as a function of RCB [Ah] (Rechargeable Electric Energy Storage System (REESS) Charging Balance) obtaining $CO_{2,CD,corrected}$ and $FC_{CD,corrected}$ at RCB=0.

Furthermore the Regulation describes three different reasons for which is possible to use the uncorrected values in PHEV and HEV both:

- The manufacturer can prove that there is no relation between the energy balance and fuel consumption.
- ΔE_{REESS} as calculated from the test result corresponds to REESS charging.
- ΔE_{REESS} as calculated from the test result corresponds to REESS discharging, ΔE_{REESS} expressed as a percentage of the energy content of the fuel consumed over the cycle, is calculated in the equation below:

$$\Delta E_{REESS} = \frac{0,0036 \cdot \sum_{i=1}^z (RCB_i \cdot U_{REESSi})}{E_{fuel}} \cdot 100 \quad (3.10)$$

where:

- U_{REESSi} =nominal REESS voltage for i_{th} REESS [V].

- RCB_i =is the charging balance over the whole cycle for the i_{th} REESS [Ah].

- E_{fuel} = is the energy content of the consumed fuel [MJ].

- i = index of REESS.

- z = number of installed REESS.

- ΔE_{REESS} is smaller than the RCB correction criteria, according to the following equation and table below:

$$\Delta E_{REESS} \leq \text{RCB correction criteria} \quad (3.11)$$

Cycle	WLTC (Low+Medium+High)	WLTC (Low+Medium+ High+Extra High)
RCB correction criteria [%]	1	0.5

TABLE 5-RCB CORRECTION CRITERIA VALUES

The correction in function of RCB is done through CO₂ emission and fuel consumption correction coefficients. They shall be calculated separately for each phase of the WLTC and corrected to zero over each WLTC phase.

The two correction factors for the individual phases as well as for the complete test cycle are defined as follow:

$$K_{CO2} = \frac{n \cdot \sum E_{REESSi} \cdot M_i - \sum E_{REESSi} \cdot \sum M_i}{n \cdot \sum E_{REESSi}^2 - (\sum E_{REESSi})^2} \quad (3.12)$$

$$K_{FUEL} = \frac{n \cdot \sum E_{REESSi} \cdot FC_i - \sum E_{REESSi} \cdot \sum FC_i}{n \cdot \sum E_{REESSi}^2 - (\sum E_{REESSi})^2} \quad (3.13)$$

with:

- K_{CO2} are the CO₂ emissions correction coefficients [g/km/Wh/km].

- M_i are the CO₂ emissions measured during the i_{th} test [g/km].

- K_{FUEL} are the fuel consumption correction coefficients [l/100 km/Wh/km].

- FC_i are the fuel consumptions measured during the i_{th} test [l/100 km].

- E_{REESSi} is the electricity balance during the i_{th} test [Wh/km].

- n is the number of measurements.

Finally the CO₂ emissions and fuel consumption at zero REESS energy balance shall be:

$$M_0 = M - K_{CO2} * \Delta E_{REESSi} \quad (3.14)$$

$$FC_0 = FC - K_{FUEL} * \Delta E_{REESSi} \quad (3.15)$$

where:

- M_0 are the CO₂ emissions at zero REESS energy balance (REB=0) [g/km].

- K_{CO2} are the CO₂ emissions correction coefficient [g/km/Wh/km].

- FC_0 is the fuel consumption at $\Delta E_{REESS} = 0$ [l/100 km].

- FC is the fuel consumption measured during the test [l/100 km].

$-\Delta E_{REESSi}$ is the electricity balance measured during test [Wh/km].

Because of only the charge sustaining mode is carried out for the conventional hybrid vehicle, the corrected value are also the final values. [9] [10]

Chapter 4

4. FIAT Panda-Demo Car

4.1. Vehicle general architecture

The kinematic model presented in this thesis has been created to simulate a real vehicle on the principal type approval cycles. This reference vehicle is a **FIAT Panda Demo-Car** built by FIAT Chrysler Automobiles (FCA) that is tested on the chassis dynamometer in the FIAT Research Center in Orbassano (Turin).



FIGURE 12-FIAT PANDA DEMO-CAR

In the FIAT Panda particular devices have been installed that will be described in the next sections:

- **BSG**
- **E-Clutch**
- **Li-Ion Battery**

Their installation in the powertrain and the functions that can be provided change completely the vehicle architecture and especially its definition in the automotive market by making this vehicle a **Micro-Hybrid** with a **P1f architecture**.

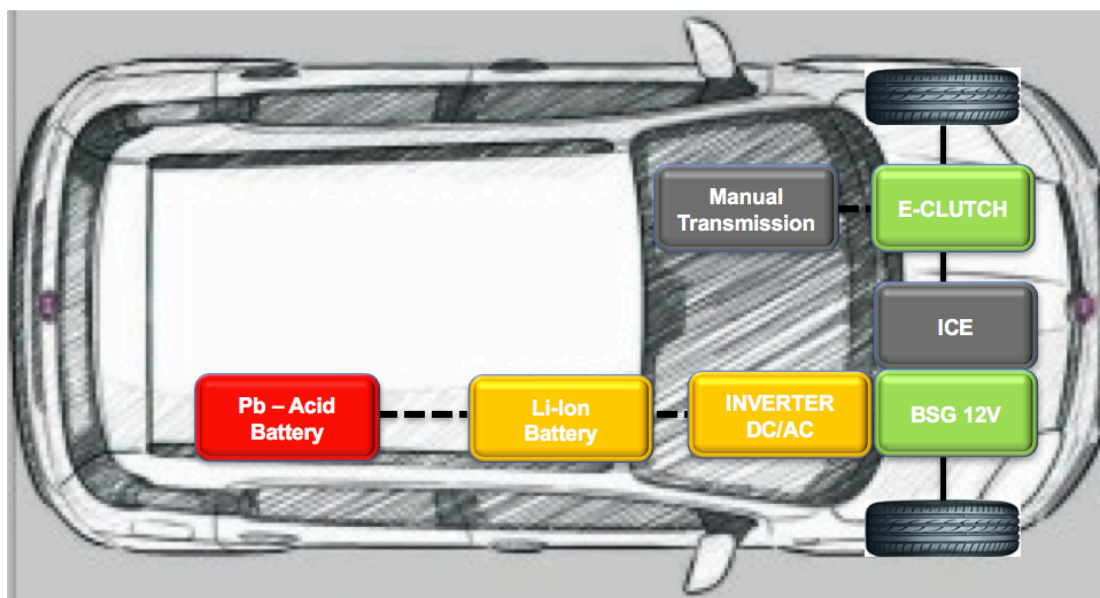


FIGURE 13-FIAT PANDA DEMO-CAR ARCHITECTURE

4.2. Belt Starter Generator

The Starter Generator (SG) system is a technology that through its functions transforms a conventional vehicle equipped by an internal combustion engine only in a micro hybrid vehicle with a P1f architecture. This configuration is one of the most analyzed during the last decade. Indeed it guarantees good reduction of carbon-dioxide emission

and fuel consumption with low delta costs and minimal modifications of the classical powertrain.

The application of this electric machine that works both as starter and alternator can be done in four different ways [11]:

- **Direct coupled drive:** The electric machine is placed on the accessory drive or on the crankshaft between the transmission and the engine in the location of the flywheel. Despite the benefits in terms of reliability and torque smoothing this application needs an increase of the powertrain length for a correct and efficient installation. In this case the starter generator is also referred as Integrated Starter Generator.
- **Chain Drive:** The application of the SG is done thanks to a chain. The chain could be smaller compared to the belt solution but this coupling requires a new design of the transmission case and an expensive cost to reduce the noise.
- **Gear Drive:** In this kind of coupling the Starter Generator is connected through the gear on the transmission side. The common problems are due to the possible teeth damages at high speed and not high loads. It involves the use of expensive materials and the reduction of benefits in terms of costs.
- **Belt Drive:** If the Starter Generator is connected to the engine through a belt drive, it can be referred to Belt Starter Generator (BSG). The connection is realized on the accessory side using a dedicated belt drive. Despite the increase of the belt and pulley widths in order to process the new load supplied by the electric motor, the BSG solution provides a lot of benefits in terms of low cost application, minimal modification of the powertrain, low noise and more

freedom in packaging. The main disadvantage is the limitation of the torque transmission through the belt drive.



FIGURE 14-BSG INSTALLED IN FIAT DEMO-CAR

In FIAT Panda Demo-Car the BSG connection is done through a belt drive with a decoupling tensioner to obtain the maximum benefits with the low delta costs.

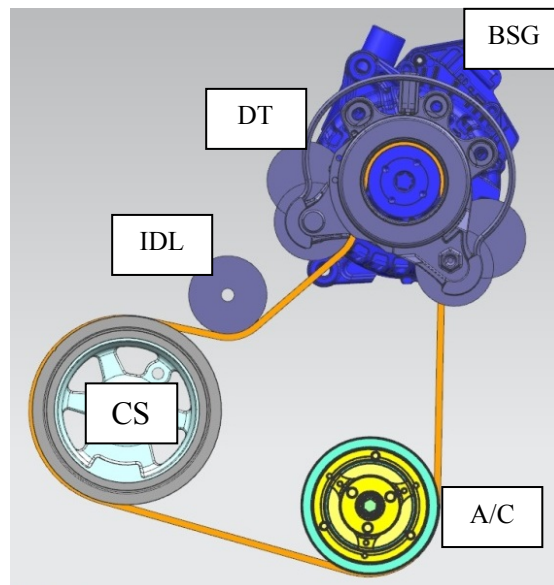


FIGURE 15-COUPLING BETWEEN BSG AND ENGINE

In the figure above it is possible to examine the complete coupling between the internal combustion engines (CS in the figure), the accessories as the A/C compressor (A/C) and the BSG. The system is driven almost exclusively by V-ribbed belts and the main differences with respect to the classical belt drive set is the use of a decoupling tensioner (DT) entailing the presence of a single idler pulley (IDL). Although the V-ribbed belt is vulnerable to power losses due to external friction (speed losses) and internal friction (torque losses) the efficiency of belt drive system is quite high [12].

Instead the decoupling tensioner automatically damps vibrations in the belt drive due to its design, when power is transferred between belt starter alternator and engine. Moreover it improves the working under transient and load conditions and its layout reduces the volume involved enhanced a simple packaging for its installation [13].



FIGURE 16-DECOUPLING TENSIONER

4.2.1. BSG functionalities

In this section the advantages due to the installation of a Belt Starter Generator are illustrated.

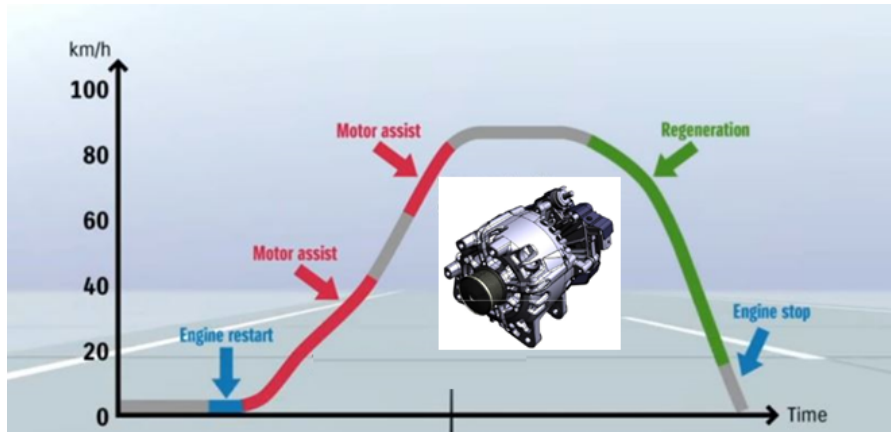


FIGURE 17-BSG MAIN FUNCTIONS

The most important functions are [14]:

- **Start&Stop (S&S):** One of the higher contribution in terms of fuel saving is the Start&Stop function. This strategy consists in switching off the ICE when it is not used to provide energy to the vehicle and turning on, quietly and quickly, in so far as possible, when the driver wants to move the vehicle. Different conditions have to be checked by the management system before enabling this strategy such as the SOC of the battery or the temperature of the exhaust after-treatment.
- **Electric power assist (EA):** With the electric power assisting the starter generator it provides an electric torque in order to reduce the load on the ICE and moreover to improve the throttle response during starting and acceleration conditions (E-Assist Mode). The instantaneous electric motor torque can enhance the vehicle drivability and its acceleration performance by reducing the slow dynamic of the ICE. The torque and the speed range for performing the E-Assist function are determined by the client requirements (figure below).

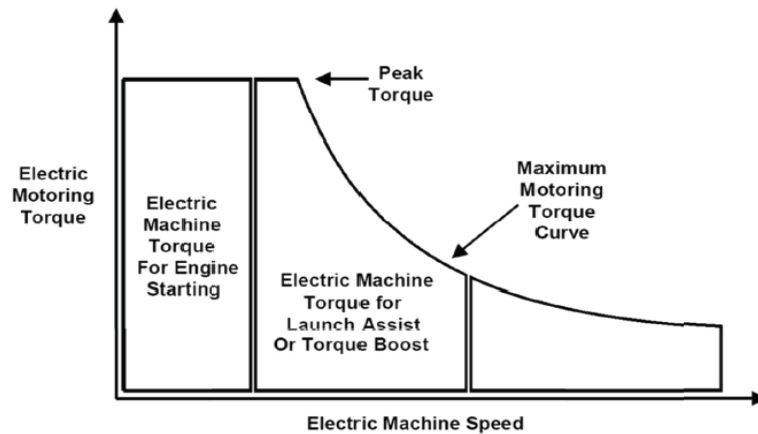


FIGURE 18-BSG MOTORING TORQUE [15]

- **Regenerative braking (RG):** The regenerative braking is another important function performed by the BSG. If the driver presses the brake pedal the kinetic energy will not be dissipated as heat in the friction brakes but it will be recovered by BSG system and stored in the battery as electric power. This energy could be used for the EA Mode or to feed the electric loads during idle stop. Obviously the management system must take into account the maximum battery power, and when the limit is achieved the kinetic energy will be lost in the friction brakes. The contribution in terms of FC and emissions reduction is given by the **cut-off** function which is on when the RG Mode is active: the fuel injection through the injector is disabled to obtain a saving of fuel consumption.

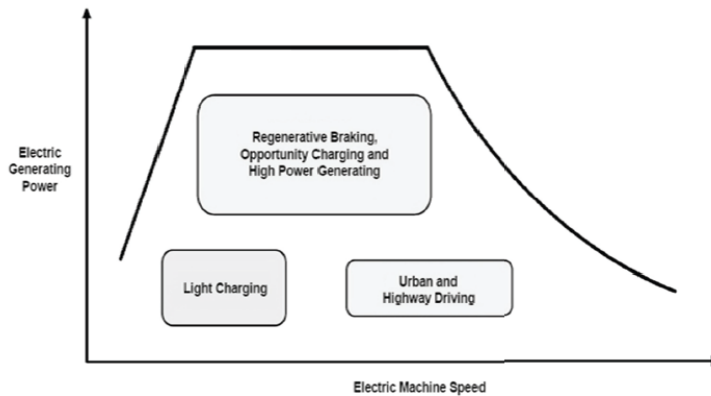


FIGURE 19-BSG GENERATING TORQUE

- **Secondary functions:** The BSG can improve the comfort and drivability of the vehicle for example smoothing the torque irregularities originated by the engine compression pulse especially during cranking.

Between the BSG and the Li-ion battery there is an **Inverter AC/DC**. This device converts the BSG alternate current (AC) to direct current (DC) that can be stocked in the Li-ion battery. It has a low weight and is linked to the belt starter generator.

4.3. Electromechanical Clutch

One of the most original device mounted in the FIAT Demo-Car is certainly the Electromechanical Clutch system called **E-Clutch**. The classic mechanical clutch has been replaced by a system more advanced that can provide several advantages. The electromechanical clutch brakes the mechanical connection between the clutch pedal and the clutch itself in the vehicles with manual transmission replacing the typical mechanical or hydraulic link. [16]

In the vehicles with the friction clutch operated by hydraulic link, the clutch pedal is connected to the master cylinder. The pedal force pressurizes a fluid in a slave cylinder

which is connected thanks to the release fork to the thrust bearing disengaging the clutch. In the mechanical link instead, the pedal is connected to the clutch by a cable. On a typical installation, one end of the cable is connected to the clutch pedal and a spring is attached to the pedal assembly (to return the clutch pedal on the rest position). The other end of the cable is connected to the clutch release fork. When the clutch pedal is depressed, the cable pulls the clutch fork, causing the release bearing to move forward against the pressure plate.

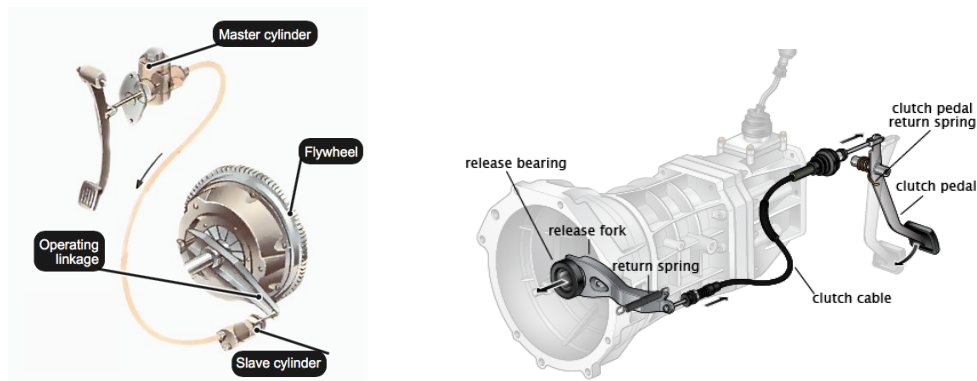


FIGURE 20-HYDRAULIC AND MECHANICAL LINK IN MANUAL TRANSMISSION

The electromechanical clutch system instead is based on a “by wire” technology (no hydraulic or mechanical connection). The classical clutch pedal presents in a manual transmission is replaced by a pedal sensor which consists in a clutch pedal and a force emulator. This one is connected to an electronic clutch control unit (CCU) which commands an electronic intelligent actuator. [17] The CCU input data are information from the vehicle control unit and from the driver intention (pedal position) and also supplementary values by on-board sensor like as transmission speed in a signal feedback loop. When the control unit acquires the data from the sensors it determines,

by predefined strategies, the target clutch torque which is transmitted thanks to an electric signal to the electronic actuator. The actuator unit usually is hydrostatic and it consists in an electric motor that sets the target clutch torque value using a spindle drive and it is transmitted to the clutch by a master cylinder and a slave cylinder. [18]

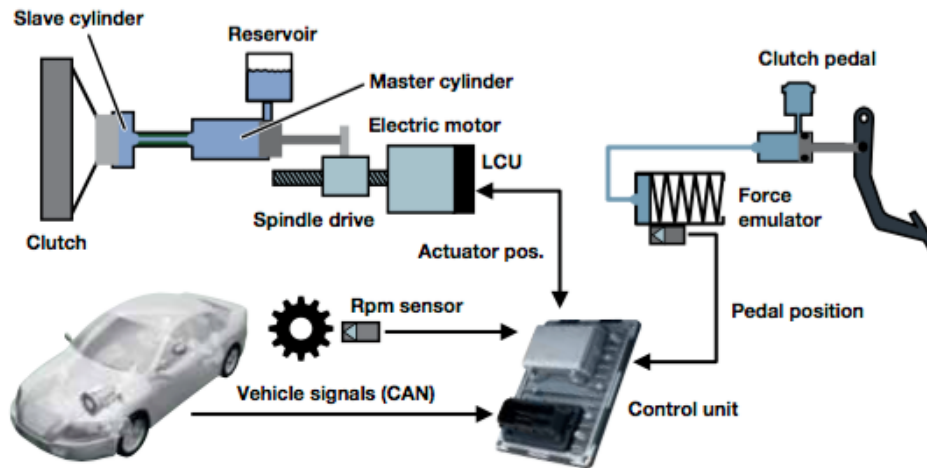


FIGURE 21-DESIGN AND COMPONENT OF THE ELECTROMECHANICAL CLUTCH SYSTEM

The main benefit of E-Clutch application is related to the presence of the control unit. The CCU using information such as the engine and transmission speed can adjust the clutch torque as a function of the pedal travel to best suit each and every driving condition. Moreover when it is required the system can correct driver inputs on the basis of the target clutch torque calculated by predefined strategies on CCU, for example when the system detects a wrong driver operation or a specific working condition such as the standing start.

If the driver inadvertently misuses the clutch or does not coordinate it properly with the gas pedal which can cause the engine to stall, the system is smart enough to override the driver commands. By keeping tabs on the vehicle speed and engine revolutions, the stop-and-go driving is simplified because the system eliminates the frequent use of the

clutch pedal (just as with an automatic transmission). The E-clutch ensures that the driver cannot forget to disengage the clutch when he changes gears: this means that the synchronizer does not have to be so robust, the transmission and axles do not need to be over-designed, which results in cost savings and reduces shift effort by improving acoustic driving comfort. The system can therefore take control at any time to increase driving comfort, safety and efficiency.

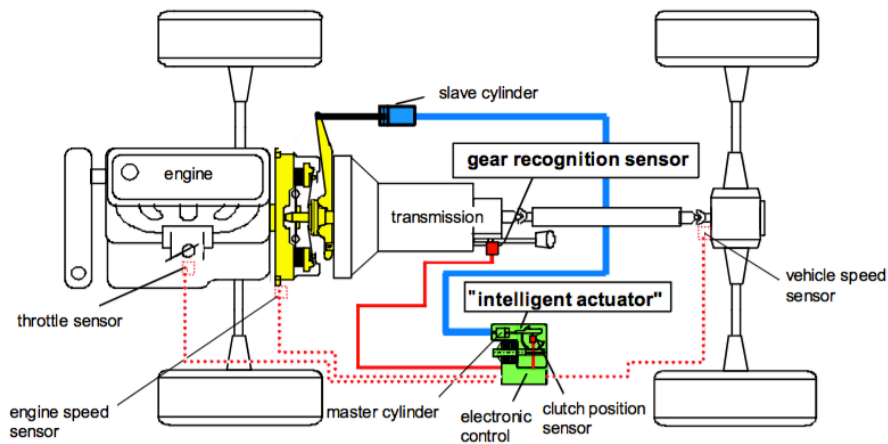


FIGURE 22-SYSTEM OVERVIEW OF A CLUTCH BY WIRE SYSTEM

The other benefits of electromechanical clutch assembly concern to the possibility to use a manual transmission in a hybrid powertrain. Up to now, it has only been possible to combine a hybrid powertrain with an automatic transmission, since it is not possible to match a combustion engine and an electrical powertrain using a manual transmission. With the new clutch technology is possible to use a classical manual gearbox mechanizing the clutch (the only automatic component) and adding only switches and actuators. This new system made up by a manual transmission and an automated clutch is cheaper of an automatic transmission. As a consequence hybrid vehicle price can

decrease by creating an attractive alternative in the passenger car segment, where price competition is quite difficult.

Furthermore in order to reduce fuel consumption and emissions, the E-Clutch enables the Start&Stop function, which shuts off the engine during longer stop phases. The engine starts again when the driver presses on the gas pedal or shifts into gear. In addition the **Idle Coasting** (IDLC) working is activated when the driver is not pressing down on the gas pedal (4.3.1). [19]

4.3.1. Idle Coasting

The Idle Coasting, also known as **sailing** or **coasting** in the simplest way, is an important function in the Demo-Car which allows a fuel consumption reduction around 1% during normal driving condition. In the last few years a lot of passenger cars with state-of-the-art automatic transmission could activate the coasting during their working. The advantage of the vehicle prototype under investigation is the possibility to active the Idle Coasting using a manual transmission thanks to the presence of E-Clutch.

Nowadays market all vehicle, in any segment and market, have available the Start-and-Stop system to avoid a wastefulness of fuel consumption when no propulsion is required. The cars technologically advanced moreover use the engine cut-off function for the same purpose: fuel injection is turned off as soon as the driver releases the gas pedal. During this working, the engine control unit supervises the mode operation to avoid the engine switching off and restoring the fuel injection if a minimum threshold of engine speed is reached. In spite of benefits in terms of emissions and fuel consumption, this system causes a significant loss of energy due to the friction and pump losses because the engine is still connected with the transmission and

consequently the ICE is driven by the vehicle. The friction losses rise if the engine speed rises so the amount of lost energy is high as much as the engine speed value is elevated [20]. In order to avoid the negative engine torque during an operation mode in which no propulsion is required, the engine can be decoupled by the drivetrain to operate such as freewheeling device.

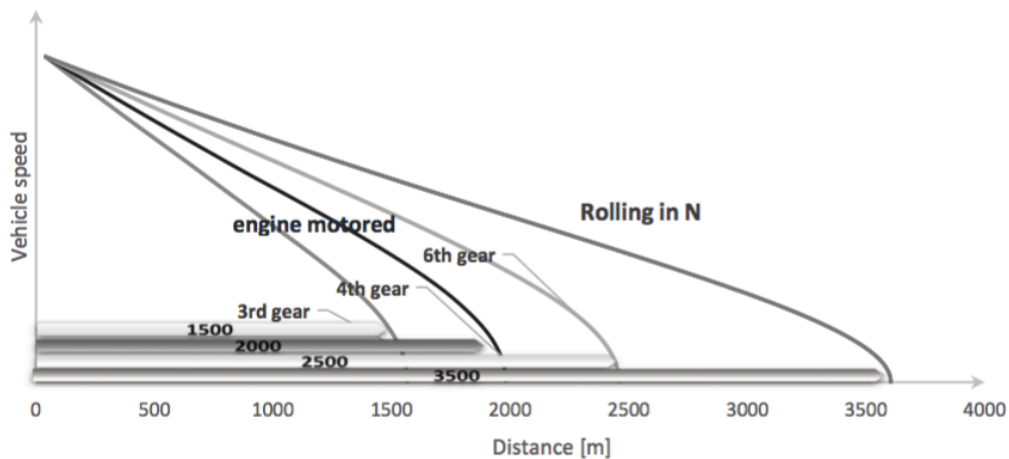


FIGURE 23-ROLLING DISTANCE WITH AND WITHOUT IDLE COASTING [21]

During the Idle Coasting mode the engine is no more linked with the transmission, it operates in idle speed by saving fuel and the kinetic energy of the vehicle is retained. The engine is not motored and the absence of the drag torque duplicates the rolling distance travelled by the vehicle when the driver releases the gas pedal obtaining an additional reduction of vehicle emissions. The engine would start again as soon as the clutch pedal or the brake pedal is depressed and the engine connected with the drivetrain again. [22] This new state of the powertrain provides different operation modes: normal driving, fuel cut-off or regenerative braking (thanks to the BSG) and Idle Coasting.

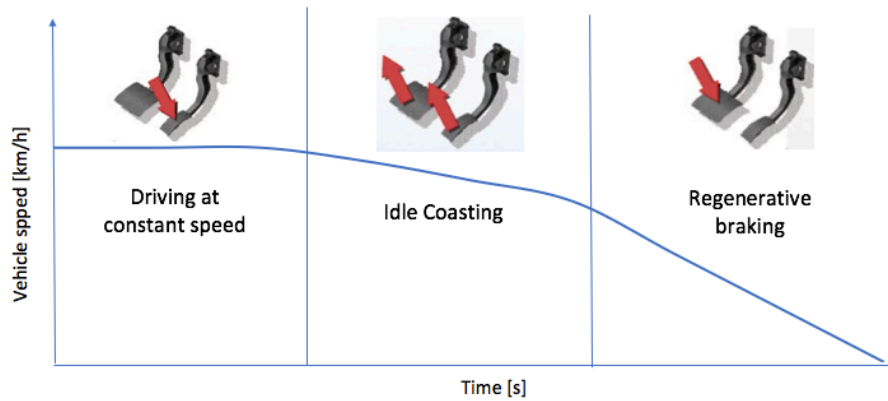


FIGURE 24-IDLE COASTING SUCH AS A TRANSITION MODE BETWEEN DRIVING AT CONSTANT SPEED AND BRAKING/RECUPERATION

Though the fuel economy potential of Idle Coasting depends strongly on driver behavior (i.e. dynamic or economic and predictive driver) and on the mission speed profile. Although its activation depends on few vehicle parameters, it is strongly conditioned by the gas and brake pedal position. Only if the driver releases these pedals, the Idle Coasting function is on. About the mission speed profile for example the NEDC does not have a correct speed profile to obtain the maximum benefit from the Idle Coasting because it consists of phases at constant speed and phases of braking. Limiting the sailing mode to the transients between these two phases, and making it dependent on the driver choice and its willingness to use the speed tolerance band in this situation the reduction of fuel consumption is quite low. Instead in a WLTC or during a real-world driving condition in which there are many phases with slightly decreasing vehicle speed, the best conditions for the Idle Coasting application are matched.

4.4. Li-ion Battery

The opportunity to recover the kinetic energy during the regenerative braking that can be progressively used during E-assist mode, requires a device in which the electric BSG

energy can be stocked. For this reason, in the Demo-Car has been installed a Li-ion rechargeable battery that allows the use of all the functions previously described.

The Li-ion battery uses a lithiated carbon intercalation material (Li_xC) for the negative electrode instead of metallic lithium, a lithiated transition metal intercalation oxide ($\text{Li}_{1-x}\text{M}_y\text{O}_z$) for the positive electrode and a liquid organic solution or a solid polymer for the electrolyte. Lithium ions swing through the electrolyte between the positive and negative electrodes during discharge and charge. During the discharge phase the lithium ions are released from the negative electrode, passed through the electrolyte, and are taken up by the positive electrode. Instead during the charge phase, the process is reversed.

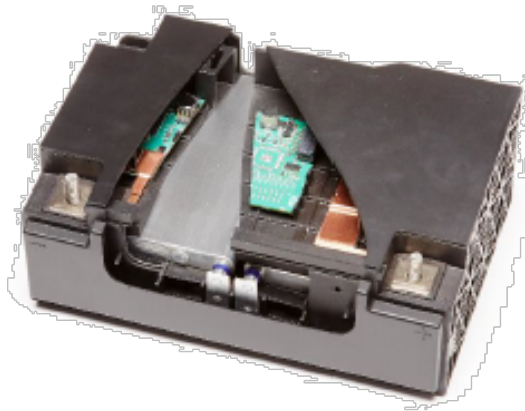


FIGURE 25-LI-ION BATTERY INSTALLED IN THE DEMO-CAR

Chapter 5

5. Vehicle model

The main purpose of this work is the creation of an hybrid vehicle simulation model for the calculus of fuel consumption and CO₂ emissions on the principal type approval driving cycles. The model reference vehicle is the FIAT Panda Demo-Car micro hybrid in which there are a Belt Starter Generator in P1f position and an electromechanical clutch: the BSG (and its coupling with the engine), Li-ion Battery and E-Clutch have been modelled. The final output is a model called **DemoBE** and the benefits due to the installation of the BSG and E-Clutch calculated on Matlab environment have been compared with the CRF experimental data later. In this section are presented the basic background knowledge used for the model creation. Firstly a basic driveline has been analysed and the power required by the vehicle (taking into account the resistance to motion), the vehicle translational inertial resistance and the inertial power of the main rotating components was obtained. Secondly, starting from the new devices modelling their inertia contribution and successively the engine final power have been obtained. The figure below shows the DemoBE complete driveline, in which the BSG (with inverter and Li-ion battery) and E-Clutch have been mounted.

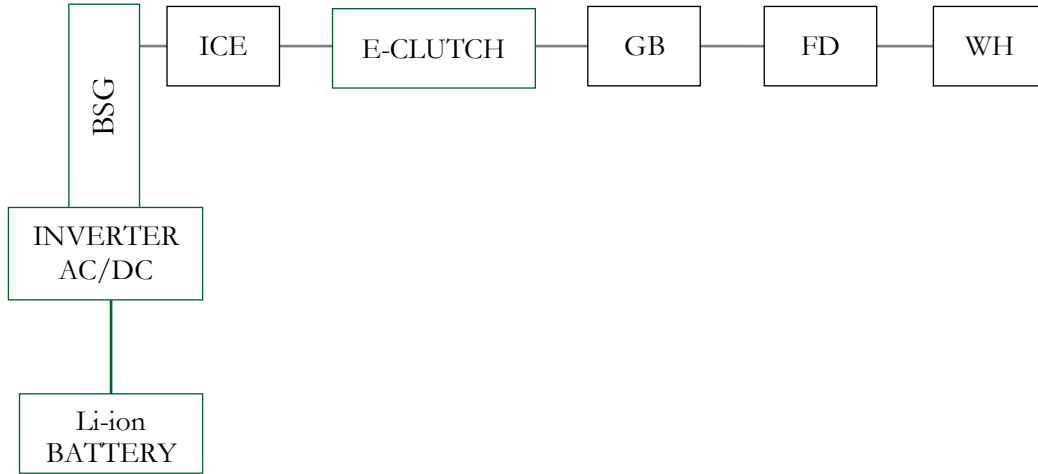


FIGURE 26-DEMOBE DRIVELINE

5.1. Driveline model

5.1.1. Resistance to motion

When the performance of a vehicle are computed in a longitudinal motion, the dynamics of a vehicle is obtained by neglecting the longitudinal slip of the wheels and supposing it as a point mass in the simplest way. [24]

In order to propel a vehicle at constant speed on a straight and level road, the vehicle should overcome different resistance forces such as aerodynamic drag resistance F_{aero} , rolling resistance F_r , grading resistance F_g and translational inertial resistance force F_{inert} .

The aerodynamic force in the x direction is proportional to air density, the air drag coefficient, the frontal area of the vehicle and the square of the vehicle speed:

$$F_{aero} = \frac{1}{2} \cdot \rho \cdot C_x \cdot A \cdot v^2 \quad (5.1)$$

With increasing the vehicle frontal area and the vehicle speed the aerodynamic drag resistance will increase.

Assuming that the rolling resistance f_r is the same for each wheels and it is not necessary taking into account the mass distribution the rolling resistance can be expressed as

$$F_r = f_r \cdot m \cdot g \cdot \cos \alpha \quad (5.2)$$

where m is the vehicle mass and α is the road angle from horizontal.

If the road is not level, the component of weight acting in a direction parallel to the velocity then the grade force due to the angle of the road is:

$$F_g = m \cdot g \cdot \sin \alpha \quad (5.3)$$

These forces are the road load and they represent the resistance to motion [25]:

$$R = F_{aero} + F_r + F_g \quad (5.4)$$

The vehicle translational inertial resistance force represents the resistance of the body to vary its kinematic state and it is related to the vehicle mass and the vehicle acceleration a :

$$F_{inert} = m \cdot a \quad (5.5)$$

The vehicle power demand taking into account only the forces just described is:

$$P_{veh} = (R + F_{inert}) \cdot v_v \quad (5.6)$$

5.1.2. Driveline components inertial power

However in a vehicle the rotating components such as motor, crankshaft, pulleys, axles and wheels have rotational inertia and consequently they affect also the vehicle performance analysis. [26] In this model only the components with high inertia are taken into account ignoring the small rotating components (bearings and little pulleys)

that instead provide a negligible contribution. The next equations evaluate the inertial power of the main rotating components which are present in the Demo-Car powertrain:

- **Wheel (WH)**
- **Final drive (FD)**
- **Gearbox (GB)**

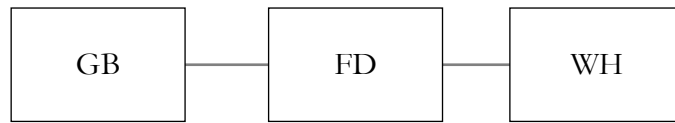


FIGURE 27-MAIN ROTATING COMPONENTS IN THE DRIVELINE

Starting from the vehicle speed and knowing the wheels radius R_{wh} , their angular velocity and angular acceleration are obtained:

$$\omega_{wh} = \frac{v_v}{R_{wh}} \quad \dot{\omega}_{wh} = \frac{\dot{v}_v}{R_{wh}} \quad (5.7)$$

and the wheels inertial power also:

$$P_{wh,inertia} = J_{wh} \cdot \dot{\omega}_{wh} \cdot \omega_{wh} \quad (5.8)$$

Where J_{wh} is the wheels inertia and η_{wh} is the tyre efficiency.

The new vehicle power demand will be:

$$P_{DRV,WH} = (P_{veh} + P_{wh,inertia}) \cdot \eta_{wh}^k \quad (5.9)$$

the coefficient k is equal to 1 if the vehicle is braking, equal to -1 otherwise for a correct analysis of braking and torque mode.

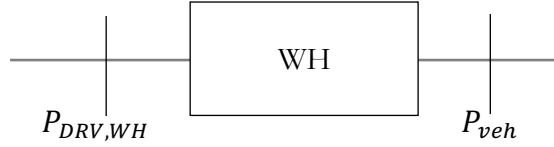


FIGURE 28-WHEELS INERTIAL POWER

Despite the final drive is a little component, its inertia contribution J_{fd} is taken into account obtaining the final drive inertial power P_{fd} . Its angular velocity and acceleration have been obtained from the wheels values previously calculated and using the final drive ratio τ_{FD} :

$$\omega_{fd} = \omega_{wh} \cdot \tau_{fd} \quad \dot{\omega}_{fd} = \omega_{wh} \cdot \tau_{fd} \quad (5.10)$$

$$P_{fd,inertia} = J_{fd} \cdot \dot{\omega}_{fd} \cdot \omega_{fd} \quad (5.11)$$

$$P_{DRV,FD} = (P_{DRV,WH} + P_{fd,inertia}) \cdot \eta_{fd}^k \quad (5.12)$$

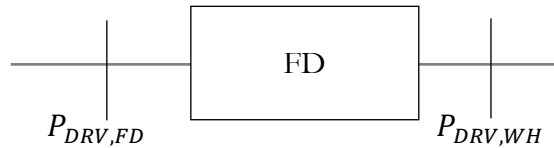


FIGURE 29-FINAL DRIVE INERTIAL POWER

The gearbox inertial contribution has been obtained with the same procedure. However in this case the ratio values τ_{gear} and efficiency values η_{gb} depend on the gear engaged in each time instant.

$$\omega_{gb} = \omega_{fd} \cdot \tau_{gear} \quad \dot{\omega}_{gb} = \omega_{fd} \cdot \tau_{gear} \quad (5.13)$$

$$P_{gb,inertia} = J_{gb} \cdot \dot{\omega}_{gb} \cdot \omega_{gb} \quad (5.14)$$

Therefore the final power required by the vehicle taking into account the main rotating powertrain components is:

$$P_{DRV,GB} = (P_{DRV,FD} + P_{gb,inertia}) \cdot \eta_{gb}^k \quad (5.15)$$

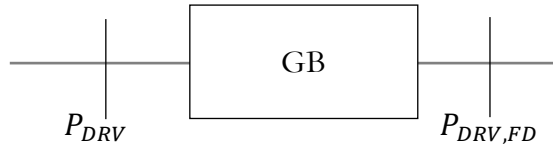


FIGURE 30-GEARBOX INERTIAL POWER

5.2. E-Clutch model

As explained in the section 4.3 the innovation of an electromechanical clutch is in terms of electronics is related to the presence of a dedicated control unit. Conversely in relation to the coupling with the engine no differences are presented with respect to a conventional clutch. Because the model takes into account the components inertia and the coupling between themselves, the only difference is the E-Clutch inertia. The clutch is a rotating component and therefore its inertia $J_{e-clutch}$ causes an inertial power that will be added to the driveline power previously calculated. Supposing that the E-clutch coupling does not reduce the gearbox speed, its angular speed $\omega_{e-clutch}$ and its angular acceleration $\dot{\omega}_{e-clutch}$ are the same of those calculated for the gearbox:

$$\omega_{e-clutch} = \omega_{gb} \quad \dot{\omega}_{e-clutch} = \dot{\omega}_{gb} \quad (5.16)$$

Therefore the E-Clutch power inertia is:

$$P_{ECL,inertia} = J_{e-clutch} \cdot \dot{\omega}_{e-clutch} \cdot \omega_{e-clutch} \quad (5.17)$$

5.3. Engine model

The engine installed in the FIAT Panda Demo-car is a 1 L gasoline engine.

The confidentiality agreements with the CRF do not allow further complementary information for a correct description. To obtain the final power supply by the engine, the inertia power of its components must be also added to the power required by the driveline (5.15). The procedure is the same of the previous components: starting from the E-Clutch angular velocity the engine angular velocity has been obtained ω_{ICE} (verifying that each values over the cycle is higher than the engine idle speed $\omega_{ICE,idle}$):

$$\omega_{ice} = \max (\omega_{ice,idle} , \omega_{e-clutch}) \quad (5.18)$$

and using the engine inertia value J_{ICE} the inertial power is defined as:

$$P_{ICE,inertia} = J_{ice} \cdot \dot{\omega}_{ice} \cdot \omega_{ice} \quad (5.19)$$

Taking into account the accessories power demand P_{ACC} , the vehicle power required to follow the mission speed profile and therefore the power supply by the engine is defined as follow:

$$P_{ICE} = P_{DRV,GB} + P_{ECL,inertia} + P_{ICE,inertia} + P_{ACC} \quad (5.20)$$

This power is not the final power because the Belt Starter Generator installation implicates an increase or a reduction of the power supply by the engine in function of the BSG working (RG or EA).

5.4. BSG model

In the DemoBE model, the power supply by the engine is not equal to the power required by the driveline, because the BSG during the standard working condition and Regenerative Braking is a load for the engine (supposing that during the RG mode load does not increase). Instead during the E-Assist the BSG helps the engine by reducing the power generated. Therefore the power supply by the engine depends on the BSG working (RG or EA). The engine final power P_{DemoBE} changes and two different conditions can be analysed:

$$P_{DemoBE} = \begin{cases} P_{ICE} + P_{BSG,inertia} & (5.21) \\ P_{ICE} - P_{EA,pwr} & (5.22) \end{cases}$$

The value of the BSG inertial power $P_{BSG,inertia}$ has been calculated by taking into account its inertia J_{BSG} and its angular velocity and acceleration. The aforementioned depend on the coupling transmission ratio BSG-ICE τ_{BSG} :

$$\omega_{BSG} = \omega_{ice} \cdot \tau_{BSG} \quad \dot{\omega}_{BSG} = \omega_{ice} \cdot \tau_{BSG} \quad (5.23)$$

$$P_{BSG,inertia} = J_{BSG} \cdot \dot{\omega}_{BSG} \cdot \omega_{BSG} \quad (5.24)$$

Moreover the BSG model simulates the power conversion from the electric to the mechanical form, and vice versa, analysing the energy losses in the BSG itself and in the inverter. About the first, they are calculated by means of efficiency map which is function of the machine mechanical torque and its speed.

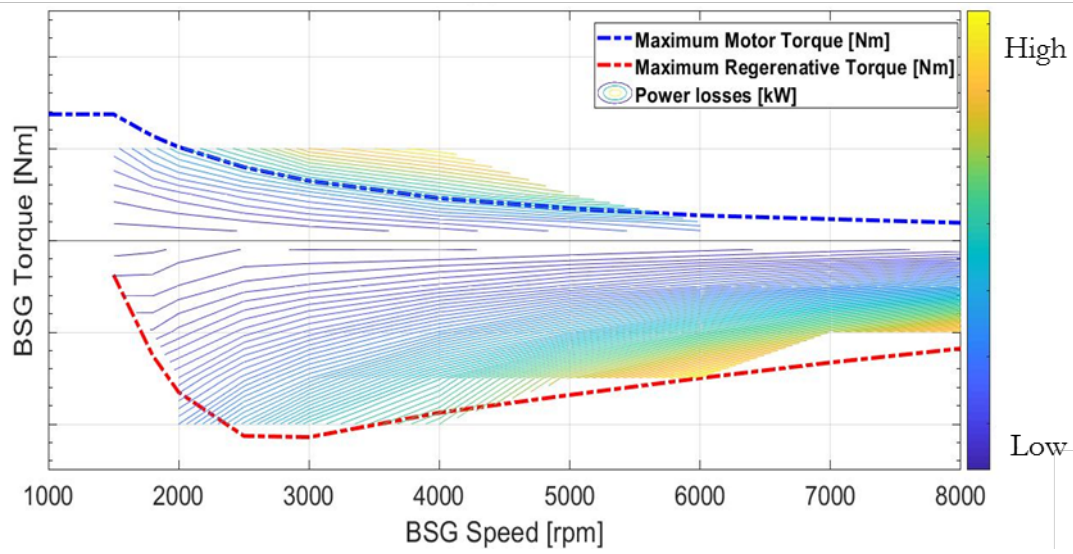


FIGURE 31-BSG EFFICIENCY MAP

Using this map it is possible to obtain the electric power after the BSG which flows towards the inverter.

Starting from the mechanical power elaborated by the BSG during the RG and EA mode, through an interpolation in the efficiency map it is possible to obtain the machine power losses. The values of BSG mechanical torque during the two working conditions were obtained by a map provided by the manufacturer: for different engine angular velocity range a value of mechanical torque is defined:

$$P_{RG,torque} = map_{manufacturer}(\omega_{ice}) \quad (5.25)$$

$$P_{EA,torque} = map_{manufacturer}(\omega_{ice}) \quad (5.26)$$

$$P_{RG,losses} = map_{BSG}(P_{RG,torque}, n_{BSG}) \quad \text{with } P_{RG,mech} < 0 \quad (5.27)$$

$$P_{EA,losses} = map_{BSG}(P_{EA,torque}, n_{BSG}) \quad \text{with } P_{EA,mech} > 0 \quad (5.28)$$

The electric power depends on the power losses inside the electric machine but above all its important the power flow analysis. Indeed the power losses in function of the

BSG working mode will be summed or subtracted. The figures below show the idea just described.

In the RG mode the power flow entails the subtraction of the power losses and the mechanical power to obtain the electric power that will be stocked in the battery:

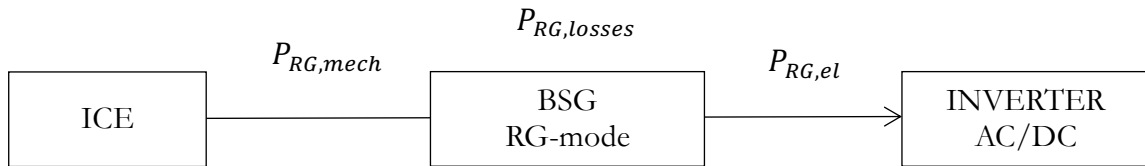


FIGURE 32-POWER FLOW IN RG-MODE

$$P_{RG,el} = P_{RG,pwr} - P_{RG,losses} \quad (5.29)$$

Instead in EA mode because the power flow is in the opposite direction the electric power that comes out from the battery is:

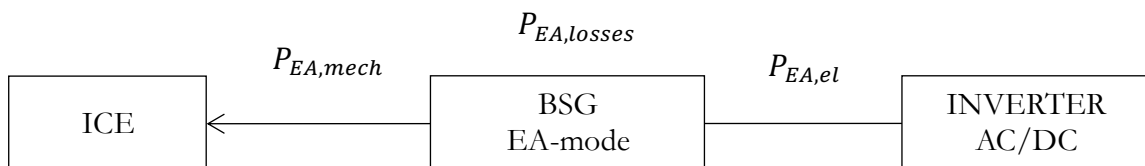


FIGURE 33-POWER FLOW IN EA-MODE

$$P_{EA,el} = P_{EA,pwr} + P_{EA,losses} \quad (5.30)$$

5.5. Battery model

The battery was modelled through an equivalent resistance circuit. [27]

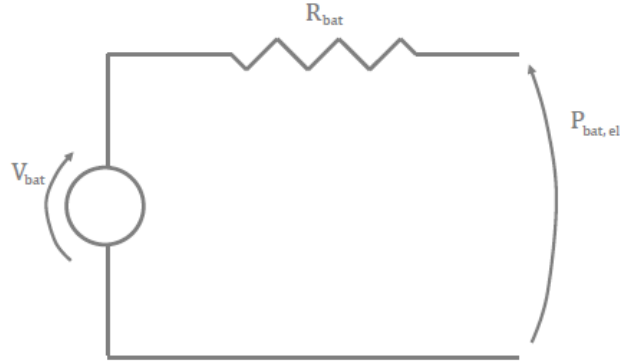


FIGURE 34-BATTERY EQUIVALENT RESISTANCE CIRCUIT

Also in this event, the battery power $P_{bat,el}$ depends on the BSG working condition:

$$P_{bat,el} = \begin{cases} P_{RG,el} \cdot \eta_{INV} & (5.31) \\ \frac{P_{EA,el}}{\eta_{INV}} & (5.32) \end{cases}$$

where η_{INV} is the efficiency inverter.

The equivalent resistance circuit modelling implies a relation between the internal resistance and the open-circuit voltage (OCV) with the battery State Of Charge.

The first two values were derived by interpolating the corresponding 1D maps, as functions of the battery SOC.

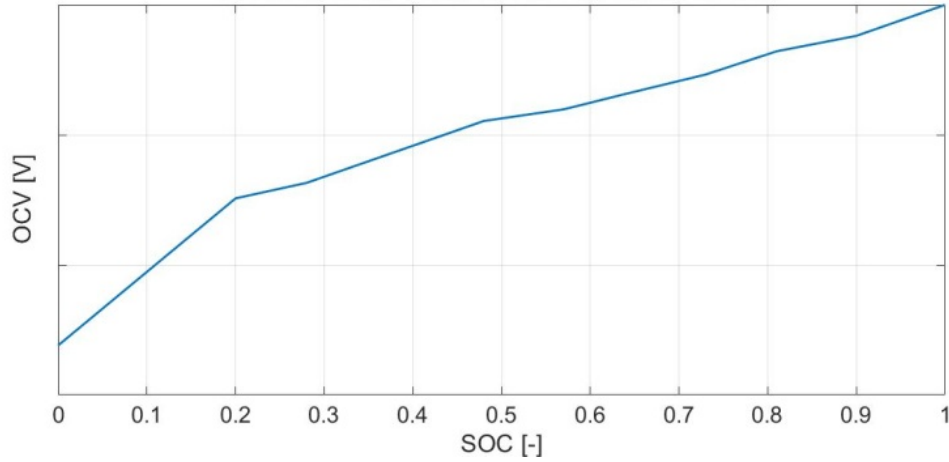


FIGURE 35-OCV VERSUS SOC

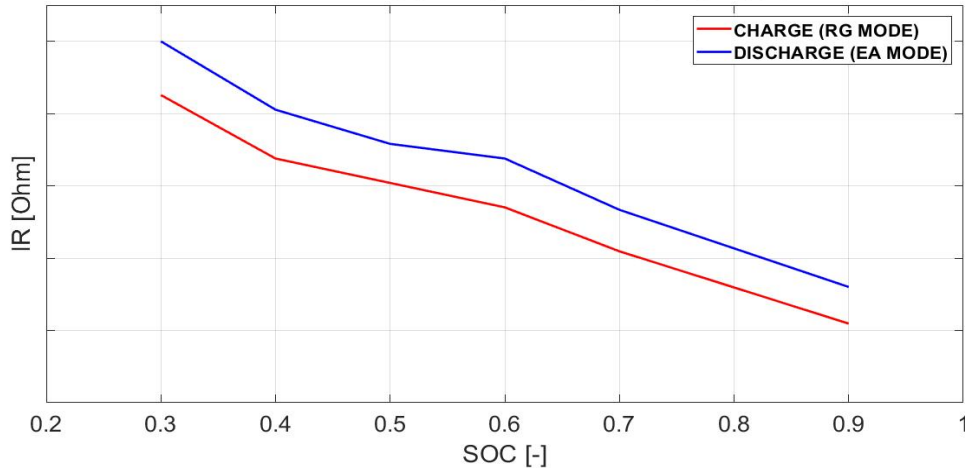


FIGURE 36-INTERNAL RESISTANCE VERSUS SOC

After the power check about the capacity of the battery to supply the energy demand and therefore the SOC value control in the previous time instant, the battery current I_{bat} is required to be obtained:

$$I_{bat} = \frac{V_{bat} - \sqrt{V_{bat}^2 - 4 \cdot R_{bat} \cdot P_{bat,elt}}}{2 \cdot R_{bat}} \quad (5.33)$$

Secondly the battery current value during RG mode and EA mode has been verified. About the Regenerative Braking working condition the map below was used. The figure

shows as the max battery current (BC) values are limited by the BSG speed and the gear ratio.

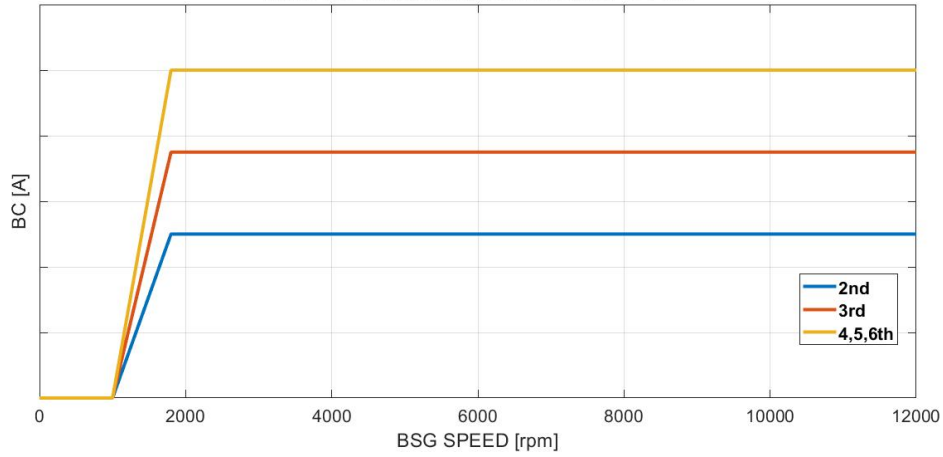


FIGURE 37-BATTERY CURRENT LIMITATIONS

For the E-Assist mode indeed, the maximum value was provided by the battery manufacturer.

The battery temperature was assumed to be constant and the temperature effect was therefore ignored.

5.6. Vehicle performances and emissions

The engine performance and the evaluation of the fuel mass flow rate have been evaluated by interpolating the fuel consumption map, which is function of the engine Brake Mean Effective Pressure (BMEP) and speed n [rpm] as follow:

$$\dot{m}_{fc} = \text{map}_{fc}(BMEP_{ICE}, n_{ICE}) \quad (5.34)$$

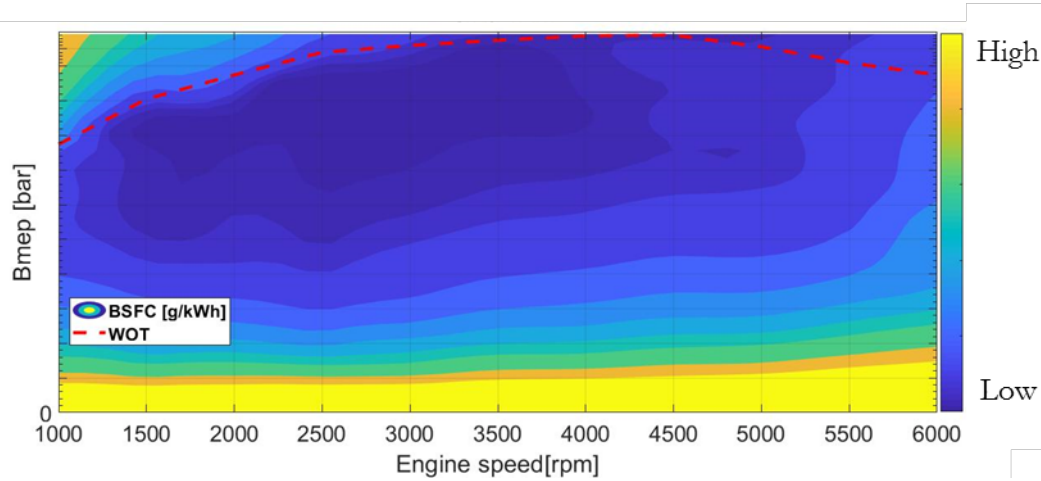


FIGURE 38-BSFC MAP

This map definition implied the calculus of the BMEP starting from the power supply by the engine P_{DemoBE} which depends on the BSG working condition:

$$BMEP[bar] = \frac{1200 \cdot P_{DemoBE}[kW]}{rpm \cdot V[dm^3]} \quad (5.35)$$

Where V is the overall engine displacement.

From the values obtained through the interpolation in the fuel consumption map the corresponding CO₂ emissions are linearly determined:

$$m_{CO_2} \left[\frac{g}{km} \right] = \frac{\rho_f [kg/dm^3]}{0.0315} \cdot L \left[\frac{l}{100km} \right] \quad (5.36)$$

where ρ_f is the fuel density and L is the fuel consumption in litres per 100 km obtained through the integration over the cycle of the fuel mass flow rate. The coefficient 0.0315 takes into account the correlation between the CO₂ and fuel molecular weights and appropriate conversion values.

Chapter 6

6. Strategy

The model creation and the identification of the correct equations is certainly the base for simulating a vehicle with the same architecture of the FIAT Panda Demo-Car. However, the presence of BSG and E-Clutch require the individuation of a correct strategy for the proper activation of their functions over the cycle. The strategy in a real vehicle is written in the vehicle control unit (VCU) and, thanks to the communication with the electronic components of each devices, allows the launch of the different vehicle functionality during the motion. For this project it was not possible to access to the Panda VCU and for this reason a new way to identify the strategy has been individuated. An Analyzer Tool has been created for the analysis and the manipulation of the VCU signals. The data have been loaded in Matlab environment which gave the opportunity to resample the signals and to plot. These steps were fundamental for the individuation of the rules. In the next section—the Tool presentation, the BSG and E-Clutch flow chart strategies and the procedure for the individuation are presented.. The strategies defined **are completely independent by the type-approval cycle**, for this reason they will be applied without no change to the NEDC and to the WLTC.

6.1. Data pre-processing

6.1.1. Chassis dynamometer emission testing

The vehicle test chassis dynamometer is used to simulate different road load models required for exhaust emission tests on vehicles. The laboratory can test any legislative

regulations or customized test cycles and it is equipped with latest emission systems and software (general test cell equipment).

The test is carried out on a chassis dynamometer in a specially designed testing facility. At least two of the wheels of the vehicle are spinning during the test, but the vehicle itself remains stationary. The driving resistances (vehicle inertia, rolling resistance, aerodynamic resistance) are previously determined in a separate test (the road load test) and are then simulated in the laboratory by adjusting the resistance of the chassis dynamometer. [28]

The vehicle laboratory testing is artificial and not fully representative of real-world driving, which often results in unrealistically low emission levels. In an attempt to overcome this shortcoming, a series of laboratory tests under different conditions can be carried out for one vehicle in order to better represent the full range of real-world driving situations.

After a test on the chassis dynamometer two different kinds of data are obtained:

- **Emission data:** The exhaust of the vehicle such as regulated emissions (HC, NH₃, CO, NO, O₂, and PM) and GHG emissions (CO₂, N₂O and CH₄) are collected and analysed on the laboratory to calculate emission levels and fuel consumption over the entire test cycle. The vehicle exhaust will be conducted to the exhaust dilution tunnel where the gaseous emissions of carbon monoxide, oxides of nitrogen (both nitric oxide and nitrogen dioxide) and carbon dioxide will be analysed as an integrated bag sample. Particulate matter instead will be measured gravimetrically thanks to the dedicated emission equipment using fluorocarbon coated glass fibre filters by weighing the filters before and after testing.

- **Vehicle Control Unit signal:** During the test on the chassis dynamometer the engine and main vehicle activities are saved by the Engine Control Unit (ECU) and they can be analysed later through computer programs. However in reference to FIAT Panda Demo-Car, the presence of the BSG and E-Clutch implicate the installation of two other control units respectively: BSG control unit (BCU) and E-Clutch control unit. These three controllers moreover can communicate each other through a BUS CAN.

6.1.2. Vehicle testing Analyzer Tool

The possibility to have complete access to the data saved during a chassis dynamometer test carried out by the Demo-Car, involved the creation of a Matlab vehicle testing Analyzer Tool for the analysis and saving of the data and signal obtained during a test.

The emission data usually are saved automatically by the laboratory software on an Excel file. The CRF chassis dynamometer laboratory after a test provides the measure of **259** emission data with values for each time instant. Instead the VCU signals total number, taking into account the engine, BSG and E-clutch control unit is around **575**.

The necessity to have a device which enables **quickly and easily** the investigation and the saving of the main data has required the creation of the Analyzer Tool.

This analyzer is **interactive so** that the user have three different choice levels:

- **Possibility to choose how many tests to analyse and therefore the test numbers to compare:**

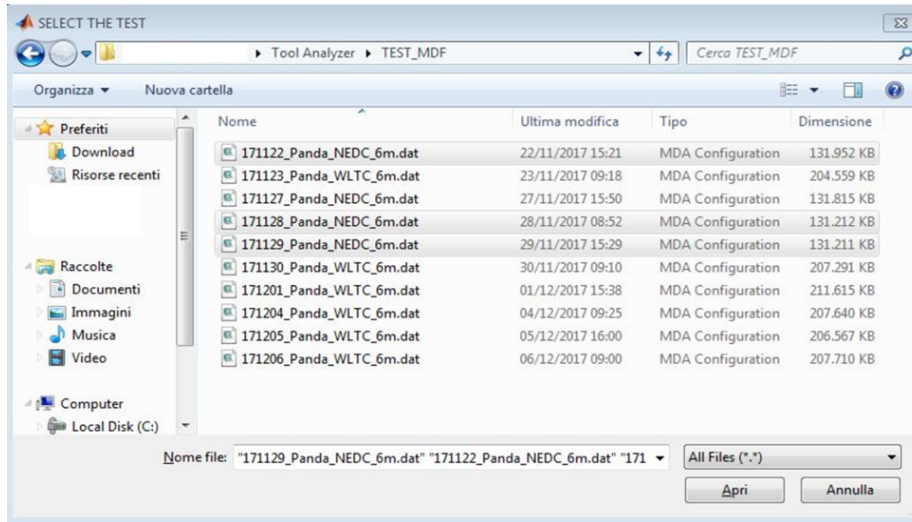


FIGURE 39-MATLAB DIALOG BOX FOR THE CHOICE OF TESTS

- Possibility to choose what kind and how many polluting substances to analyse:

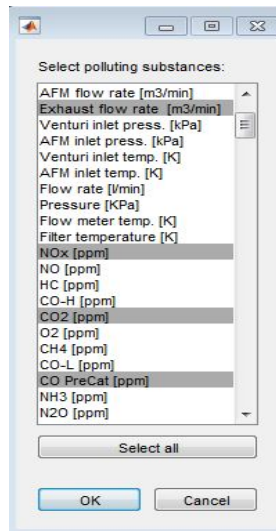


FIGURE 40-MATLAB DIALOG BOX FOR THE CHOICE OF POLLUTING SUBSTANCES

The final values of the main emissions are reported automatically. In this window it is possible choose the variables for which will be calculated the cumulative values and their trend in function of time will be plotted.

- **Possibility to choose what kind and how many Vehicle Control Unit signals to analyse:**

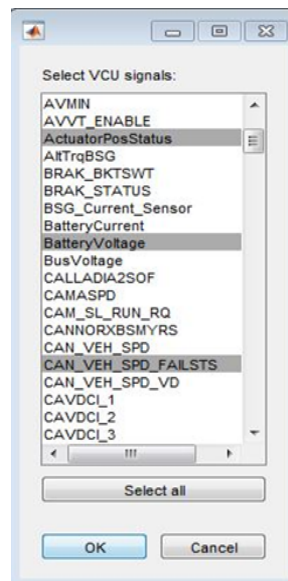


FIGURE 41-MATLAB DIALOG BOX FOR THE CHOICE OF VCU SIGNALS

The calculus for the most important electric are reported automatically for each test. In this window it is possible to choose the variables that will be plotted in function of time.

- **Automatic creation of a visual comparison between different tests results and saving of the trend and of the main values calculated on a Excel file for the comparison.**

This possibility for the VCU signals implicates the automatic resampling to the vehicle velocity time acquisition for each signal (usually 12 ms).

The Analyzer utility was fundamental for the saving and sampling of different tests and for the creation of the model strategy. Indeed the strategy rules for the activation of BSG and E-Clutch functions have been obtained after the signals manipulation through the Analyzer.

6.2. BSG function

6.2.1. Enhanced Start & Stop

The first function for the reduction of the fuel consumption by means of the use of the BSG is the Enhanced Start&Stop (ENHSS). In this specific case no VCU signal have been analysed but the activation rules were provided by the manufacturer. The Enhanced S&S with respect to the conventional, turns off the engine when the vehicle velocity is lower than 12 km/h. The classic S&S instead is active for speed lower the 3 km/h. The figure below shows the flow chart for the Enhanced Start & Stop activation.

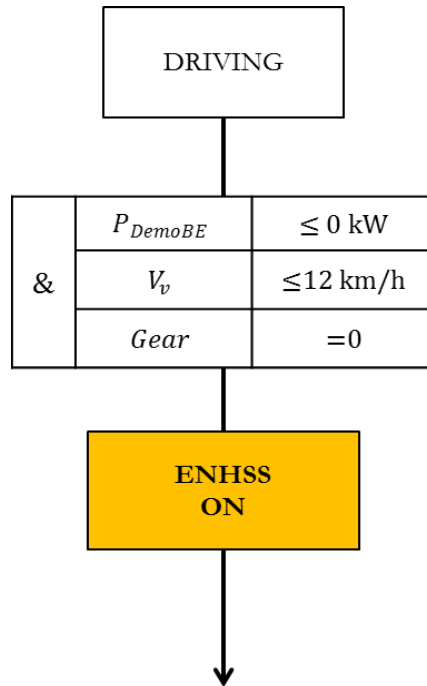


FIGURE 42-ENHANCED START & STOP STRATEGY FLOW CHART

6.2.2. Regenerative Braking

The starting point for the regenerative braking function has been the MM_STATE signal of the BCU that described the BSG state during the working condition. Thanks to the Analyzer, after a resampling it was plotted with the vehicle velocity trend in function of time.

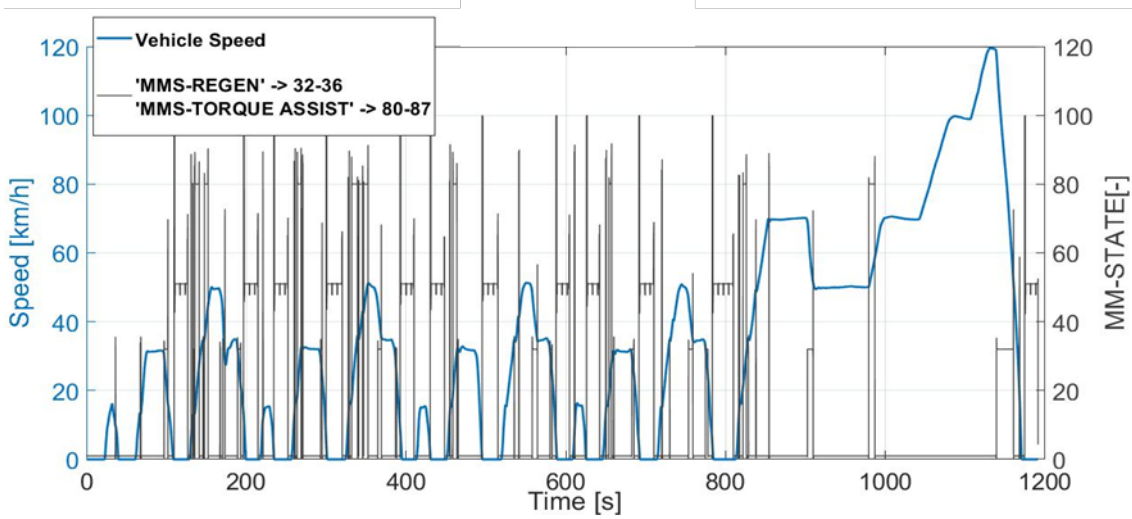


FIGURE 43-BSG MM_STATE SIGNAL

As shown in the legend, the BSG state depends on the MM_STATE value in a specific time instant. If the value is included between 32 and 36, the BSG is in Regenerative Braking Mode, instead if it is higher than 80 and lower than 87, the working condition is E-Assist. Isolating the RG Mode, the moments in which the BSG working as generator are identified:

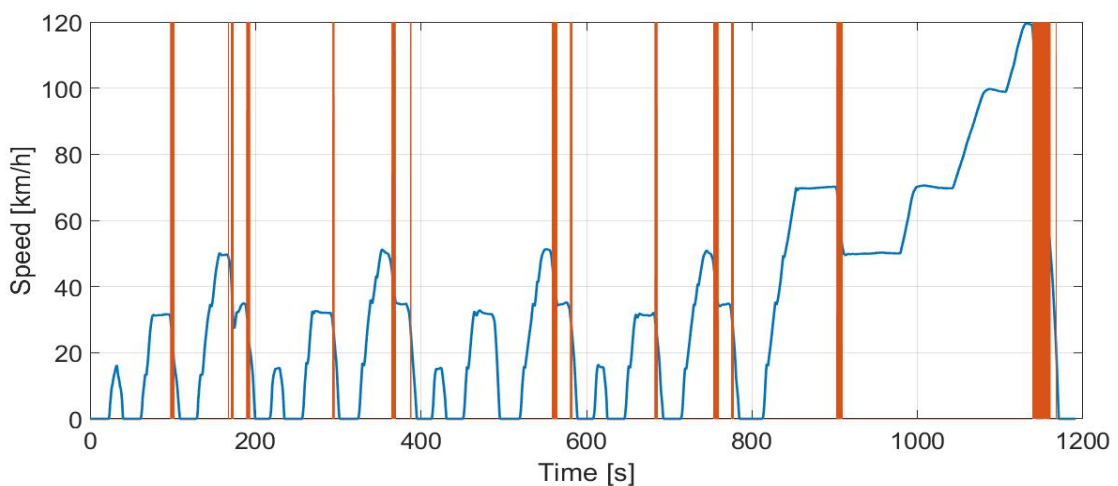


FIGURE 44-BSG MM_STATE SIGNAL-RG MODE

Thanks to the figure above the first rules for the activation have been individuated: velocity decreases, the driver is braking and therefore the power supply by the engine in the kinematic model is minor or equal to zero; the velocity is higher than a threshold value of 25 km/h; the gear engaged must be at least the first.

&	P_{DemoBE}	≤ 0 kW
	V_v	≥ 25 km/h
	$Gear$	≥ 1

TABLE 6-RG MODE STRATEGY RULES A

Secondly an engine speed threshold value $nrpm_{ICE,th}$ was identified by means of a signals plotting. As you can see in the figure below it is possible to identify a minimum value for the engine speed below which the RG mode turns off.

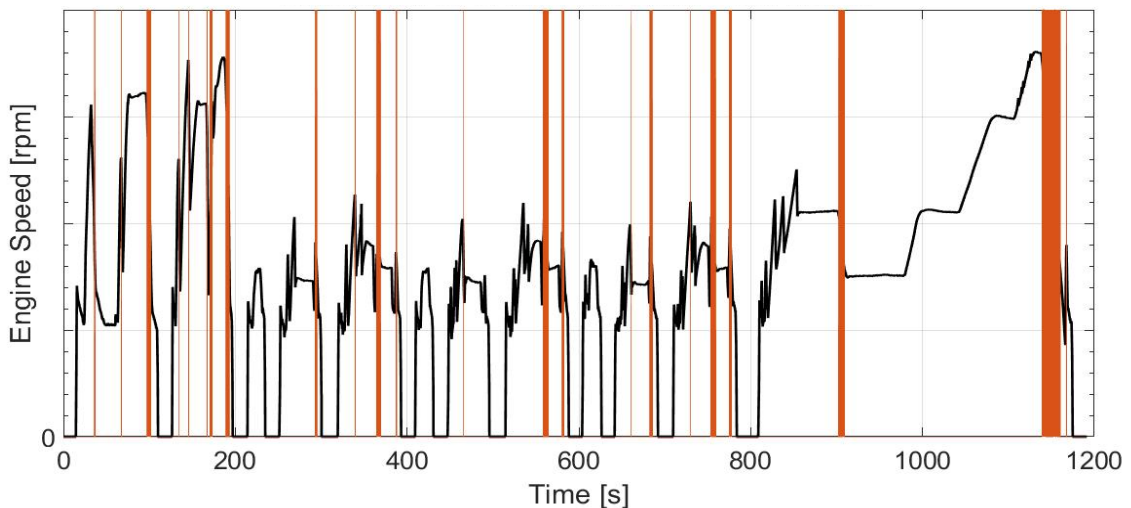


FIGURE 45-ENGINE SPEED AND MM_STATE-RG MODE

&	$nrpm_{ICE}$	$\geq nrpm_{ICE,th}$
---	--------------	----------------------

TABLE 7-RG MODE STRATEGY RULES B

The partial strategy flow chart will be:

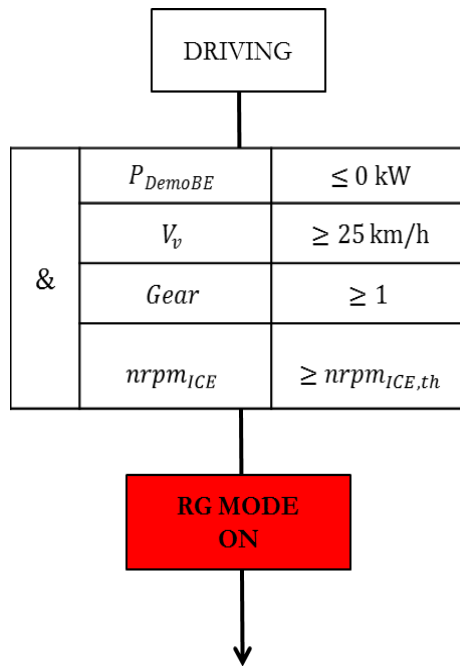


FIGURE 46-REGENERATIVE BRAKING PARTIAL STRATEGY FLOW CHART

The rules until now described are based on vehicle and engine parameters for the activation of RG Mode. However the possibility to stock electric power to the battery depends on its State Of Charge and on the amount of energy that it can be store even. For this reason it is necessary to introduce a State Of Charge check for the evaluation of the SOC instantaneous level and the calculus of storable electric energy. The final flow chart will be:

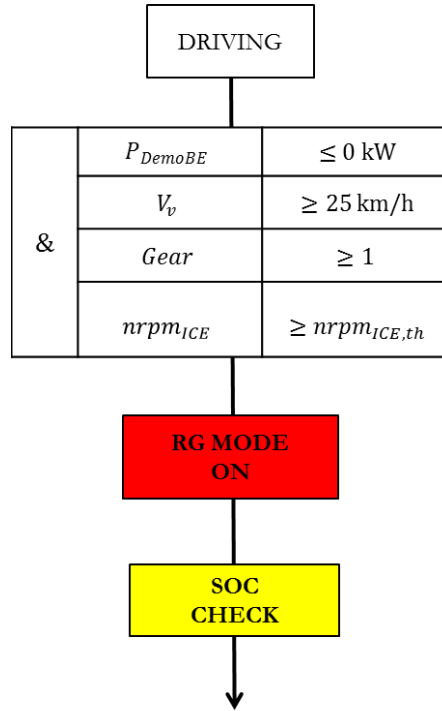


FIGURE 47-REGENERATIVE BRAKING STRATEGY FLOW CHART

The idea behind the SOC check level and the respective energy flow is based on the BSG and Li-ion Battery models described in the previous chapter. Indeed starting from the BSG mechanical torque during the RG mode and taking into account the electric motor's power losses and the efficiencies respectively of BSG η_{BSG} and of inverter η_{INV} , it is possible find out the amount of energy in terms of SOC that shall be stored into the battery $SOC_{RG,i}$ and therefore verify that the new level SOC is lower than the maximum. After the individuation of a possible time instant in which the RG Mode shall be active the BSG mechanical torque value is determined $P_{RG,mech}$. Secondly by means of an interpolation on the 2D BSG map the power losses are obtained a therefore the electric power before the invert $P_{RG,el}$. Taking into account the inverter efficiency the new power value is identified (5.29) and it is possible use the battery maps for the resistance and for the OCV to obtain firstly the battery current $I_{batt,i}$ (5.31) and the

$SOC_{RG,i}$ value later. If this value is lower than the difference between the maximum level SOC and the SOC level in the previous instant, the Regenerative Braking can be activated actually and the State Of Charge will be updated. Instead if the condition is false, the RG Mode will be off.

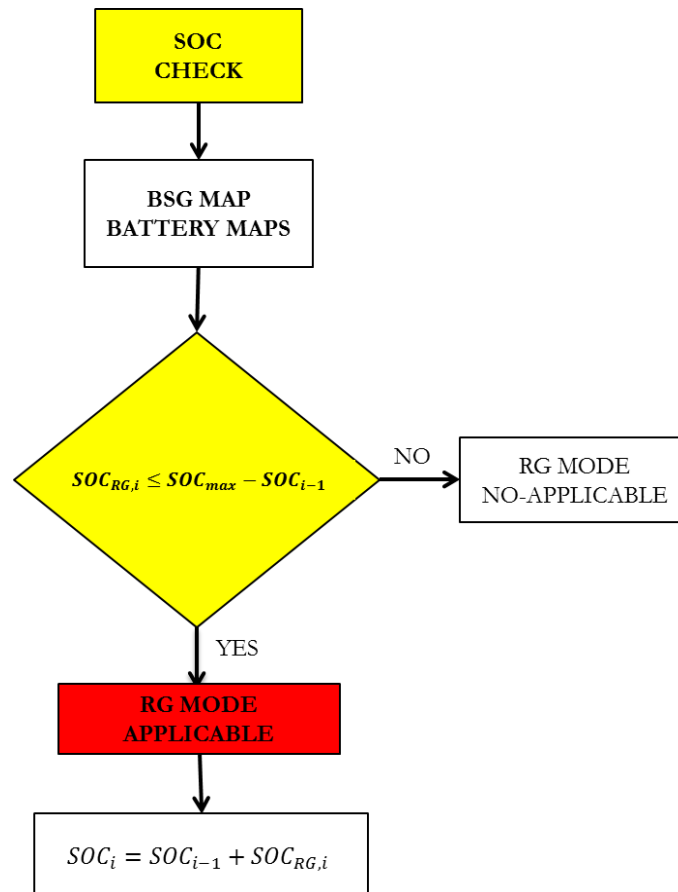


FIGURE 48-REGENERATIVE BRAKING SOC CHECK

6.2.3. E-Assist

For the EA Mode the procedure is quite similar to that previous described for the Regenerative Braking. Starting from MM_STATE signal of the BCU and isolating the

values included between 80 and 87, the time instants in which the EA Mode is active have been identified.

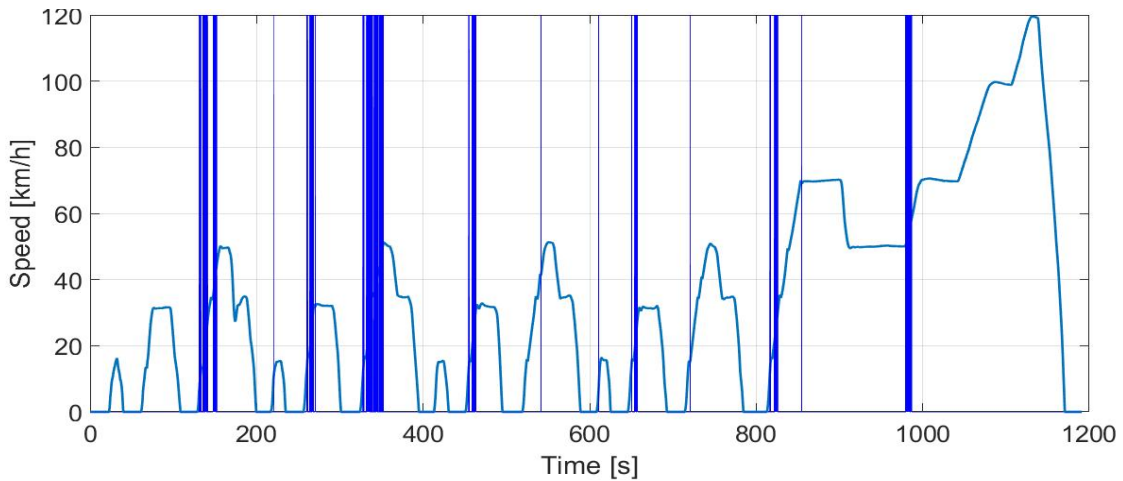


FIGURE 49-BSG MM_STATE SIGNAL-EA MODE

By means of the figure above three rules have been achieved:

&	P_{DemoBE}	> 0 kW
	V_v	>0 km/h
	$Time$	≥ 120 s

TABLE 8-EA MODE STRATEGY RULES A

The last rule presents in the table is implemented to obtain the time interval in which the three-way catalyst (TWC) reaches the light-off temperature and therefore an efficiency of 50% for the NO_x reduction, HC and CO oxidation. Even if a warm cycle is simulated (please refer the next chapter), this time interval is considered in order to obtain results coherent with the CRF experimental data which are evaluated on a cold cycle. Indeed

because of the results are present in terms of benefits with respect to a reference vehicle, the additional fuel consumptions during the warm up are annulled each other.

Moreover also in this case, the engine speed threshold values (minimum and maximum) were identified thanks to a signals plotting:

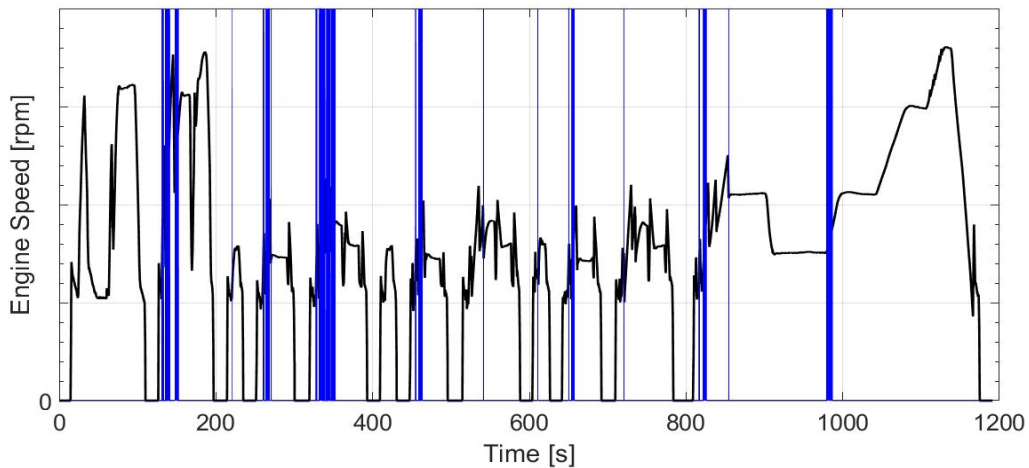


FIGURE 50-ENGINE SPEED AND MM_STATE-EA MODE

&	$nrpm_{ICE}$	$\geq nrpm_{ICE,th,MIN}$
	$nrpm_{ICE}$	$\leq nrpm_{ICE,th,Max}$

TABLE 9-EA MODE STRATEGY RULES B

For the E-Assist strategy also the control about the SOC level is fundamental for a correct simulation to check that in the battery enough energy is stored for the vehicle propulsion. The process is similar to the process described for the RG Mode. The difference is the power flow direction and therefore the equation used to take into account the devices efficiency. Through the interpolation on the BSG map and on the battery maps the energy $SOC_{EA,i}$ that shall be flowed away from the battery for the i_{th}

EA operation is obtained. After the comparison of this value with the previous SOC of battery, the controller decides if the EA Mode shall be active and the SOC level will be update or if not enough energy is present and the function is not applicable.

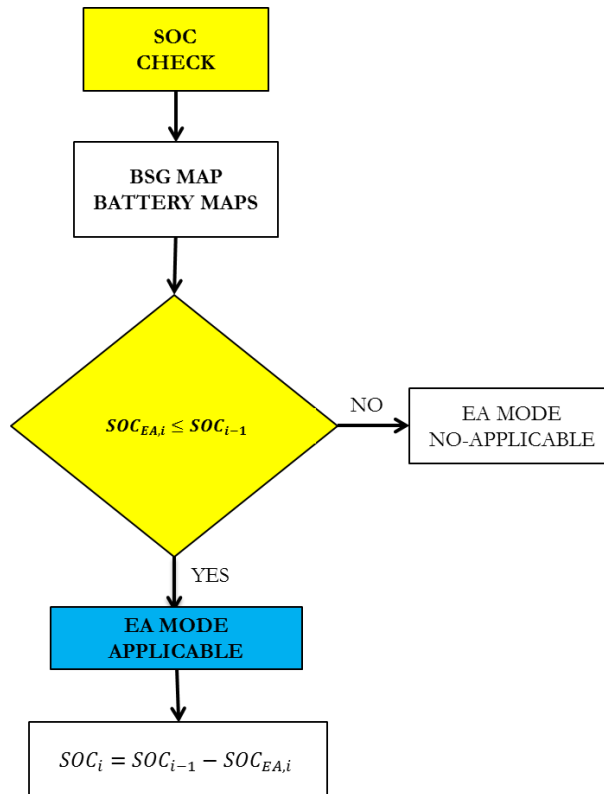


FIGURE 51-E-ASSIST SOC CHECK

The final flow chart for the EA strategy will be:

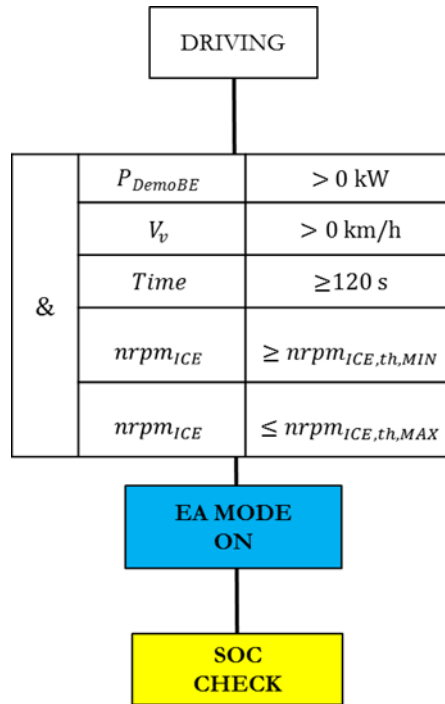


FIGURE 52-E-ASSIST STRATEGY FLOW CHART

6.3. E-Clutch function

6.3.1. Driver Behaviour

The Idle Coasting activation is related to engine and vehicle parameters during the test but it is also strictly conditioned by the driver behavior. Instead for a correct activation of the Idle Coasting function the driver has to release the brake pedal and the gas pedal when no propulsion is required and the engine will be decoupled by the drivetrain to operate such as freewheeling device. For a more precise simulation of the Idle Coasting, mode the driver behavior has been modelled. Particular attention has been given to the force on the brake and on the accelerator pedal. This approach was necessary to individuate pedals position threshold values below which the pedals release by the driver can be assumed. The analysis has been done over the WTLC cycle because its speed profile is more realistic with respect to the NEDC.

For the gas pedal, it is assumed that the relationship between the pedal position and the power supply by the engine P_{DemoBE} will be such as that described in the figure below:

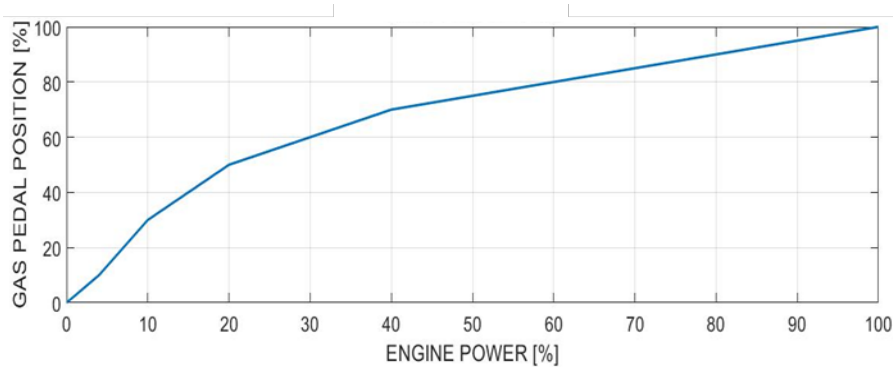


FIGURE 53-GAS PEDAL MODEL

Actually this trend described the relationship between a comfortable accelerator pedal travel and the torque required by the driver. This one is not ever equal to the torque provided by the engine because in the modern car the ECU is the final devices which decides what is the torque delivered taking into account all the parameters during the motion. The modern engine control system are equipped with a Torque-Based unit control. The driver indeed can require a torque level but is the engine control unit after an electronic control (EGAS) to decide the final torque: all this system is based on the drive by wire technology. In conclusion because of the structure model and of the impossibility to simulate a control unit, the accelerator characteristic has been readjusted ignoring the ECU operation.

The figure below shows the gas pedal position over the WLTC cycle, calculated with the Panda Demo-Car powers in each time instant:

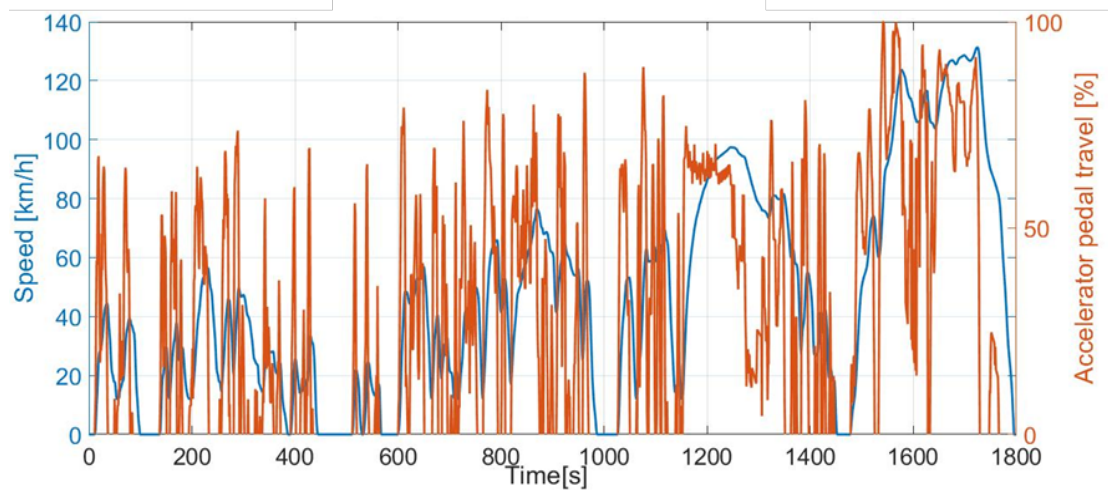


FIGURE 54-ACCELERATOR PEDAL TRAVEL OVER THE CYCLE

As you can see the trend is quite similar to the ECU accelerator pedal position signal obtained by means of the Analyzer, neglecting a scaling factor which depends on the characteristics of the real pedal:

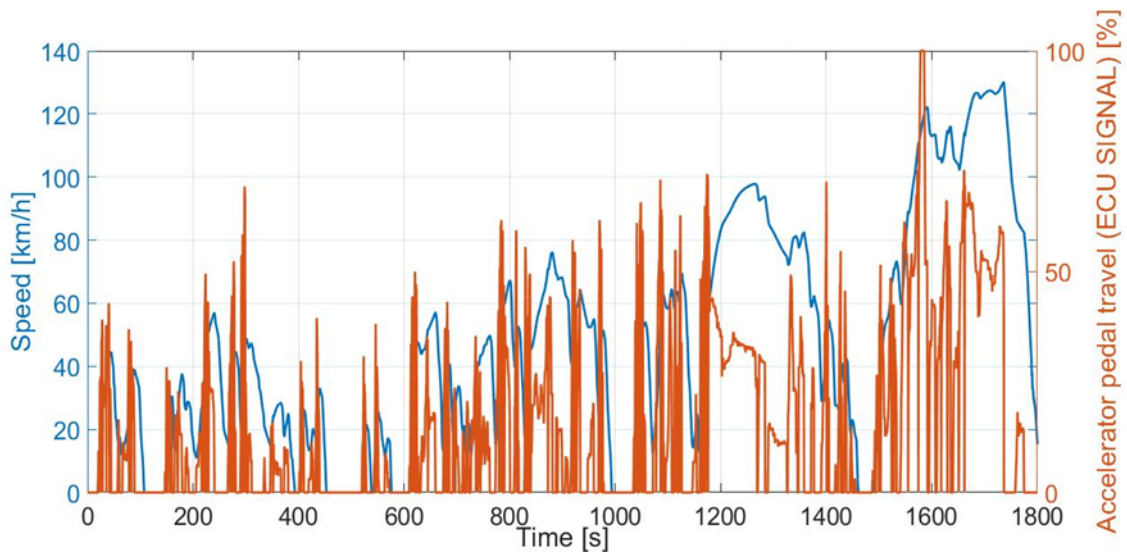


FIGURE 55- ACCELERATOR PEDAL ECU SIGNAL

Obviously in term of pedal travel the intensity the two signals are different, but considering the time instants over the cycle in which the values increase or decrease the overall trend is the same.

For the brake pedal position instead its model is based on the vehicle deceleration. After a study about the vehicle deceleration during the motion, a relationship between the brake pedal position and vehicle deceleration has been found. The parameterization of this trend and the calculus with the Demo-Car deceleration over the WLTC cycle allows to obtain the brake pedal position for each time instants:

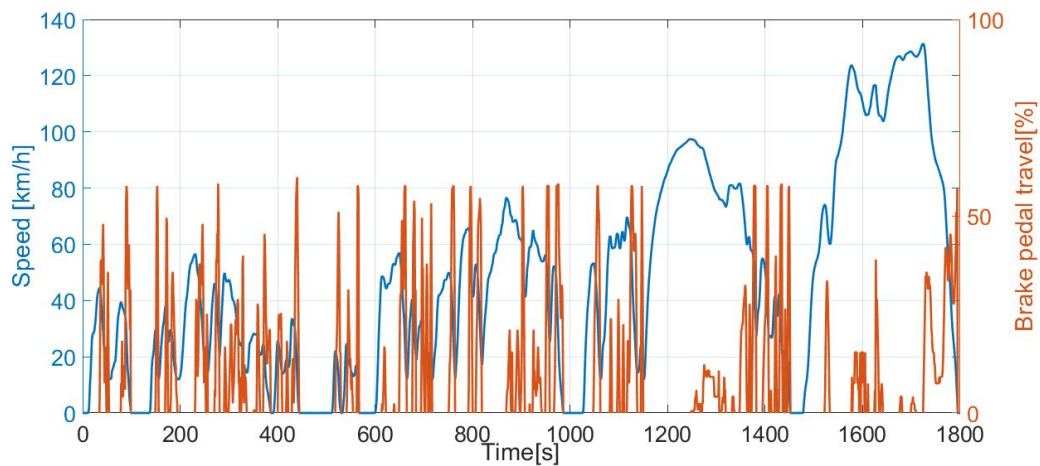


FIGURE 56-BRAKE PEDAL TRAVEL OVER THE WLTC CYCLE

Taking into account all the hypothesis done for the driver behavior modelling, the trend shown in the figures above were considered very similar to reality.

6.3.2. Idle Coasting

The method for the individuation of the E-Clutch function activation is based on the same procedure described for the BSG. The starting point indeed is the E-Clutch control unit signal which shows the activation of the Idle Coasting function over the cycle. This

study has been done over the WLTC cycle because for this cycle more CCU signals are recorded with respect to NEDC test. The E-Clutch as a matter of fact was not tested on the NEDC with the same frequency as WLTC because the starter experiments have showed how the IDLC would have not provided any benefits in terms of FC or CO₂ emissions and on the this mission speed profile: it consists of phases at constant speed and phases of braking in which the IDLC mode can not work with the maximum efficiency.

From the Coasting_Phase CCU signal:

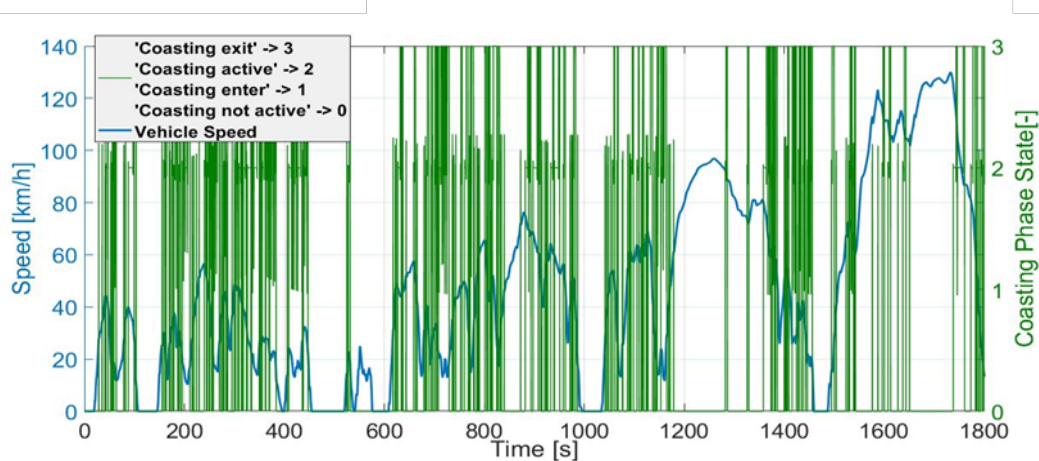


FIGURE 57-E-CLUTCH COASTING_PHASE_STATE SIGNAL

and isolating the values equal to 2 , the time instants in which the IDLC Mode is on have been obtained:

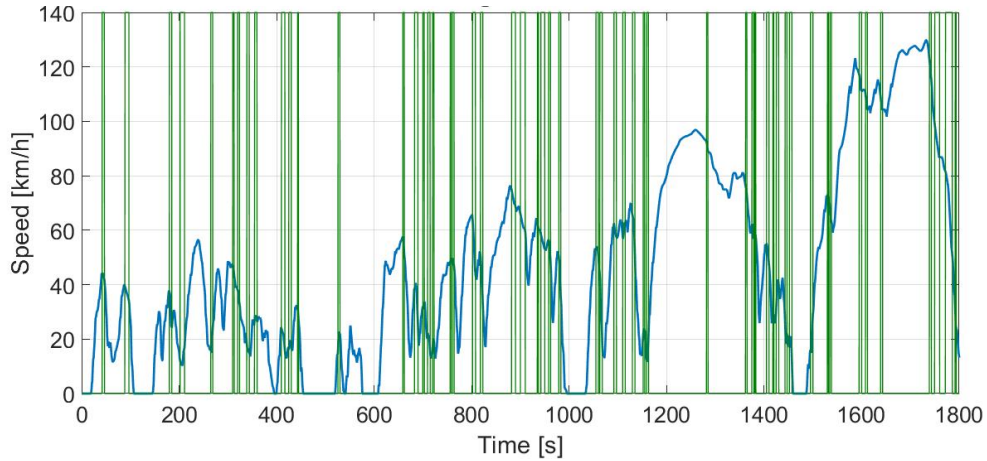


FIGURE 58-E-CLUTCH COASTING_PHASE_STATE ACTIVE

From the graph above the first rule strategy has been obtained and a minimum velocity value has been identified:

&	V_v	$\geq 15 \text{ km/h}$
---	-------	------------------------

TABLE 10-IDLC MODE STRATEGY RULE A

The other strategy rules have not been obtained by the VCU signals due to acquisition problems. For this reason and to create a E-Clutch strategy activation as much real as possible, the literature review was used. After different researches and many studies on the last scientific paper [23] and on the main manufacturer's presentation [17], two other rules have been defined:

&	<i>Gear</i>	≥ 2
	$nrpm_{ICE}$	$\geq 1200 \text{ rpm}$

TABLE 11-IDLC MODE STRATEGY RULES B

Finally the driver behaviour has been taken into account and two different threshold values have been defined. If the accelerator or gas pedals travels are lower than the 15%, it is possible to assume the cycle conditions allow the pedals release and therefore the Idle Coasting Mode activation.

&	Acc_{pdl}	$\leq 15\%$
	Brk_{pdl}	$\leq 15\%$

TABLE 12-IDLC MODE STRATEGY RULES C

Summarizing the final flow chart for the E-Clutch and the base rules for the Idle Coasting activation is:

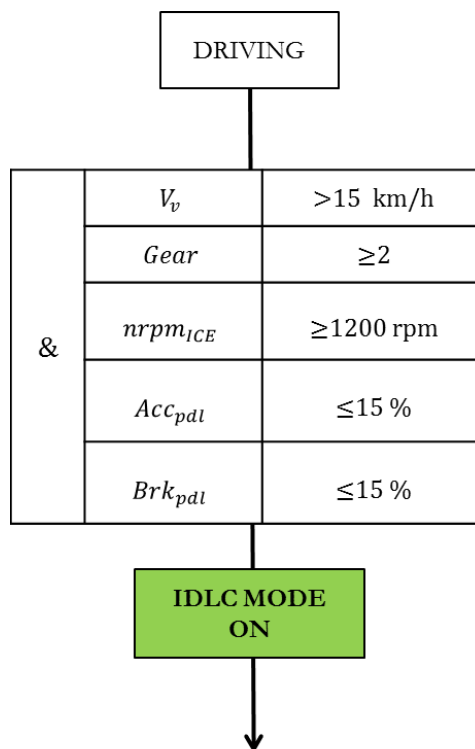


FIGURE 59-IDLE COASTING STRATEGY FLOW CHART

Chapter 7

7. Results

In this chapter the model validation and the final results are presented. The CRF database presents a lot of test with the BSG active on the NEDC and no one with the E-Clutch function on. For these reasons the model validation for the BSG has been done by taking into account the experimental data over the NEDC, instead for the E-Clutch the reference cycle was the WLTC. After the model validation the results in terms of CO₂ benefits are showed and the final impact of the combined use of the BSG and of the E-Clutch no tested yet, will be presented. Finally an energy analysis about the energy recover and the energy supply by the BSG was carried out. Because of the confidentiality of the data, it was not possible used the fuel consumption or the emissions values and all results are shown with respect to a reference vehicle. It is important to underline that the model simulation on the type-approval cycle is based on different hypothesis:

- A **warm cycle** is simulated. It was assumed that before the cycle start the engine has completed yet the warm-up phase. The additional FC and CO₂ emissions due to the low temperature of the three-way catalyst are not taken into account.
- It was used a **kinematic approach**. Therefore it was assumed that the driver follows always in the best way possible the speed profile defined by the regulation.

- **Gearbox efficiency** is assumed **constant**, even if in reality it depends on the torque.
- Transitional phase are neglected and it was assumed that the cycle is a **stationary phase succession**.

7.1. BSG benefits

7.1.1. NEDC and model validation

As said in the introduction, for the BSG working functions the NEDC cycle is the reference type-approval cycle. Using the strategy described in the previous chapter, the points in which the main Belt-Starter Generator functions are on (Enhanced Start Stop, Regenerative Braking and E-assist) were plotted over the vehicle speed profile:

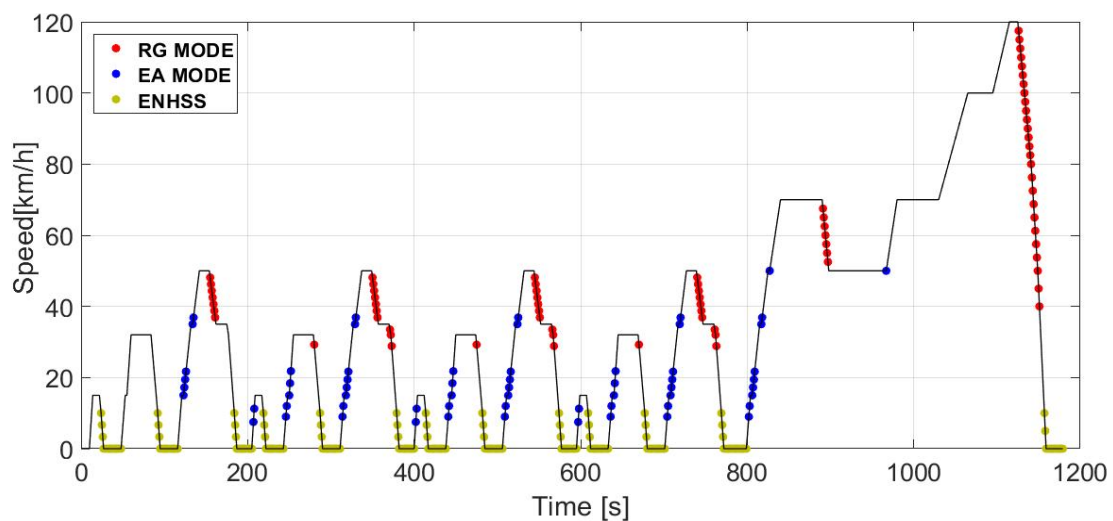


FIGURE 60-BSG FUNCTIONS OVER THE NEDC

If you compare the time instants where the EA mode and the RG mode are active in the figure above with the MM_STATE signal for the same working condition, it is clear how the model is validated for the duration of electric function over the cycle.

Otherwise it is possible to look the figures below. By means of the Analyzer, it was possible to recorder the electric function duration for each tests and therefore the average values were individuuated. The simulation with the DemoBE model and the respective calculus provides the same results:

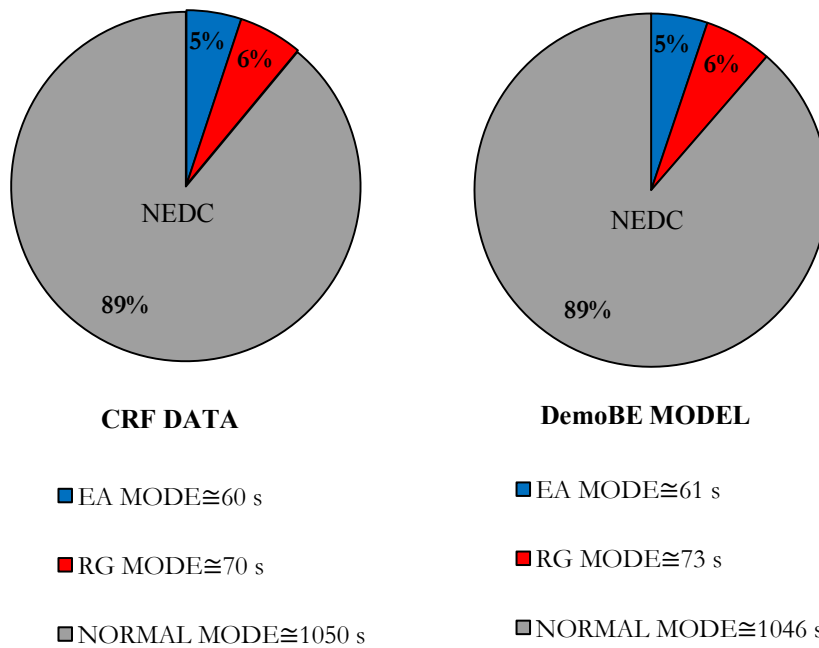


FIGURE 61-BSG ELECTRIC FUNCTIONS DURATION OVER THE NEDC

To expose the correct model working, the BSG operative points for each time instants in which the EA and RG Mode are on, are reported in the BSG map below:

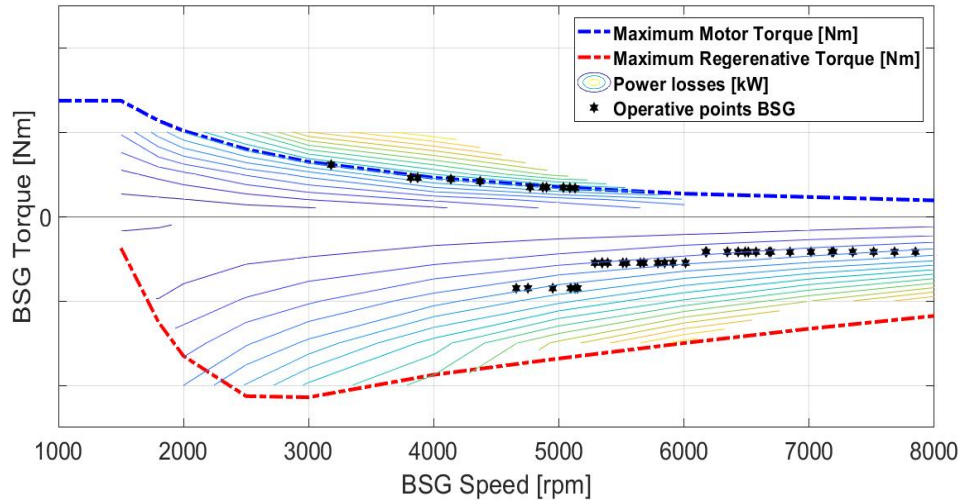


FIGURE 62-BSG OPERATIVE POINTS- NEDC

The SOC check control and the consequent upload of the SOC level allows the possibility to obtain the trend level in function of time.

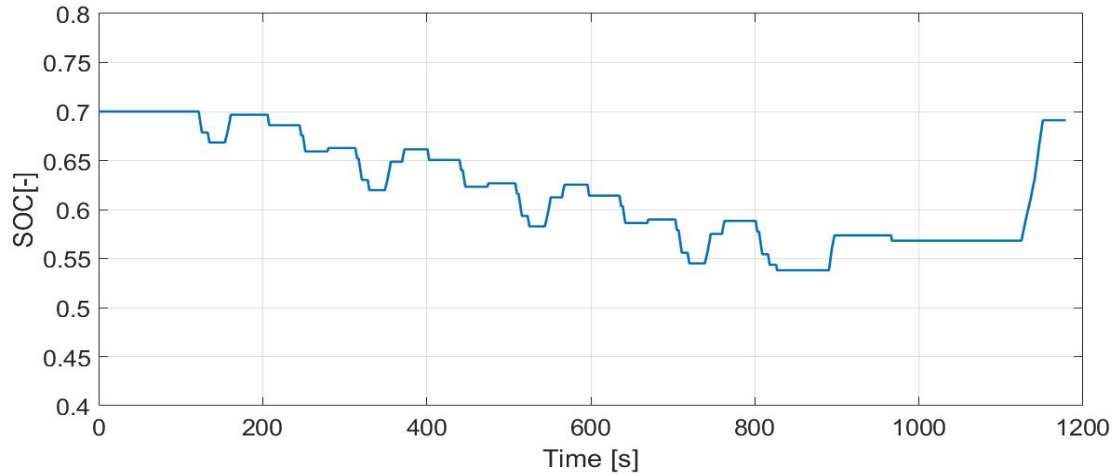


FIGURE 63-SOC LEVEL-NEDC

Taking into account the start and the end value it is possible the calculus of the

$$\Delta SOC = SOC_{end} - SOC_{START} \quad (7.1)$$

The figure above shows as for the simulation the $\Delta SOC \cong 0$. Indeed the regulation defines a constraint for the state of charge of the traction battery (for the FIAT Panda is the Li-ion battery) before and after the test. This condition is fundamental for the vehicle homologation.

The calculus of the CO₂ benefits due to the installation of the BSG has been done with respect to a reference vehicle with a conventional Start&Stop in which the engine is turn off for speed lower than 3 km/h. For a correct and clear data representation and an effective comparison between CRF data e DemoBE results an histogram is used. The total benefits may be-subdivided in different CO₂ reduction contributions considering the BSG functionalities and the table shows the benefits provided by each of them. Beyond the Enhanced Start&Stop and the E-assist which are the main functionalities developed by the BSG, its installation and therefore the dual battery system (DB) presence on the vehicle causes an additional fuel consumption reduction. Because of the Demo-Car is a vehicle with two batteries (Li-ion and Pb-Acid), the Pb-Acid battery can provide power to the accessories, reducing the engine load and its fuel consumption. Although this function causes a Pb-Acid battery discharge, no constraints for the NEDC regulations are defined about the its final state of charge.

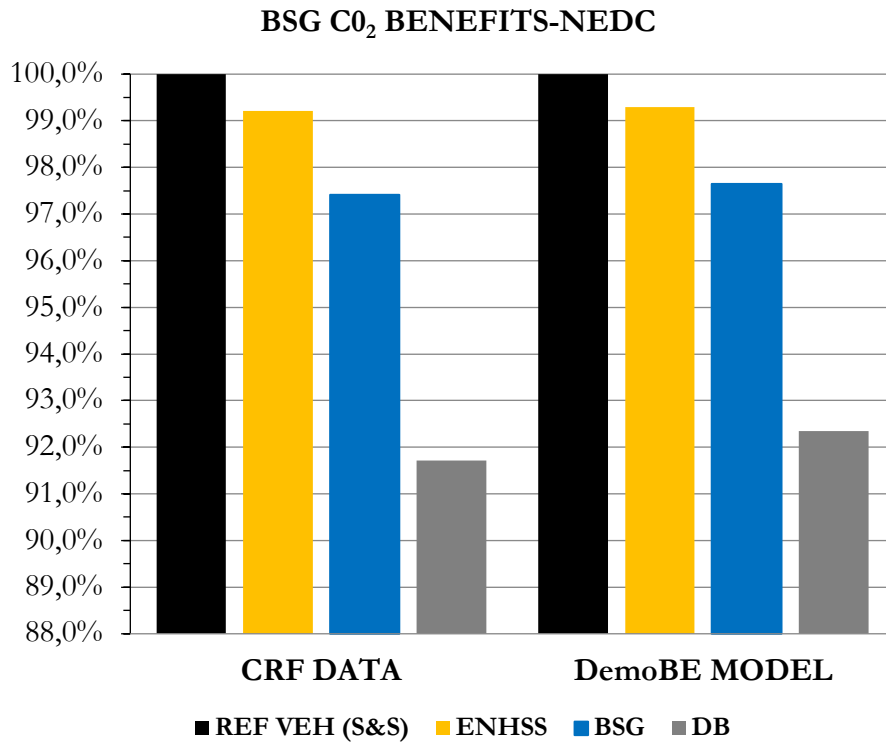


FIGURE 64-BSG CO₂ BENEFITS - NEDC

	ENHSS	BSG	DB	TOT.
CRF DATA	0.8%	1.8%	5.6%	8.2%
DemoBE MODEL	0.7%	1.7%	5.3%	7.7%
$\varepsilon = \text{CRF-DemoBE} $	0.1%	0.1%	0.3%	0.6%

TABLE 13-CONTRIBUTION OF EACH BSG FUNCTIONALITIES FOR CO₂ REDUCTION-NEDC

The value ε indicates the difference in percentage between the CRF and the DemoBE model data.

From the values obtained through the interpolation in the fuel consumption map the corresponding CO₂ emissions are linearly determined by means of the equation (5.34).

By means of the cumulative integral via trapezoidal , the final value of CO₂ is obtained.

The figures below are the validation for histogram data illustrated before. As you can see the final benefits is equal to the final benefits showed in the Figure 64.

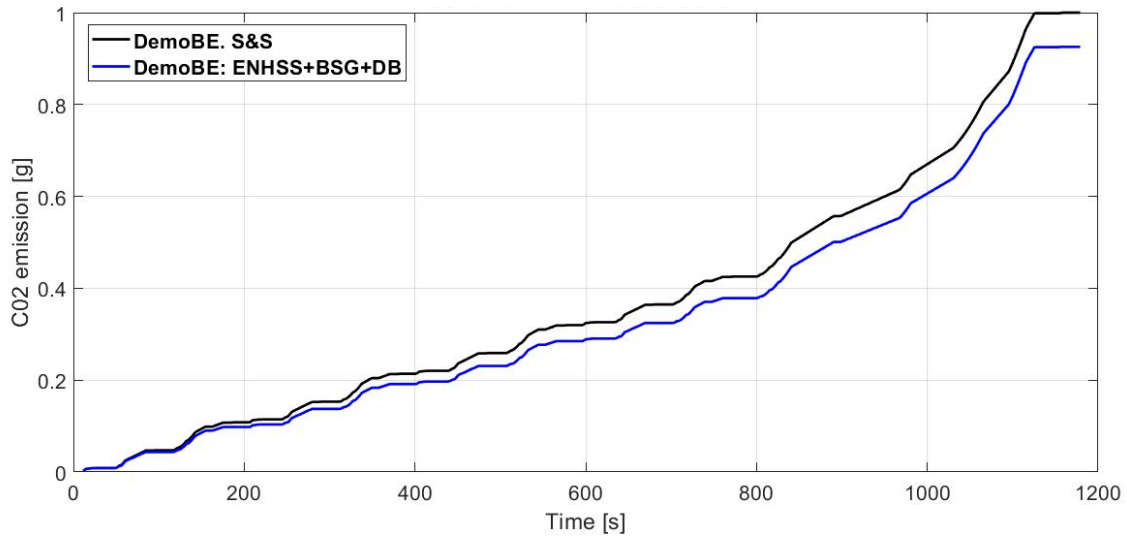


FIGURE 65-CUMULATIVE CO2 EMISSION WITH BSG-NEDC

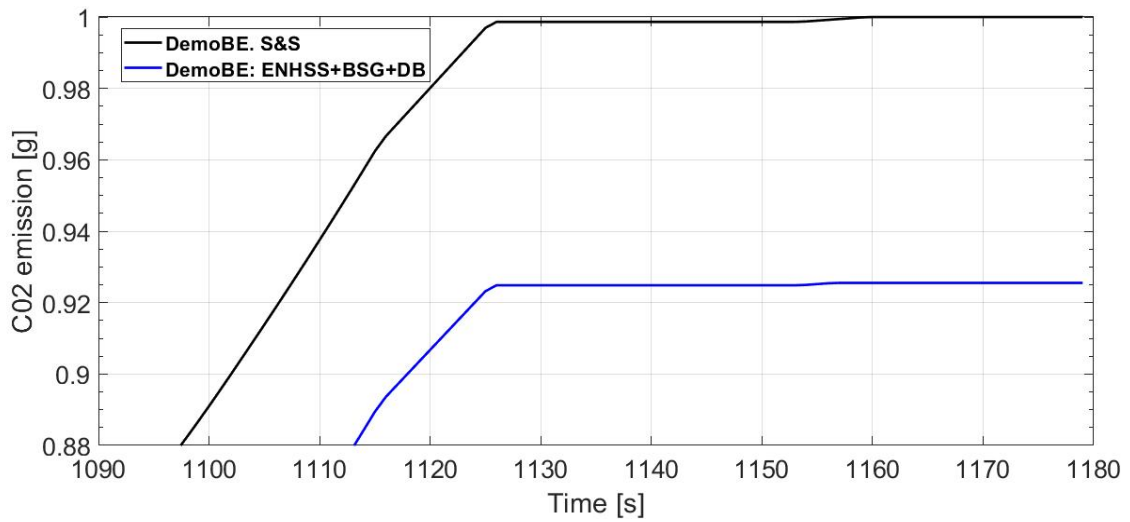


FIGURE 66- ZOOM OF THE CUMULATIVE CO2 EMISSION WITH BSG-NEDC

7.1.2. WLTC

After the model validation over the NEDC, the strategy has been applied over the WLTC. It is important to underline how the strategies are completely independent by the type-approval cycle therefore the rules defined previously can be applied for any cycle tests. For this reason it was applied without any modification. The results are presented below.

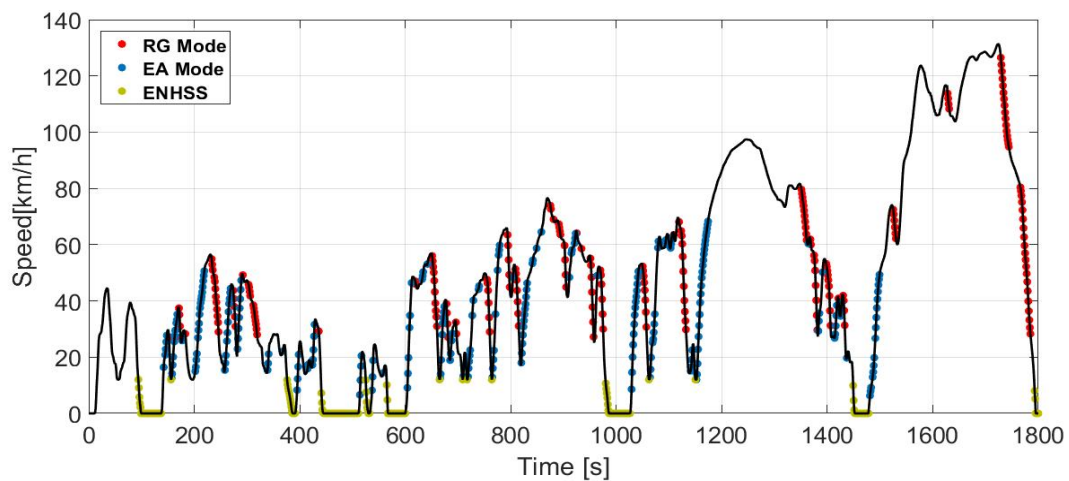


FIGURE 67-BSG FUNCTIONS OVER THE WLTC

Although the few experimental test in which the BSG was tested on the WLTC, also in this case an average duration of the electric functions was individuated (left cake diagram). The results obtained using the DemoBE model are consistent with the CRF data.

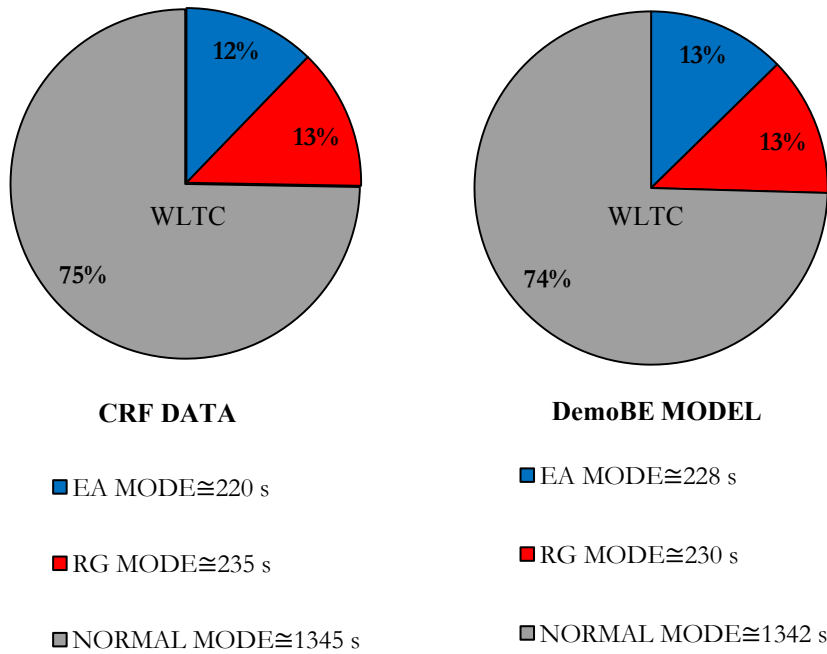


FIGURE 68-BSG FUNCTIONS DURATION OVER THE WLTC

Because of the time instants activation are higher with respect to the previous case, the operative points on the BSG are:

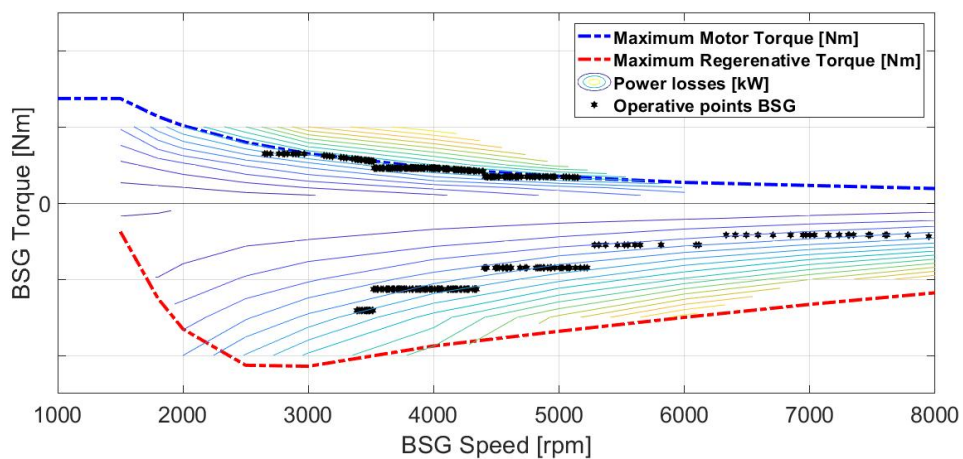


FIGURE 69-BSG OPERATIVE POINTS-WLTC

The SOC values uploading by means of the SOC check, provide the trend in function of time. As you can see by the figure below, the strategy allows to reach the value $\Delta SOC \cong 0$ but it does not violate the regulation request about the state of charge of the traction battery.

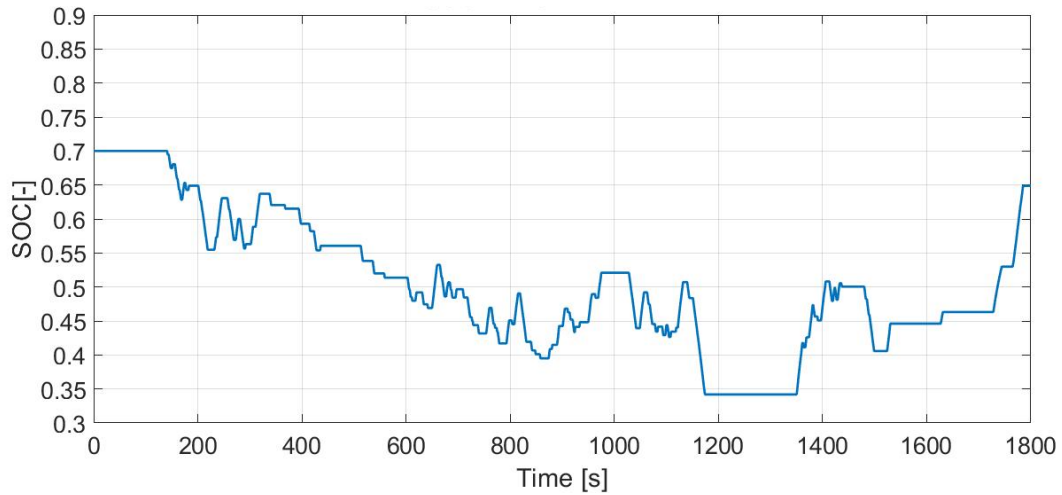


FIGURE 70-SOC LEVEL-WLTC

Even though the model validation was done for the NEDC, in this section also the CRF data related to the benefits by means of the BSG use as additional validation example is reported. However the WLTC regulation does not allow the possibility to use the Pb-Acid battery to supply power to the accessories, because a constraint on its state of charge is defined. For this reason only the Enhanced Start&Stop and E-Assist benefits were evaluated:

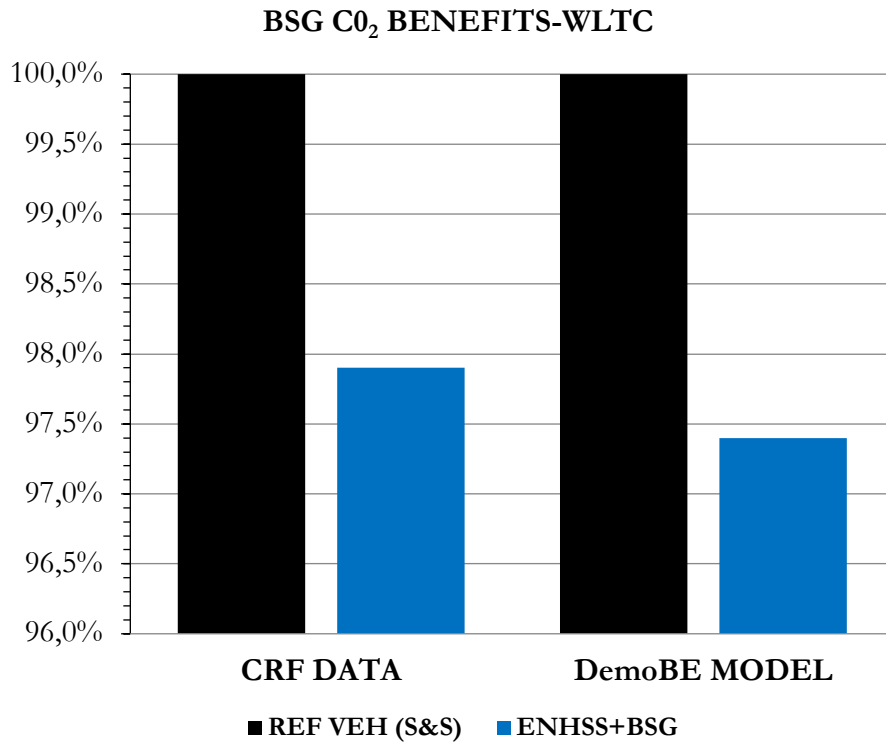


FIGURE 71-BSG CO₂ BENEFITS-WLTC

	ENHSS+BSG
CRF DATA	2.1%
DemoBE MODEL	2.6%
$\varepsilon = \text{CRF-DemoBE} $	0.5%

TABLE 14-CONTRIBUTION OF EACH BSG FUNCTIONALITIES FOR CO₂ REDUCTION-WLTC

The CO₂ cumulative trends give a visual result of that has been already explained through the histogram.

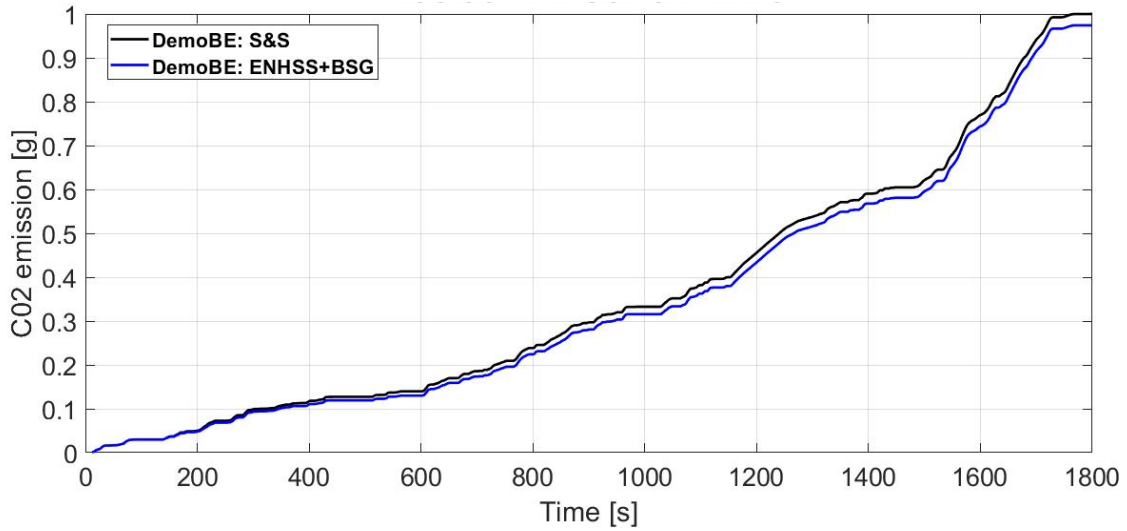


FIGURE 72-CUMULATIVE CO2 EMISSION WITH BSG-WLTC

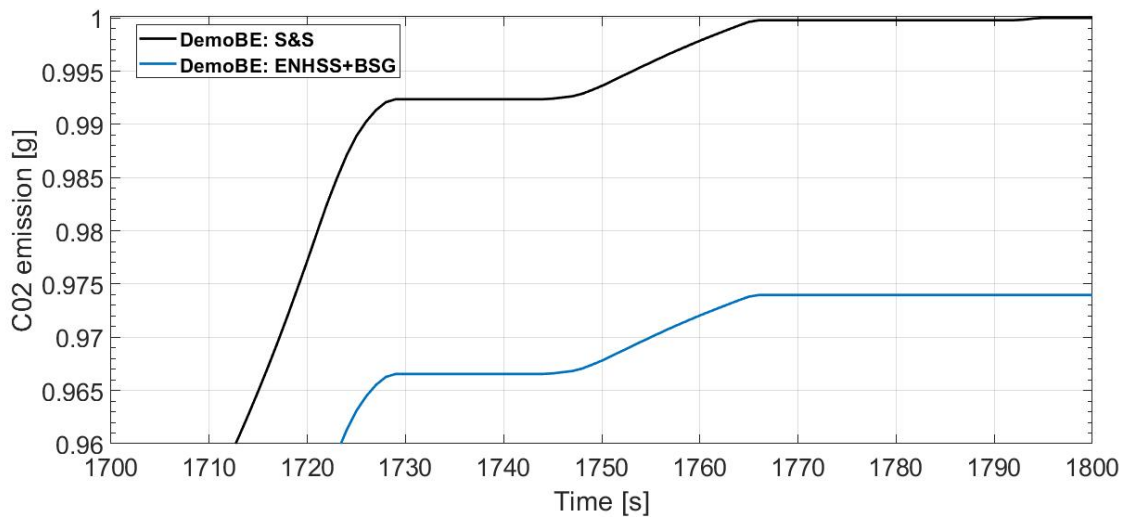


FIGURE 73-ZOOM OF THE CUMULATIVE CO2 EMISSION WITH BSG-WLTC

7.2. E-Clutch benefits

7.2.1. WLTC and model validation

The E-Clutch and therefore the Idle-Coasting strategy were validated thanks to the experimental data obtained by the tests on the WLTC. The time instant, where the E-Clutch is active, are showed in the figure below:

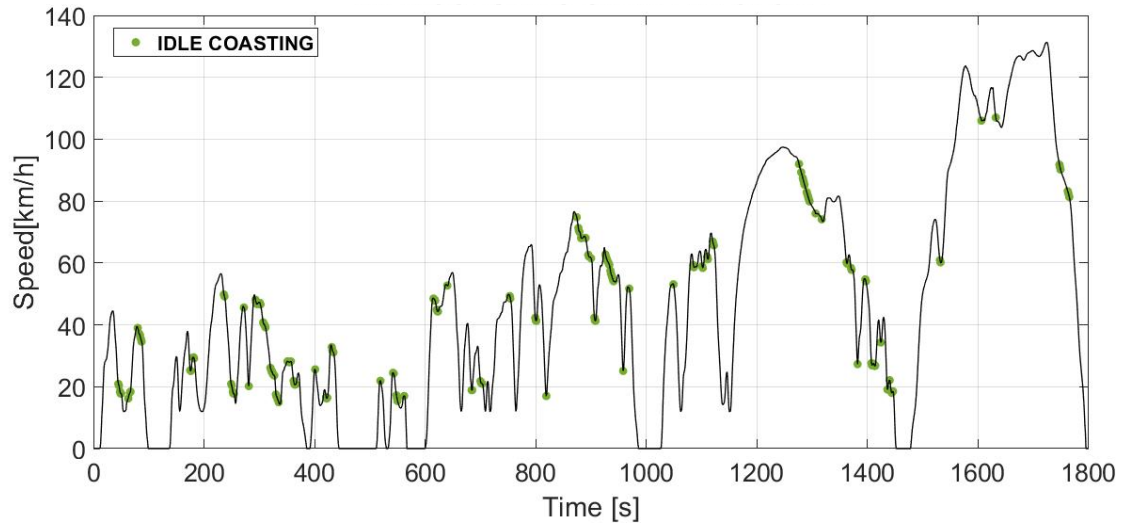


FIGURE 74-IDLE-COASTING OPERATIVE POINTS OVER THE WLTC

The figure illustrates a typical Idle Coasting event where, despite the high vehicle speed when the IDLC is on, the engine is decoupled and the gear shifts to the neutral.

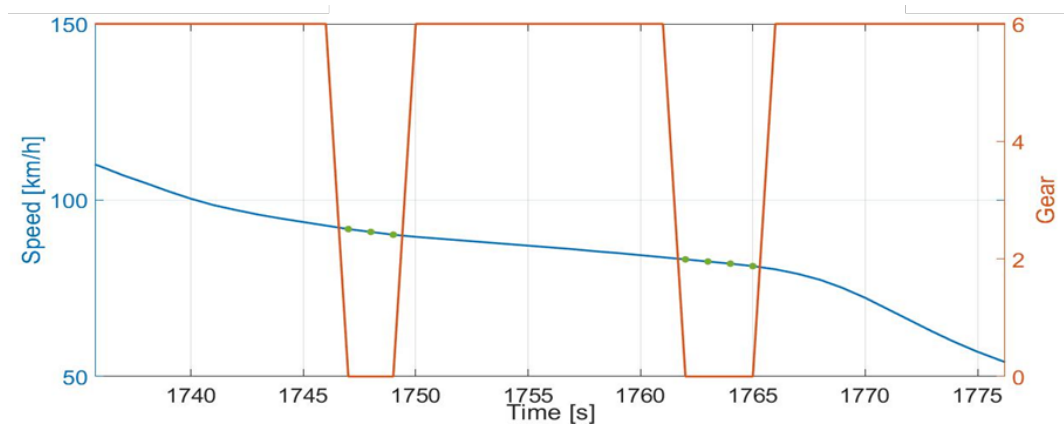


FIGURE 75-GEAR VARIATION DURING THE IDLE-COASTING

Despite of the simplest driver behaviour model, necessary for a correct simulation of the E-Clutch activation, the points over the cycle are distributed consistently with respect to the COSATING_PHASE_STATE signal. Moreover the analysis about the overall

duration of the Idle Coasting over the total cycle time discloses again how the strategy created is very similar to the real strategy which is present in the clutch control unit.

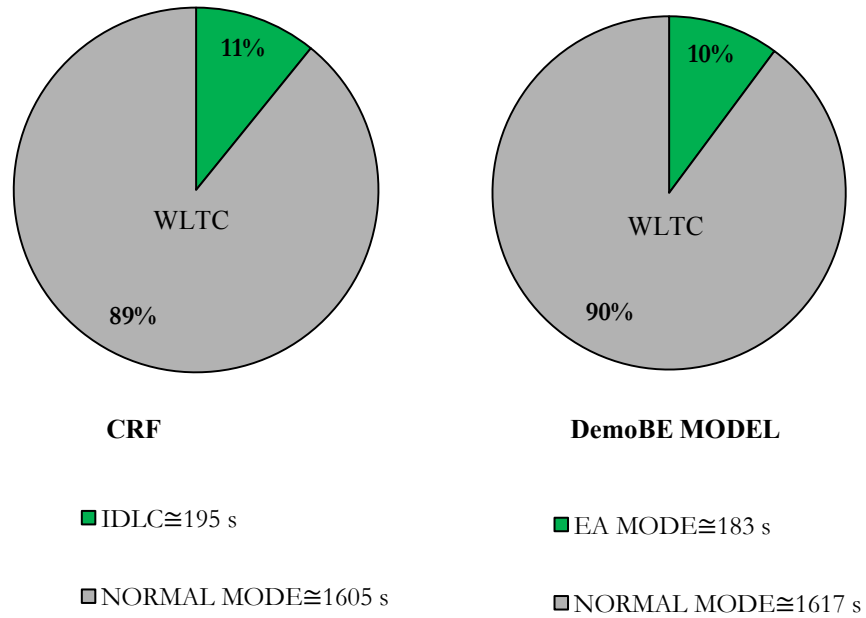


FIGURE 76-E-CLUTCH FUNCTION DURATION OVER THE WLTC

The last validation modality is CO₂ benefits calculus due to the function activation:

E-CLUTCH CO₂ BENEFITS-WLTC

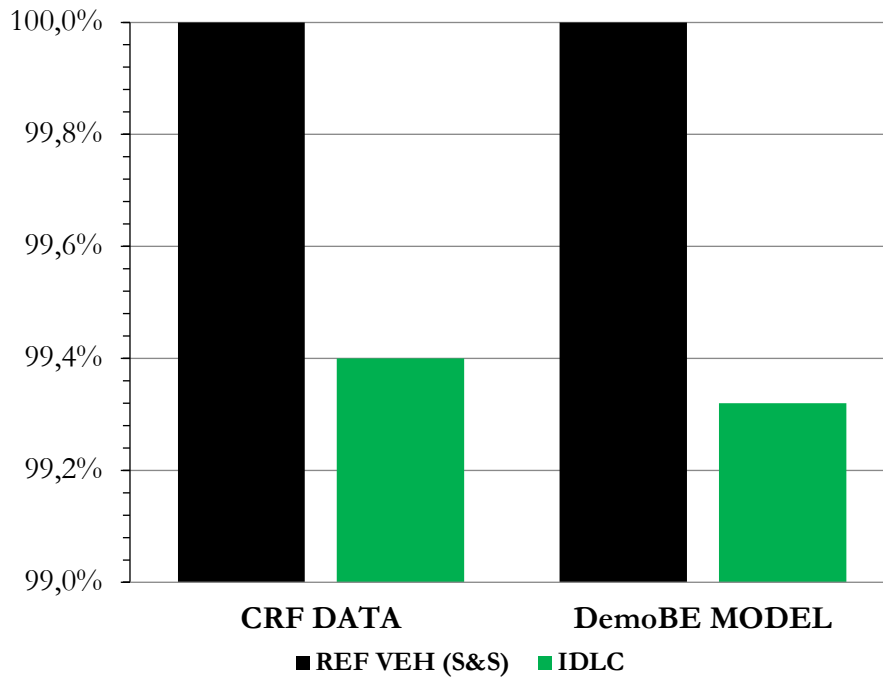


FIGURE 77-E-CLUTCH CO₂ BENEFIT-WLTC

	IDLC
CRF DATA	0.6%
DemoBE MODEL	0.7%
$\varepsilon = \text{CRF-DemoBE} $	0.1%

TABLE 15- CONTRIBUTION OF E-CLUTCH FUNCTION FOR CO₂ REDUCTION-WLTC

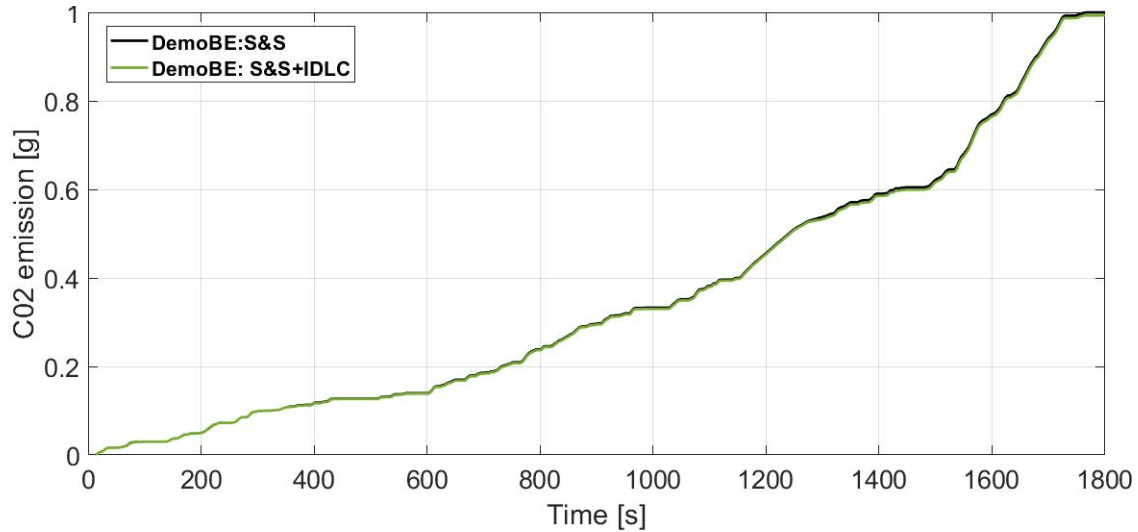


FIGURE 78-CUMULATIVE CO2 EMISSION WITH E-CLUTCH-WLTC

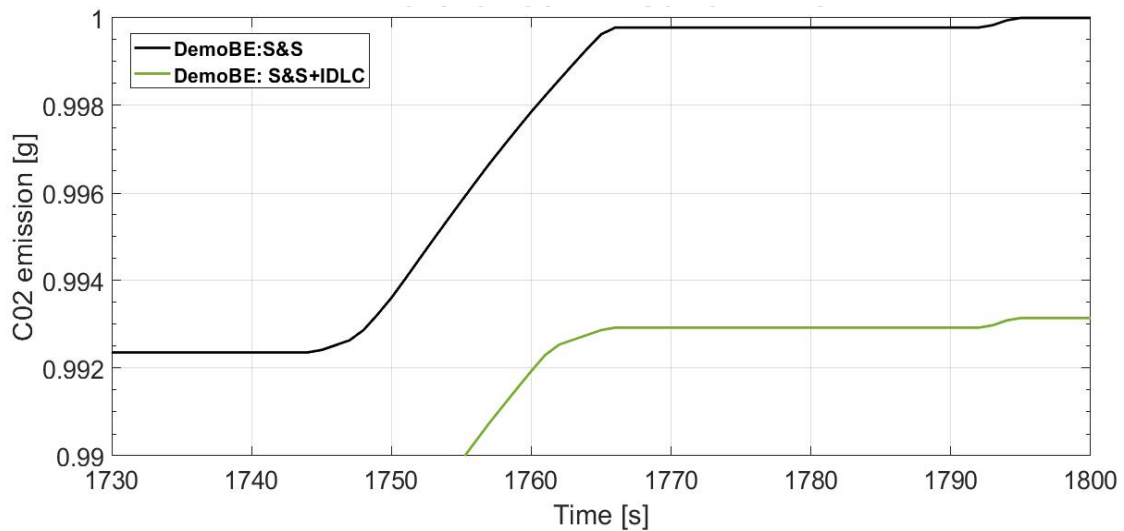


FIGURE 79-ZOOM OF THE CUMULATIVE CO2 EMISSION WITH E-CLUTCH-WLTC

7.3. Combined use of the BSG and of the E-Clutch

In the end, the two strategies defined for the BSG and for the E-Clutch activation have been combined to evaluate the overall benefit due to the simultaneous use of the devices over the WLTC. Because of the strategies definition, the different threshold values

which allows the activation of the two devices do not conflict even when the E-Clutch and the BSG work together. For this reason, the combined use was evaluated through the activation of the flow charts strategies during the simulation. The activation points over the cycle will be:

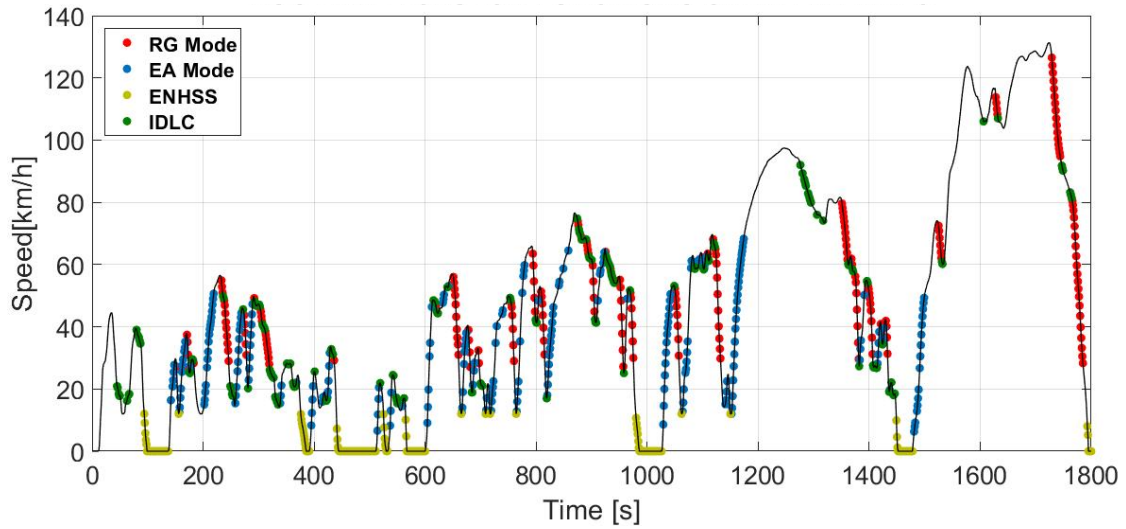


FIGURE 80-BSG AND E-CLUTCH FUNCTIONS OVER THE WLTC

As you can see by the figure below the activation points are never superimposed and the BSG does not prevent the E-Clutch working and vice versa. The CO₂ benefits are reported in the histogram below:

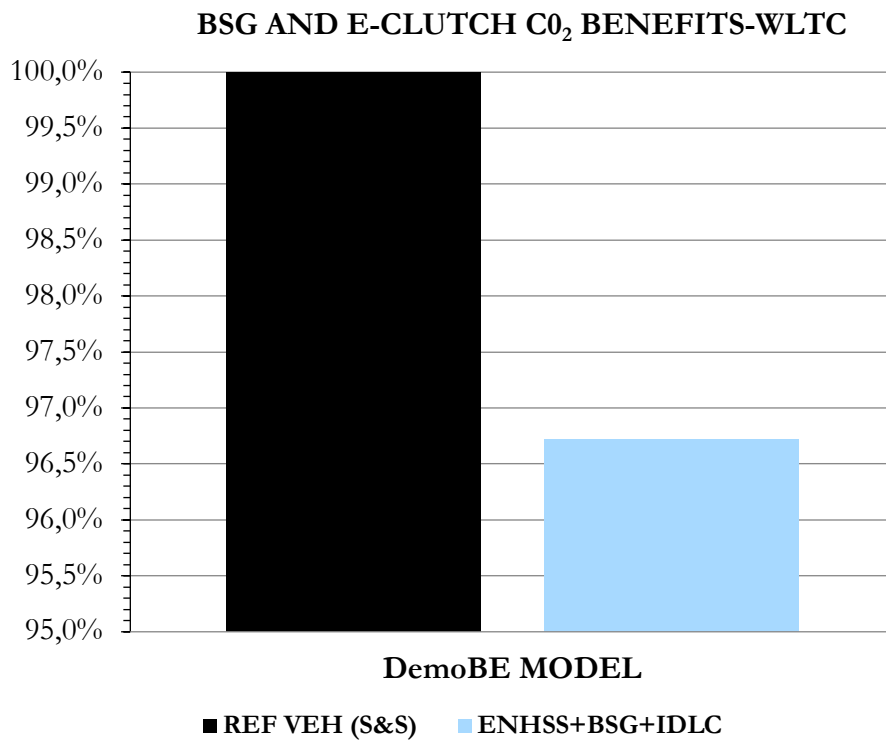


FIGURE 81-BSG AND E-CLUTCH CO₂ BENEFITS-WLTC

	BSG+ENHSS	IDLC	TOT.
DemoBE MODEL	2.6%	0.7%	3.3%

TABLE 16- CONTRIBUTION OF BSG AND E-CLUTCH FUNCTIONS FOR CO₂ REDUCTION-WLTC

As it was done previously the cumulative, CO₂ obtained by the simulation are reported:

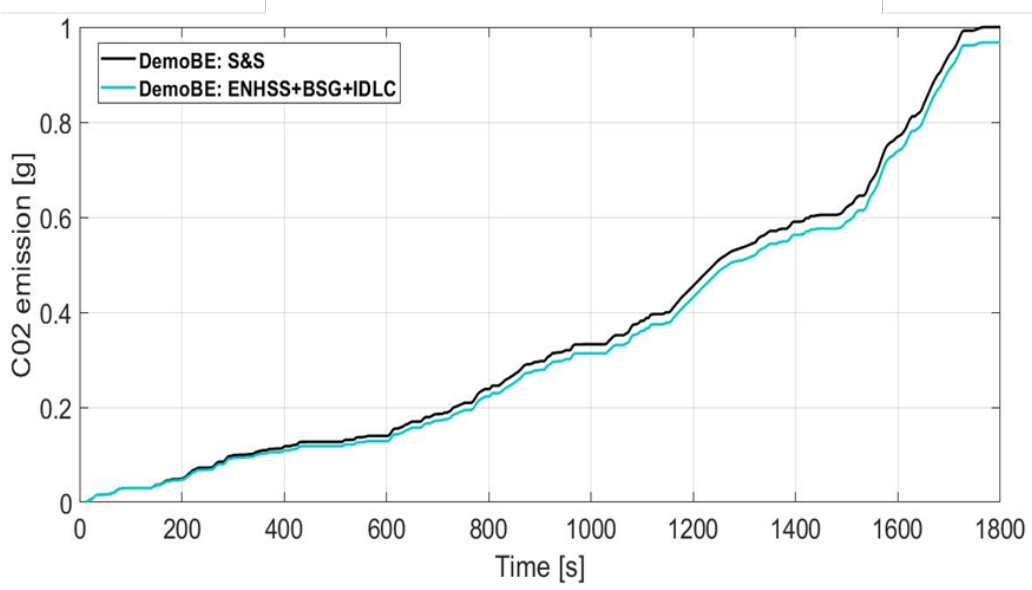


FIGURE 82-CUMULATIVE CO2 EMISSION WITH BSG AND E-CLUTCH-WLTC

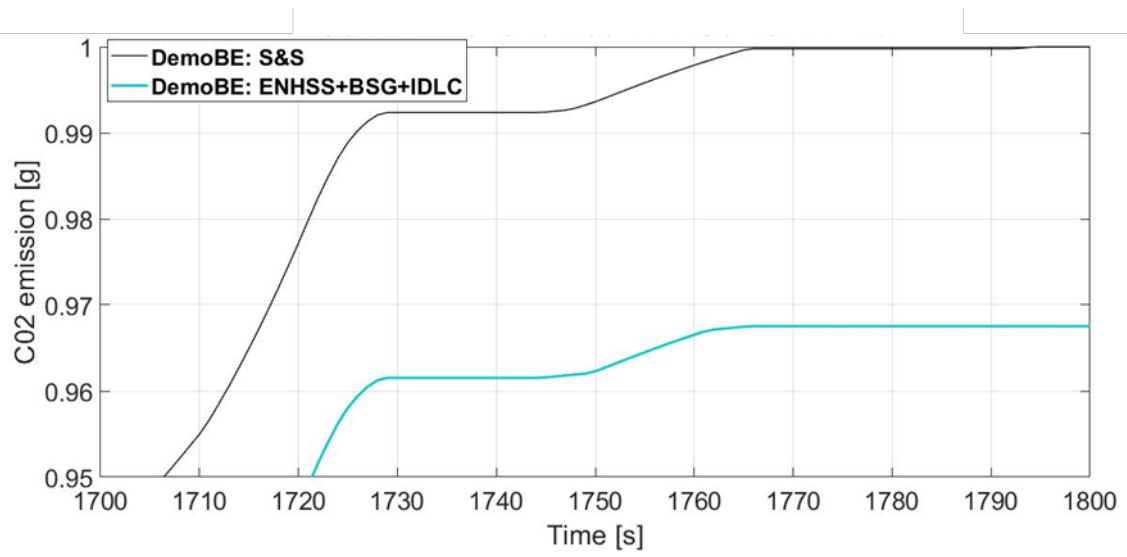


FIGURE 83-ZOOM OF THE CUMULATIVE CO2 EMISSION WITH BSG AND E-CLUTCH-WLTC

7.3.1. Energy analysis

Because in this case the values are more general and significant, an energy analysis has been carried out. The percentage of energy recovered during RG Mode with respect to the energy potentially recoverable during all brakes over the cycle was calculated.

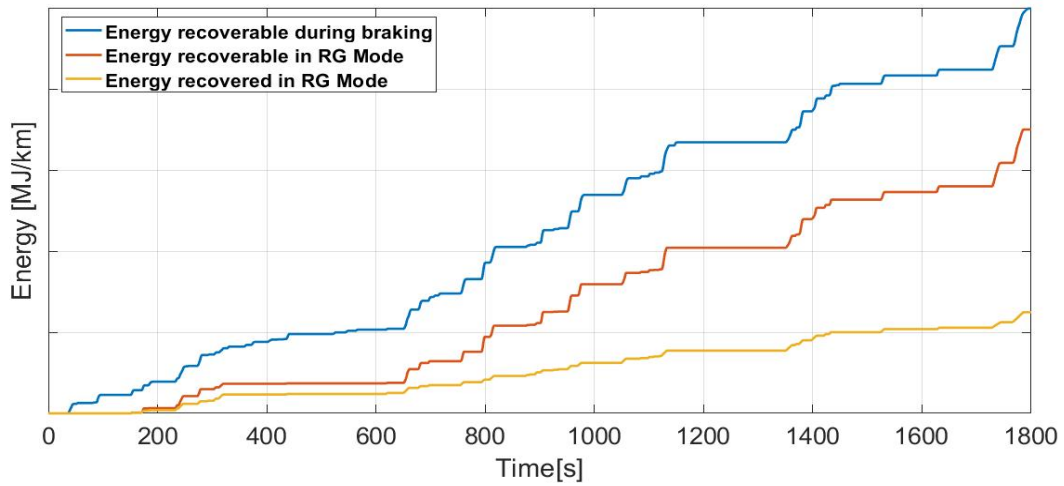


FIGURE 84-ENERGY RECOVER ANALYSIS

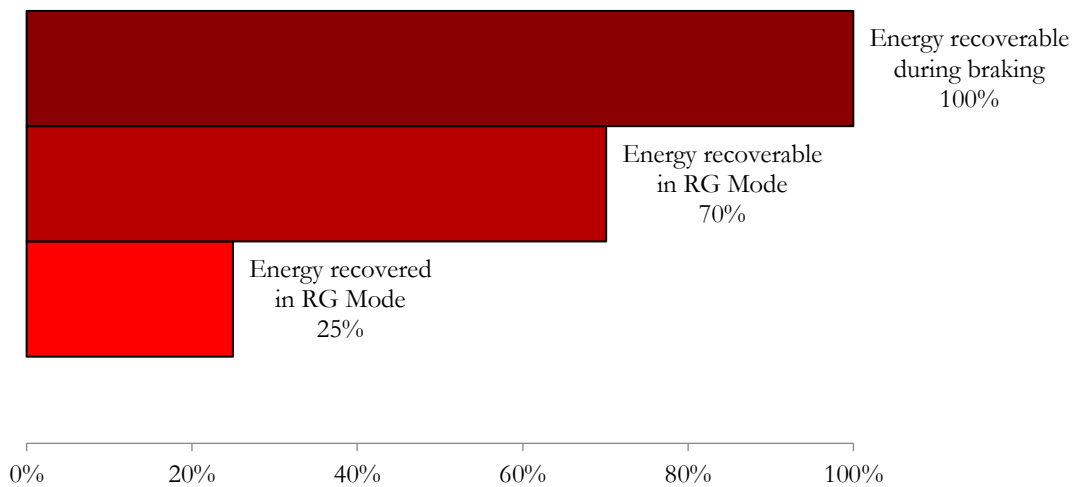


FIGURE 85-ENERGY RECOVER PERCENTAGE REDUCTION

The strategy implementation and therefore the impossibility to use the BSG during all brakes causes a reduction of 30% of the energy recoverable. Moreover taking into account the power losses throughout the electric power flow, the BSG and inverter efficiencies, the energy actually recovered is the 25% compared with the ideal energy recoverable.

For the energy supply the approach is similar. Indeed, starting from the energy potentially available by the BSG when a propulsion is required and therefore when the power provided by the ICE is higher than zero, the application of the EA strategy and the conditions that should respect the energy that the BSG can supply are around the 22% of the overall required. Furthermore, the power losses causes a further reduction of 7% and the energy actually provided by the BSG is less or more the 15% of the total.

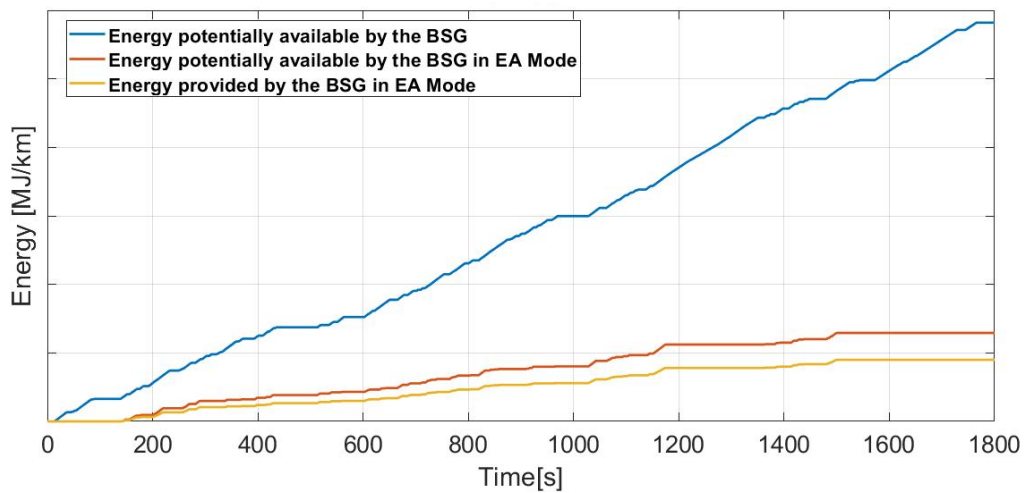


FIGURE 86-ENERGY SUPPLY ANALYSIS

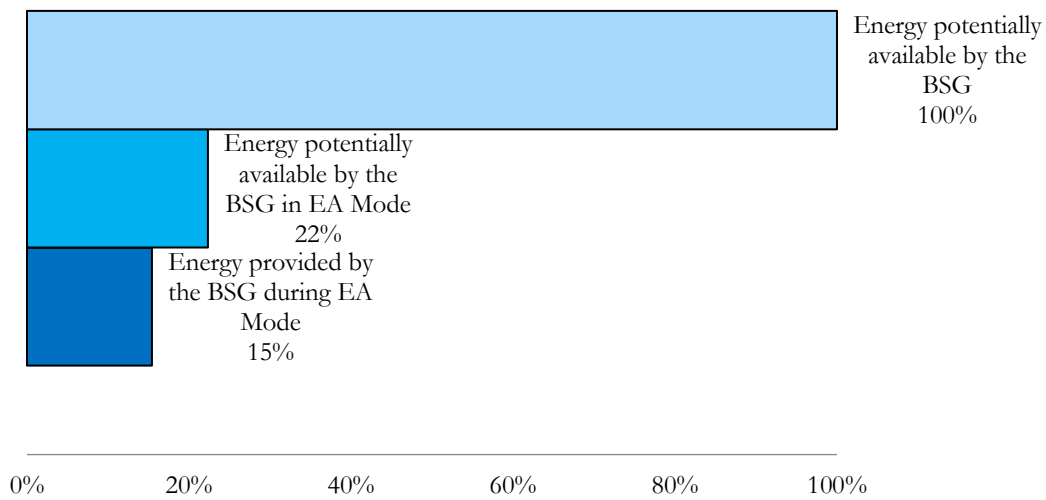


FIGURE 87-ENERGY SUPPLY PERCENTAGE REDUCTION

The Idle Coasting activation indeed allows to retain the kinetic energy which otherwise is dissipated. All the vehicle wheels are fitted with brake pads which apply a friction force that inhibits the motion of the wheels. Frictional braking results in a conversion of the kinetic energy gained from fuel consumption to thermal energy. This thermal energy is dissipated in the atmosphere in the form of waste heat. By means of the Idle Coasting function, the brake pedal is not depressed and the kinetic energy is not wasted. The figure below shows the kinetic energy retained when the IDLC is on. By summing the contribution in each time instants the total kinetic energy saved through the Idle Coasting over the WLTC is defined.

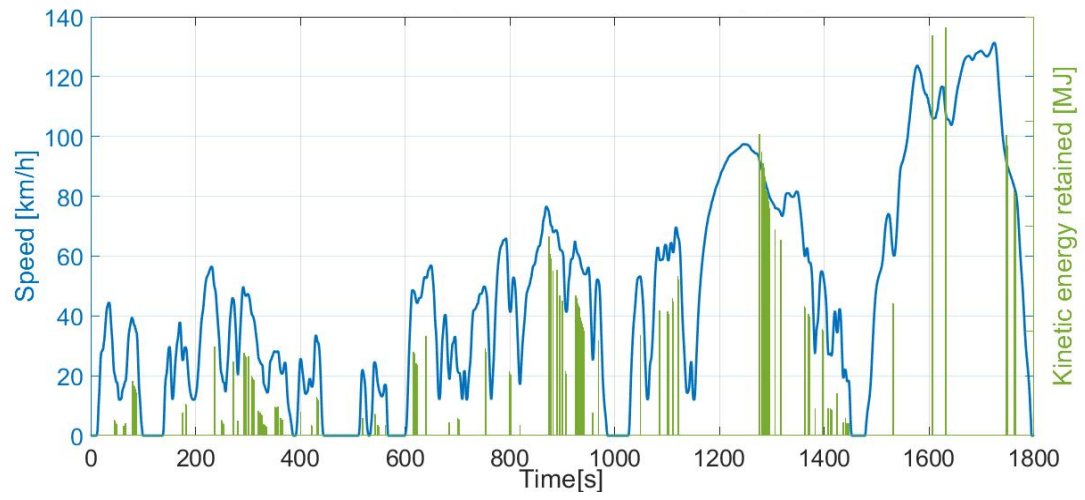


FIGURE 88-KINETIC ENERGY RETAINED

Chapter 8

8. Conclusion

This study is focused on impact of the BSG and of the E-Clutch on the CO₂ emission of a micro-hybrid vehicle. The calculus of the fuel consumption and of the carbon dioxide emissions was done by means of a kinematic model in which different strategies, for the activation of the electric devices, have been implemented. The reference's model is a real vehicle, actually tested in the CRF chassis-dynamometer in Orbassano (Turin). The results show that the model is precise and the benefits calculated are congruent with the experimental data. The combined use of the BSG and of the E-Clutch is never evaluated by the CRF, and through to the model it is possible estimate the CO₂ reduction if the devices are both active during a type-approval test. This final strategy can be the starting point for the future work to achieve more efficient calibration of the electric functions and therefore to optimize the combined use of the BSG and of the E-Clutch. Moreover the Tool Analyzer created for the data pre-processing and therefore for the analysis of the vehicle control unit signals, thanks to its functions and the possibility to resample the signals, is actually used in CRF for the saving and the comparison of different tests in terms of polluting substance emissions and different electric calibration installed on the VCU. The future work could be focused on the model improvement for the evaluation of the other polluting substances, for example by means of the NO_x map in which the emissions are in function of the engine BMEP. Moreover, the addition of a model for the estimation of the time in which the TWC light-off temperature is reached and the respective calculus of additional polluting substance emissions could be

evaluated in future. Ultimately, it is important to underline how the model strategies have been built by the VCU signal and certainly they could be improved if the admission to the DSPACE database (environment in which the real strategy rules used by the Demo-Car are saved) is allowed. Furthermore the possibility to increase the BSG voltage (48 V for example) to allow a pure electric propulsion could be investigated by identifying the respective FC and emissions.

In conclusion the vehicle electrification is undoubtedly a good way to reduce the fuel consumption and the polluting substances emissions and therefore to respect the more stringent limits imposed by the regulation for the vehicle homologation.

Bibliography

- [1] K. G. Høyer, “The history of alternative fuels in transportation: The case of electric and hybrid cars.,” *Utilities Policy* 16, pp. 63-71, 2008.
- [2] E. Spessa, “Hybrid Vehicles,” in *Control of polluting substances emission*, Politecnico di Torino, 2017.
- [3] M. Velardocchia, “Electrically Variable Transmission (EVT),” in *Meccanica del Veicolo*, Politecnico di Torino.
- [4] Union of Concerned Scientists-Science for healthy planet and safer word, “Series vs Parallel vs Series/Parallel Drivetrains,” [Online]. Available: <https://www.ucsusa.org>. [Accessed 22 December 2017].
- [5] Macomb Community College-Center for Advanced Automotive Technology (CAAT), “Hybrid and Battery Electric Vehicles,” [Online]. Available: <http://autocaat.org>. [Accessed 21 December 2017].
- [6] Economic Commission for Europe of the United Nations (UN/ECE), “Regulation No 83,” *Official Journal of the European Union*.
- [7] Economic Commission for Europe of the United Nations (UN/ECE), “Addendum 100: Regulation No 101,” *Official Journal of the European Union*.
- [8] United Nations, “Addendum 15:Global technical regulation on Worldwide harmonized Light vehicles Test Procedure No. 15,” *Global Registry*.
- [9] C. Cubito, “A policy-oriented vehicle simulation approach for estimating the CO2 emissions from Hybrid Light Duty Vehicles,” *Ph.D. Dissertation*, 2017.

- [10] F. Millo, L. Rolando, R. Fusco and F. Mallamo, "Real CO₂ emissions benefits and end user's operating costs of a plug-in Hybrid Electric Vehicle," *Applied Energy*, vol. 114, pp. 563-571, 2014.
- [11] R. Henry, B. Lequesne, S. Chen, J. Ronning and Y. Xue, "Belt-Driven Starter-Generator for Future 42-Volt Systems," *SAE Technical Paper*, no. 2001-01-0728, 2001.
- [12] M. di Napoli, "Modelling and Experimental Characterisation of Belt Drive System in Micro-Hybrid Vehicles," *Ph.D. Dissertation*.
- [13] A. Stuffer, T. Schmidt, D. Helnrich and H. Stlef, "Introduction of 48 V Belt Drive System: New tensioner and decoupler solutions for belt driven mild hybrid systems," in *Schaeffler Kolloquium*, 2014.
- [14] M. Cossale, "Multi-phase Starter-Generator for 48 V Mild-Hybrid Powertrains," *Ph.D. Dissertation*, 2017.
- [15] J. Walters, R. Krefta, G. Gallegos-Lopez and G. Faticc, "Technology Considerations for Belt Alternator Starter Systems," *SAE Technical Paper*, no. 2004-01-0566, 2004.
- [16] M. Zink, M. Hausner, R. Welter and R. Shead, "Clutch and release system-Enjoyable clutch actuation," in *LuK Symposium*, 2006.
- [17] J. Kroll, M. Hausner and R. Seebacher, "Mission CO₂ Reduction-The future of the manual transmission," in *Schaeffler Kolloquium*, 2014.
- [18] B. Müller, M. Kneissler, M. Gramann, N. Esly, R. Daikeler and I. Agner, "Smaller, Smoother, Smarter-Advance development components for double-clutch transmissions," in *Schaeffler Symposium*, 2010.

- [19] B. Kremmling and R. Fischer, "The Automated Clutch- The new LuK ECM," in *LuK Symposium*, 1994.
- [20] P. Shakouri, A. Ordys, P. Darnell and P. Kavanagh, "Fuel Efficiency by Coasting in the Vehicle," *International Journal of Vehicular Technology*, 2013.
- [21] G. Brunetti, "Development of a Clutch Assisted-Enabling Stop & Start Sailing on next generation powertrain," *Ph.D. Dissertation*, 2014.
- [22] N. Muller, S. Strauss, S. Tumback and A. Christ, "Coasting-Next Generation Start/Stop System," *ATZ Autotechnology*.
- [23] P. Griefnow and J. Andert, "Next-Generation Low-Voltage Power Nets Impacts of Advanced Stop/Start and," *SAE Int. J. Fuels Lubr*, 2017.
- [24] G. Genta and A. Genta, *Road Vehicle Dynamics: Fundamentals of Modelling And Simulation*, World Scientific, 2016.
- [25] G. Genta and L. Morello, in *The Automotive Chassis*, vol. II: System Design, Springer, 2009.
- [26] J. Lee, "Rotating Inertia Impact on Propulsion and Regenerative Braking for Electric Motor Driven Vehicles," *Ph.D Dissertation*, 2005.
- [27] M. Venditti, "Innovative Models and Algorithms for the Optimization of Layout and Control Strategy of Complex Diesel HEVs," *Ph.D. Dissertation*, 2015.
- [28] W. Graus and E. Worrell, "Methods for calculating CO2 intensity of power generation and consumption: A global perspective," *Energy Policy* 39 (2011) 613-627.
- [29] International Energy Agency, "Energy efficiency indicators for public electricity production from fossil fuels," *IEA Information Paper*.

- [30] B. Baldissara, U. Ciorba, M. Gaeta, M. Rao and M. R. Viridis, “Verso un'Italia low carbon: sistema energetico, investimenti e innovazione,” *ENEA Energia, Ambiente e Innovazione*.
- [31] European Commission, “EU Reference Scenario 2016:Energy, Transport and GHG Emissions trends to 2050,” July 2016.
- [32] Ministero dello Sviluppo Economico, “Italy's National Energy Strategy: For a more competitive and sustainable energy,” March 2013.
- [33] U.S Energy Information Administration (EIA), “International Energy Outlook 2016,” *U.S. Energy Information Administration*, May 2016.
- [34] K. C. Prajapati, R. Patel and R. Sagar, “Hybrid Vehicle: A study on Technology,” *International Journal of Engineering Research and Techonology (IJERT)*, vol. 3, no. 12.
- [35] S. D. Belsare, D. Khairnar and M. Mishra, “Benchmarking, Target setting & Evaluation of a BSG for 2.0 L Diesel Engine,” *International Journal of Recent Trends in Engineering and Research*.
- [36] R. R.Henry, B. Lequesne, C. Shaotang and J. J.Ronning , “Belt-Driven Starter-Generator for Future 42-Volt Systems,” no. SAE Technical Paper 2001-01-0728, 2001.